Prof. Günter Allmaier

TECHNISCHE UNIVERSITÄT WIEN
Vienna University of Technology

M A S T E R A R B E I T

# Capillary Electrophoresis in combination with a Gas Phase Electrophoretic Mobility Molecular Analyzer

Ausgeführt am
Institut für Chemische Technologien und Analytik
der Technischen Universität Wien

unter der Anleitung von
Prof. Günter Allmaier, Prof. Martina Marchetti-Deschmann und Dr. Victor Weiss

durch

Lukas Kerul, BSc

Kardinal-König-Platz 3
1130, Wien

13.10.2014

Lukas Kerul, BSc

# Abstract

Nanoparticles are widely used in many fields of our lives including pharmaceutics as well as food technology, electronics, optics or cosmetics. For the characterization of nanoparticles microscopy based methods like transmission electron microscopy (TEM) can be applied. Another method which provides information about the nanoparticle size distribution receiving increasing attention is gas phase electrophoretic mobility molecular analysis (GEMMA). GEMMA separates single-charged analytes after they have been transmitted to the gas phase according to their electrophoretic mobility (EM) diameter. At standard conditions, analytes are fed continuously (in steady state) to a fused silica capillary, aerosol is generated at the tip of this capillary in the electrospray (ES) unit of the instrument due to applied pressure, voltage as well as a mixed air / $CO_2$ sheath flow. Aerosol droplets are dried and at the same time charge reduction in a bipolar atmosphere occurs. All non-volatile components of a given droplet aggregate to a single particle upon drying. Therefore, for complex samples, e.g. samples with a high salt content, the detection of individual analytes without salt aggregates on the surface of molecules is not possible: Corresponding EM diameters of analytes detected in GEMMA appear higher. In this work the additional electrophoretic separation of analytes in the liquid phase of the nano ES capillary of a standard, commercially available GEMMA instrument was developed. This additional electrophoretic separation of analytes in the liquid phase was demonstrated (proof of principle of operation) via two standard proteins, BSA and IgG. Furthermore, *on-line* desalting of these analytes could be shown. The new method was also applied for the analysis of biological nanoobjects (e.g. vaults or functional protein complexes). The separation of vault artifacts and vsvg-MVP vaults was demonstrated.

# Kurzfassung

Nanopartikel finden im täglichen Leben in vielen Bereichen, wie beispielsweise der Pharmazie, Lebensmitteltechnologie, Elektronik, Optik oder Kosmetik Verwendung. Für die Charakterisierung von Nanopartikeln werden zumeist mikroskopische Methoden wie *Transmission Electron Microscopy* (TEM) verwendet. *Gas Phase Electrophoretic Mobility Molecular Analysis* (GEMMA) stellt hierzu eine äußerst interessante Alternative dar, die Auskunft über die Größenverteilung der Nanopartikeln bietet. Bei GEMMA Messungen werden einfach geladenen Teilchen nach ihrem *Electrophoretic Mobility (EM)* Durchmesser aufgetrennt, nachdem sie zuvor in den gasförmigen Zustand übergeführt worden sind. Unter Standardbedingungen erfolgt durch eine *fused silica* Kapillare eine kontinuierliche Analytzufuhr. An der Kapillarspitze (innerhalb der Elektrosprayeinheit (ES) des Instruments) entsteht ein Aerosol durch Wirkung eines angelegten Druckes an die Probelösung, einer angelegten Hochspannung sowie einer Luft / $CO_2$ Strömung um die Kapillarspitze. Die Aerosoltropfen trocknen im Luftstrom und gleichzeitig wird die Ladungszahl in einer bipolaren Atmosphäre reduziert. Alle nichtflüchtigen Komponenten eines gegebenen Tropfens aggregieren bei Trocknung zu einem einzigen Teilchen. Das hat zu Folge, dass die Detektion für komplexe Proben (z.B. mit hohem Salzgehalt) unmöglich ist: die ermittelten EM Durchmesser und deren Verteilung erscheinen durch Anlagerungen von z.B. Verunreinigungen an Analytmolekülen deutlich höher und breiter. In dieser Arbeit wurde die vorherige elektrophoretische Auftrennung von Analyten in der Flüssigphase der nano ES Kapillare eines kommerziellen GEMMA Standardinstrumentes entwickelt. Diese zusätzliche elektrophoretische Auftrennung der Analyten in der Flüssigphase wurde mittels zweier Standardproteine (BSA und IgG) gezeigt. Desweiteren wurde das *on-line* Entsalzen derartiger Analyten damit demonstriert. Die neue Methode wurde auch für die Analyse von Bionanopartikeln (z.B. Ribonukleoproteinkomplexe - *Vaults* oder funktionelle Proteinkomplexe) verwendet. Die Analyse von *Vault* Artefakten und *Vaults* Konstrukten wie vsvg-MVP wurde gezeigt.

# Zusammenfassung

In dieser Arbeit wurde die elektrophoretische Auftrennung von Standardproteinen in der Flüssigphase (nano ES Kapillare) eines kommerziellen GEMMA Standardinstrumentes sowohl durch theoretische Modellrechnungen als auch experimentell gezeigt. Der angelegte Druck in der Probenkammer, die verwendete Luft / $CO_2$ Strömung an der Spitze der nano ES Kapillare sowie der pH des verwendeten Puffers, die Konzentration der Probe und die Zeitdauer zur Erstellung eines *sample plugs* innerhalb der Kapillare wurde optimiert. Danach konnte die Auftrennung von BSA und IgG mit unterschiedlichen Migrationszeiten beobachtet werden. Desweiteren ermöglichte die neu entwickelte Methode die Analyse von nano ES inkompatiblen Proben mit hohem Salzgehalt (bis 2 mM) dank *on-line* Entsalzens: Unter GEMMA Standardmessbedingungen kommt es zur Aggregation von Analyt- mit Salzmolekülen bei Trocknung der Aerosoltröpfchen in der ES Einheit des Instrumentes. Das hat zu Folge, dass weitaus heterogenere Verteilungen sowie höhere EM Durchmesser für Analyten detektiert werden, was die Bestimmung des EM Durchmessers der Analyten erschwert oder sogar unmöglich macht. Durch *on-line* Entsalzen der Probe entsprach der ermittelte EM Durchmesser jedoch wiederum dem EM Durchmesser der reinen Analyten. Der nächste Schritt in der Anwendung dieser Methode kann die Analyse von Detergentien enthaltenden Proben sowie elektrophoretisches *sample stacking* sein.

Die neu entwickelte Methode für die elektrophoretische Auftrennung in der Flüssigphase eines kommerziellen GEMMA Instruments wurde auch für reelle biologische Proben angewandt: *Vault* Partikel wurden mit einem GEMMA Instrument an der UCLA analysiert. Auch hier konnte eine Auftrennung zweier Analyten gezeigt werden. Zusätzlich wurden noch Stabilitätsmessungen von *Vault* Partikeln (Lagerung bei -20°C für 48 Stunden sowie Zugabe von Methanol zu Proben) durchgeführt.

Auch Hemoglobin-N2N3 Receptor Komplexe sowie TriC-Didemnin B Komplexe wurden von mir an der UCLA mittels GEMMA analysiert. Es wurde auch die Stabilität des Mmm1-D5-Fusion Komplexes in Lösungen mit MeOH-Gehalten bis 30% v/v untersucht.

# Acknowledgements

Oh, the depth of the riches
both of the wisdom and the knowledge of God!
How unsearchable His judgments
and untraceable His ways!
For who has known the mind of the Lord?
Or who has been His counselor?
Or who has ever first given to Him,
and has to be repaid?
For from Him and through Him
and to Him are all things.
To Him be the glory forever. Amen. [Romans 11:33-36]

My deepest thanks belongs to God, who fills my life with mercy, love, and blessings. Through Him I was able to finish my work and studies. I would like to express my tremendous appreciation to Prof. Günter Allmaier for his guidance, valuable reviews, and help with the arrangement and financial support of my research stay at UCLA. I would like to offer my special thanks to Dr. Victor Weiss for guidance through the entire project, his patience, his friendliness, and his availability in every moment. I want to acknowledge the help provided by Prof. Martina Marchetti-Deschmann, who provided valuable and constructive suggestions during the planning and development of the research work. A special thanks is extended to Prof. Joseph Loo for inviting me into his research group at UCLA, as well for his guidance and availability. I am particularly grateful to his entire research group and Dr. Jan Mrazek for the great cooperation and nice work environment. I would also like to thank Angelika Schweighart for finding the solution to a complicated situation regarding my research stay at UCLA. Lastly, I wish to thank my parents for their support and encouragement throughout my study.

# Table of Contents

# 1 List of abbreviations

**BGE**, background electrolyte; **BSA**, bovine serum albumin; **CE**, capillary electrophoresis; **CM**, capillary electrophoresis mode; **CPC**, condensation particle counter; **DMA**, differential mobility analyzer; **DMSO**, dimethyl sulfoxide; **EM**, electrophoretic mobility, **EOF**, electroosmotic flow; **ES**, electrospray; **FM**, flushing mode; **GEMMA**, gas phase electrophoretic mobility molecular analysis; **$H_2O$**, water; **IgG**, γ globuline; **MES**, 2-(*N*-morpholino)ethanesulfonic acid; **MVP**, major vault protein ; **m-Cherry**, m-Cherry-MVP vaults; **mix**, vsvg-MVP and m-Cherry-MVP vaults; **MS**, mass spectrometry; **$NH_3$**, ammonia; **$NH_4OAc$**, ammonium acetate; **NM**, normal mode; **TEM**, transmission electron microscopy; **TUVIE**, Vienna University of Technology, **UCLA**, University of California, Los Angeles; **vsvg**, vsvg-MVP vaults

# 2 Introduction

## 2.1 Gas-phase electrophoretic mobility molecular analysis (GEMMA)

In the past years there is an increasing interest in the research and application of nanoparticles (particles of any shape with dimensions of 1 nm to 100 nm or occasionally up to 500 nm diameter [1]). The application of nanoparticles includes biomedical [2], optical [3] as well as electronic [4] fields. After the use of nanoparticles was spread rapidly, the safety evaluation of nanoparticles became necessary [5] which made the characterization of nanoparticles more important.

For the determination of size distributions of nanoparticles several methods can be applied, for example transmission electron microscopy (TEM) [6] or inductively coupled plasma mass spectrometry (ICPMS) [7]. Gas phase electrophoretic mobility molecular analysis (GEMMA) is an electrospray-based method that can provide information about EM diameter and the size distribution of nanoparticles as well, even allowing single-particle and number-based detection. It was found that the EM diameter is in an excellent correlation with molecular mass of peptides, proteins and proteinaceous noncovalent complexes up to 2 MDa in case of spherical shape of analytes [8].

GEMMA has the following advantages in comparison to other methods (like mass spectrometry based methods and TEM): (i) fast analysis, (ii) minimal sample preparation, (iii) lower instrumentation costs and the (iv) capability to provide molecular “size” information with number-based quantification [9]. A typical GEMMA instrument consists of three components: (i) a nano Electrospray (nano ES) unit including a neutralization chamber including a $^{210}$Po-source (ii) a nano Differential Mobility Analyzer (nano DMA) for particle separation and (iii) a Condensation Particle Counter (CPC) for detection. A photo of the instrument is depicted in Figure 2.1.

**Figure 2.1: Photo of GEMMA instrument at TUVIE**

A cone tipped fused silica capillary is immersed into the liquid sample (volatile electrolyte solution) in a pressure chamber, pressure up to 5 psid (= 0.34 bar) is applied. Additionally, voltage is employed by a Pt-electrode. Such, the sample is introduced to the capillary (flow rate 10-100 nL/min) [9a, 10] and an electrospray is generated (Taylor-cone) at the cone-tipped end of capillary by (i) the applied pressure difference, (ii) the applied voltage and (iii) an applied $CO_2$ and air sheath flow at the capillary tip. The diameter of multiply-charged aerosol droplets is decreased due to solvent evaporation until analytes are dried and concomitantly their charge is reduced by $^{210}$Po-source. The majority of particles become neutral, only about 1% of particles are single charged, a negligible part double or multiple charged (in case of new $^{210}$Po-source with age not exceeding 1 year). The charged particles enter the DMA in a laminar flow where the separation of particles with different EM diameters due to a variable potential difference between an outer and a central rod-shaped electrode takes place. Charged particles are attracted to the central electrode. For one specific applied voltage, only particles with a narrow EM diameter range possess a correct trajectory for passing a slit that connects the DMA with the CPC, where particle detection occurs.

The variation of the applied field strength allows scanning of a whole EM diameter size range. In this way the separation and selection of particles is performed in the DMA (for more details about DMA see [11]). A schematic diagram of a nano-DMA is depicted in Figure 2.2.

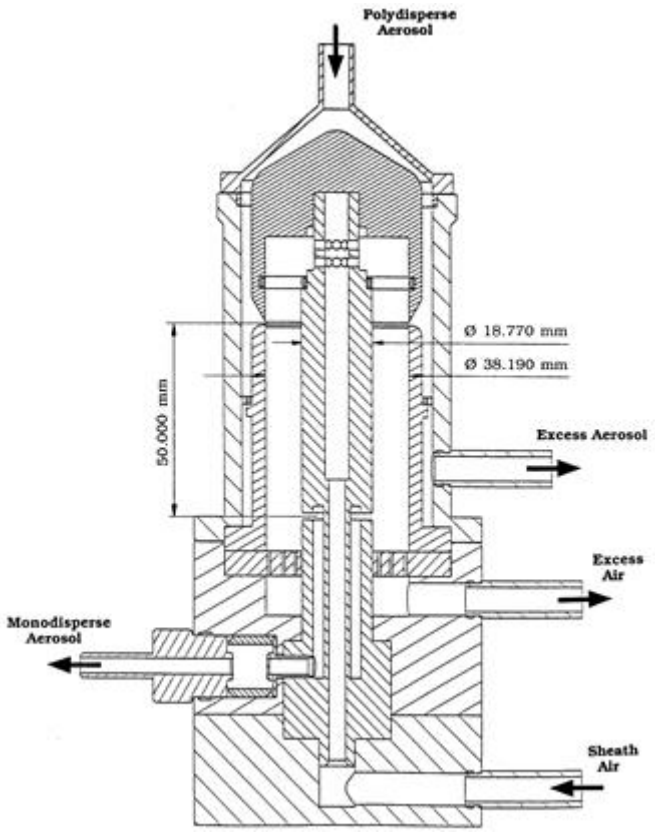


**Figure 2.2: Schematic diagram of nano-DMA described in [12]**

In the CPC, particles are enlarged by a condensation of supersaturated n-butanol vapor. The particles are then detected by a diffraction of a focused laser beam [13].

GEMMA has been already applied for analysis of peptides, proteins, polysaccharides, glycoproteins, viruses and nanoparticles with success [14].

## 2.2 Capillary electrophoresis (CE)

CE is a separation method based on differences of analyte migration in an electrolyte solution (background electrolyte = BGE) upon application of an electric field to a capillary. The migration of analytes is determined by an accelerating force (charge of analyte = z * e) and a retarding force (friction – determined by the size and shape of analyte = ξ). The migration velocity of analytes $v_i$ can be so described as:

$$v_i = E * \frac{z * e}{\xi}$$

To describe the mobility of analytes independent of the strength of the electric field E, the electrophoretic mobility term $\mu_i$ (equal to $\frac{z*e}{\xi}$) was introduced. Additional factors that influence analyte migration are temperature, viscosity, ionic strength and pH [15]. At basic pH-levels the surface accessible silanol groups of the fused silica capillary are deprotonated, cations from the solution are attracted to capillary walls, where they form the so-called Debye layer (electrical double layer). After application of an electric field to the system, the cations are attracted to cathode inducing movement of the whole solution bulk in the direction of the cathode (electroosmotic flow = EOF). The mobility of EOF ($\mu_{EOF}$) can exceed the mobility of analytes $\mu_i^{eff}$. In case analytes are negatively charged (attracted to the anode) this can even result in the detection of analytes at the cathodic side of the capillary ( = $\mu_{app}$). The mobility of analytes, $\mu_i^{eff}$, independent from the EOF can be calculated as: $\mu_{eff} = \mu_{EOF} - \mu_{app}$.

As already described in a previous chapter, the capillary in the nano ES unit of a GEMMA instrument is a fused-silica one with a voltage applied along the capillary. Therefore, the question of electrophoretic separation in the liquid phase of this capillary is discussed in this work. Until now only the combination of capillary electrophoretic separation of protein standards with CPC detection [16] or capillary isoelectric focusing combined with GEMMA [17] has been investigated.

In this master thesis the main interest is the electrophoretic separation of analytes in the liquid phase (inside the nano ES capillary) of a commercially available, standard GEMMA instrument. Upon application of standard conditions for sample introduction to a GEMMA instrument, the electrophoretic separation of analytes within the nano ES capillary is not desired - a high pressure is applied (about 4 psid = 0.3 bar) and the sample is injected continuously to the system. The problems in this case are the analysis of complex samples as well as samples with high salt concentrations (analytes are covered by an unspecified amount of salt upon drying of droplets, therefore, a shift in EM diameter to higher values can be observed).

For this reason the pressure in the nano ES capillary of GEMMA was decreased, the sample was injected to system only for a few seconds prior immersion of the capillary to a buffer vial and the scan time and range was also decreased to enable the separation and detection of sample components in a CE-GEMMA spectrum. By application of these changes, the system is capable of preseparation of salts and other sample components from analytes in the liquid phase before GEMMA takes place. A resulting manuscript (see Results and

Discussion part) consists of (i) the discussion of the theoretical background and computational results after application of the theoretical force distribution model, (ii) the presentation of obtained experimental data and (iii) the application of the new method (CE-GEMMA) for online-desalting of samples. Additionally, (iv) analyses of real biological samples (vaults, for detailed description see the introduction part below) applying standard GEMMA measurements and applying the new developed CE-GEMMA method were carried out.

## 2.3 Vault particles

Vaults are ribonucleoprotein particles present in eukaryotic cells, as for example in protozoa, molluscs, the slime mold *Dictyostelium discoideum*, echinoderms, fish, amphibians, avians and mammals [18]. Vaults are highly conserved particles [18a], barrel-shaped with two protruding caps, an invaginated waist and a hollow space inside [19]. A reconstructed vault particle is depicted in Figure 2.3. Vault from rat liver has a calculated mass of up to 12.9 ± 1 MDa (examined by scanning transmission electron microscopy) [20]. Several indications point to the transport function of vaults in the intracellular transport, however, the function of vaults still remains unclear. There were also studies published in recent years where the possibility of transport of biomolecules (cytosolic ribotoxin, secondary lymphoid chemokine) [21] [22] by recombinant vaults was shown.

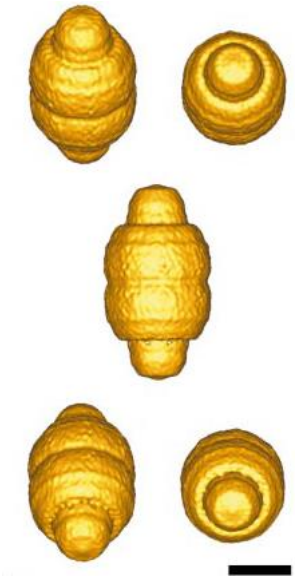

**Figure 2.3: The vault reconstruction depicted from different positions, the scale bar represents 250 Å [19]**

The further characterization of vault nanoparticles could help to explain the mechanism of vault expression (vaults are consisting of 78 - 96 MVP units) [23] [24]. For this purpose, the EM diameter analysis of vsvg-MVP vaults (vsvg) and m-Cherry-MVP vaults (m-Cherry) expressed in one system was investigated with GEMMA. The vsvg (8 MDa – 9MDa) are composed of rat MVP units, each MVP (96.8 kDa, see the amino acid sequence in 5.2) is modified with vsvg tag (1.0 kDa, see the amino acid sequence in 5.2). The m-Cherry (10 MDa – 12 MDa) are composed of rat MVP units, each MVP (96.8 kDa, see the amino acid sequence in 5.2) is modified with an m-Cherry molecule (26.7 kDa, see the amino acid sequence in 5.2) and a linker (= one leucine molecule, 131 Da).

Given that two analytes are detectable in GEMMA (vaults formed from MVP with and without m-Cherry modification separately), different building blocks are not combined spontaneously to one vault particle. Instead, the creation of vaults should be considered to be conducted by a ribosomal complex or other cell mechanism immediately after expression of MVPs without mixing of building blocks. This would help to understand more the assembly of large ribonucleoid particles.

The analysis of vaults was performed at University of California, Los Angeles (UCLA) in the research group of Prof. Joseph Loo. Ribonucleoprotein vaults were prepared and the analysis of vaults in normal mode (NM) was performed.

The NM represents the conventional GEMMA setup used for analysis. The sample is placed into the pressure chamber, and about 4 psid (which corresponds to approximately 0.3 bar) pressure and 2.7 ± 0.1 kV voltage are applied. This results typically in 400 ± 100 nA current. The sheath flow in the nano ES unit is set on 1.1 liters per minute (Lpm) (0.1 Lpm $CO_2$, 1.0 Lpm air), the sheath flow in the nano DMA is at 13.5 Lpm. The scanning process begins when a steady state is reached, i.e. when the sample is continuously fed to the system (about 5 minutes after the sample has initially been introduced to the GEMMA instrument). The scan range covers particles with EM diameter e.g. between 2 nm and 60 nm, however, also a shorter scan range can be set. For every analysis a number of scans (n=6 for the current work) are taken and a resulting GEMMA spectrum is obtained as a median of these scans (individual scans are not depicted).

Additionally, a new method for electrophoretic separation in the nano ES capillary of a commercially available standard GEMMA instrument (CE-GEMMA) was applied for the analysis of vaults as well. To demonstrate the separation potential of this method, samples containing vaults and Ovalbumin were measured in CE-GEMMA mode as well.

# 3 Results and Discussion

The main aim of this master thesis was to demonstrate that a CE separation in the liquid phase occurs during sample introduction to a Gas Phase Electrophoretic Mobility Molecular Analyzer (GEMMA).

Therefore, a model of forces acting on analytes in the capillary of a CE-GEMMA as well as calculated separations and the very first measurements with this method are explained in 3.1. Forces that influence analyte migration through the nano ES capillary include: (i) EOF (ii) mobility of analytes (iii) applied pressure across the capillary and (iv) CO2 / air sheath flow at the capillary tip. Regarding the impact of these force contributions, the electrophoretical separation of analytes was calculated. Theoretical considerations showed that analytes with different mobility $\mu_{app}$ should be separable during sample introduction to the GEMMA instrument via electrophoresis in the liquid phase (CE-GEMMA). Theoretical considerations were checked via experiments. CE-GEMMA was applied for separation of two standard proteins (BSA and IgG) as proof of principle of the applied method. Furthermore, online desalting of these proteins was shown. The results were presented in the publication "Liquid phase separation of proteins based on electrophoretic effects in an electrospray setup during sample introduction into a gas-phase electrophoretic mobility molecular analyzer (CE–GEMMA/CE–ES–DMA)" given in chapter 3.1.

The next step was the application of CE-GEMMA on complex biological analytes. Vault particles were chosen as analytes. For this purpose a research stay at UCLA was arranged. Vaults are large ribonucleotid particles found in eukaryotic cells. The size of vaults is 40 * 40 * 70 nm [25] forming a barrel-shaped hollow particle [19]. First, the GEMMA instrument at UCLA had to be prepared for measurements. Subsequently, the instrument was checked with standard proteins (under reference conditions = normal mode, NM) and compared with results obtained at TUVIE. Further measurements included other bionanoparticles in order to train the handling of complex samples. Subsequently, vaults were analyzed under reference conditions (NM) as well as in CE-GEMMA mode (CM). Samples containing standard proteins and vaults were employed for optimization of the CM method. Results are shown in section 3.2.

# 3.1 Liquid phase separation of proteins based on electrophoretic effects in an electrospray setup during sample introduction into a gas-phase electrophoretic mobility molecular analyzer (CE–GEMMA/CE–ES–DMA)

## Liquid phase separation of proteins based on electrophoretic effects in an electrospray setup during sample introduction into a gas-phase electrophoretic mobility molecular analyzer (CE–GEMMA/CE–ES–DMA)

Victor U. Weiss [a], Lukas Kerul [a], Peter Kallinger [b], Wladyslaw W. Szymanski [b], Martina Marchetti-Deschmann [a], Günter Allmaier [a,*]

[a] Institute of Chemical Technologies and Analytics, Vienna University of Technology, Vienna, Austria
[b] Faculty of Physics, University of Vienna, Vienna, Austria

### HIGHLIGHTS

- First demonstration of a hyphenated CE–GEMMA combination for proteins.
- Feasibility of *on-line* CE–GEMMA in a commercial device at ambient pressure.
- *On-line* combination of liquid phase and gas phase electrophoretic separation.

### GRAPHICAL ABSTRACT

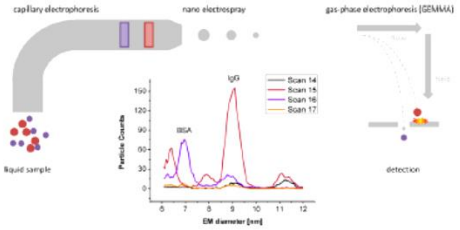


### ARTICLE INFO

*Article history:*
Received 10 January 2014
Received in revised form 22 May 2014
Accepted 23 May 2014
Available online 28 May 2014

*Keywords:*
GEMMA
Ion mobility spectrometer
Scanning mobility particle sizer
Capillary electrophoresis
Electrospray
Desalting

### ABSTRACT

Nanoparticle characterization is gaining importance in food technology, biotechnology, medicine, and pharmaceutical industry. An instrument to determine particle electrophoretic mobility (EM) diameters in the single-digit to double-digit nanometer range receiving increased attention is the gas-phase electrophoretic mobility molecular analyzer (GEMMA) separating electrophoretically single charged analytes in the gas-phase at ambient pressure. A fused-silica capillary is used for analyte transfer to the gas-phase by means of a nano electrospray (ES) unit. The potential of this capillary to separate analytes electrophoretically in the liquid phase due to different mobilities is, at measurement conditions recommended by the manufacturer, eliminated due to elevated pressure applied for sample introduction. Measurements are carried out upon constant feeding of analytes to the system. Under these conditions, aggregate formation is observed for samples including high amounts of non-volatile components or complex samples. This makes the EM determination of individual species sometimes difficult, if not impossible. With the current study we demonstrate that liquid phase electrophoretic separation of proteins (as exemplary analytes) occurs in the capillary (capillary zone electrophoresis, CE) of the nano ES unit of the GEMMA. This finding was consecutively applied for *on-line* desalting allowing EM diameter determination of analytes despite a high salt concentration within samples. The present study is to our knowledge the first report on the use of the GEMMA to determine EM diameters of analytes solubilized in the ES incompatible electrolyte solutions by the intended use of electrophoresis (in the liquid phase) during sample delivery.

*Abbreviations:* BGE, background electrolyte; BSA, bovine serum albumin; CM, CE mode; CPC, condensation particle counter; DMA, differential mobility analyzer; EM, electrophoretic mobility; ES, electrospray; FM, flushing mode; GEMMA, gas-phase electrophoretic mobility molecular analyzer; IgG, γ globulin; MW, molecular weight; NM, normal mode; TEM, transmission electron microscopy.

* Corresponding author at: Institute of Chemical Technologies and Analytics, Vienna University of Technology, Getreidemarkt 9/164, Vienna A-1060, Austria. Tel.: +43 1 58801 15160; fax: +43 1 58801 16199.

http://dx.doi.org/10.1016/j.aca.2014.05.043

Results demonstrate the proof of concept of such an approach and additionally illustrate the high potential of a future *on-line* coupling of a capillary electrophoresis to a GEMMA instrument.


## 1. Introduction

Recent years saw a fast growing interest in nanoparticles, i.e., particles up to the range of a few 100 nm in diameter. However, research concerning the applicability of nanoparticles in various fields like biotechnology, medicine, pharmaceutical or food industry, and as well risk assessment of nanoparticle application relies on well-defined material (so-called certified reference material) for experimental work. Severe concerns relating to the safety of application of certain types of nanoparticle have currently been raised [1–6]. Typically, methods like transmission electron microscopy (TEM) are employed for the analysis of nanoparticle size distributions (as recently shown by Lin *et al.* [7]). Ion mobility mass spectrometry (IM-MS, as for instance reviewed in [8]) can be used to determine collision cross section values of biological macromolecules and protein assemblies. However, also gas-phase electrophoretic mobility molecular analysis (GEMMA) was introduced, which separates single charged analytes in the gas-phase at ambient pressure according to the analytes electrophoretic mobility (EM) diameters. In case of singly charged, spherical shaped analytes EM diameters correspond to particle diameters [9–12]. Recently, the GEMMA acronym is often being replaced by other terms like macroion mobility spectrometer (macroIMS), LiquiScan-ES, nES-DMA or ES-SMPS spectrometer for the same instrument [13]. Nevertheless, for reasons of consistency with previous work we still employ the acronym GEMMA in this manuscript. Some very interesting instrumental characteristics like (i) fast analysis times, (ii) minimal sample pretreatment, (iii) low cost instrumentation (especially when compared to TEM instruments or mass spectrometers) and most importantly, (iv) the possibility of single, number based particle detection (i.e., determination of number concentrations) make the GEMMA very attractive, especially for the characterization of analytes in the nm size range (for a selection of papers concerning proteins [14,15], viruses [14,16,17], and polymer materials [18,19] refer to respective publications).

The GEMMA device [9] consists of three parts: (i) a charge reducing nano electrospray (nano ES) unit for aerosolization of analytes from an aqueous liquid solution and charge conditioning in a bipolar atmosphere induced by a $^{210}$Po $\alpha$-radiation source, (ii) a nano differential mobility analyzer (nano DMA) as separation/sizing device, and (iii) an ultrafine condensation particle counter (CPC) as detector. In the nano ES unit, samples are electrosprayed from a cone tipped fused silica capillary in the cone–jet mode [20]. Additional forces influencing analyte migration though the nano ES capillary are (i) the applied high voltage along the capillary and (ii) the $CO_2$/particle-free air sheath flow at the capillary tip. Subsequently, multiple charged, aerosolized droplets are dried and charge reduction occurs leading to a predictable equilibrium charge distribution of the nanoaerosol [21,22]. Particles are further transported *via* a sheath flow of air and $CO_2$ (typically about 1 liter per minute, Lpm) into the nano DMA. There, particles are classified according to their EM diameter. An applied electric field with tunable strength between the electrodes of a cylindrical capacitor acts as orthogonal force to the high sheath flow applied between the electrodes to carry analytes through the instrument. It enables only nanoparticles of a certain (and narrow) EM diameter range to pass through the ion mobility analyzer. By variation of the applied field strength, a given EM diameter range can be scanned. (For a more detailed description of possible DMA setups refer to Flagan [23] and Intra and Tippayawong [24]). After passing the nano DMA, monodisperse analytes are transported to the CPC. There, particles are enlarged by condensation of supersaturated *n*-butanol or water vapor to optically detectable micrometer size for single particle detection upon passing of analytes through a focused laser beam [25]. In the past, GEMMA allowed already the determination of EM diameters for a number of analytes like large peptides and proteins [26,27], polysaccharides [19], glycoproteins [15], intact viruses [12,14,27,28], virus-like particles [29], vaccines [30], virus–antibody complexes [31], and gold particles [32–34], gelatin nanoparticles up to several 100 nm EM diameter [35] or carbon nanotubes [36]. Given a suitable, analyte specific calibration exists, the GEMMA derived EM diameter values can be converted to MW values, hence allowing MW determination of analytes even in a range which cannot be addressed by mass spectrometry.

Capillary electrophoresis (CE) separates analytes in solution (background electrolyte, BGE) upon application of an electric field. Analytes migrate with specific velocities through the capillary after equilibrium between an accelerating force (determined by the charge of an analyte and the electric field) and a retarding friction force (according to Stokes' law) is reached. Analyte migration is described by the ratio between its velocity and the applied field strength (electrophoretic mobility, $\mu_i$). Additionally, factors like the ionic strength of a given electrolyte solution and its pH play a role. For instance, BGEs with basic pH lead to movement of the solution bulk inside a fused silica capillary in direction of the cathode (electroosmosis) [37,38]. As the mobility of the electroosmotic flow (EOF) typically exceeds the electrophoretic net mobility (effective mobility) $\mu_i^{\text{eff}}$ of analytes, their overall movement is directed to the cathodic side of the capillary. In case the EOF mobility is known and the apparent mobility of an analyte is calculated from its migration behavior following standard protocols, $\mu_i^{\text{eff}}$ can be calculated by subtraction.

As the capillary employed for the nano ES unit of a conventional, commercially available GEMMA instrument fulfills all requirements of a standard CE setup, we investigated if electrophoretic separations can also be observed upon sample introduction to the GEMMA instrument. To our knowledge, until now, only the direct combination of a conventional CE instrument with a CPC detector (without a nano DMA in between) has been reported [39] and a non-commercially capillary isoelectric focusing instrumentation coupled to the GEMMA presented at a conference [40]. For standard measurements, electrophoretic separation of analytes in the nano ES capillary of a GEMMA instrument is not desired, instead analytes are continuously fed to the system. Therefore, electrophoretic effects in the liquid phase are suppressed by a relatively high pressure applied to the sample chamber (approximately 4 pounds per square inch differential, psid, which corresponds to approximately 0.3 bar along a 26 cm long capillary). However, this setup causes problems with samples either with complex composition or containing high amounts of salts (e.g. samples at physiological conditions). Note that the sample pretreatment by dilution in a volatile electrolyte solution is only practicable to a certain degree, because intended analytes would also become too diluted for analysis. With increasing concentration of non-volatile sample compounds, aerosolized droplets contain aggregates of sample components that make the determination of EM diameter values for actual analytes difficult, in the worst case even impossible. With the current study we therefore suggest to solve this problem by concentrating on the CE separation potential of a typical, commercially available GEMMA

setup: by reduction of the applied pressure to the pressure chamber conditions in the nano ES capillary allowing electrophoresis can be obtained. This approach enables separation of analytes in the liquid phase of the nano ES source (i.e., in the capillary) prior to the determination of the analytes gas-phase electrophoretic mobilities coupling two electrophoresis based methods. It is therefore the aim of the current study (i) to present theoretical considerations considering CE separation of analytes in the capillary of the nano ES unit, (ii) to confirm these findings with experimental data obtained for two proteins as exemplary analytes to show the feasibility of this approach, and (iii) to demonstrate the applicability of our setup in the *on-line* desalting of a protein containing sample, which would otherwise only yield poorly interpretable spectra.

## 2. Materials and methods

### 2.1. Chemicals and reagents

Ammonium acetate (≥99.99%) and ammonium hydroxide (28.2% ammonia in water) were purchased from Sigma–Aldrich (St. Louis, MO, USA), sodium chloride (≥99.5%) as well as sodium hydroxide (≥99%) were obtained from Merck (Darmstadt, Germany). Ultra-high quality water was delivered from a Simplicity UV apparatus (Millipore, Molsheim, France) with 18.2 MΩ cm resistivity at 25 °C. Albumin (bovine, ≥96%, BSA, MW of 66 kDa according to manufacturing company, pI = 5.4 [41]) and γ globulin (bovine, ≥99%, IgG, MW 150 kDa according to manufacturing company, pI = 6.6 [41]) were purchased from Sigma–Aldrich as was dimethyl sulfoxide (DMSO, ≥99.9%). Benzoic acid (≥99.9%) was obtained from Fluka (Buchs, Switzerland).

### 2.2. Buffers

For CE and GEMMA analysis, ammonium acetate with identical ionic strength ($I$ = 25 mmol $L^{-1}$) but different pH values were employed: pH 7.4, 8.4, and pH 9.4 solutions were prepared. Ammonium hydroxide was used for pH adjustment of electrolytes. Solutions were filtered *via* >0.2 μm pore size syringe filters (sterile, surfactant free cellulose acetate membrane, Sartorius, Goettingen, Germany) prior application. Sodium hydroxide was at 1 mol $L^{-1}$ concentration for flushing of the CE capillary between runs.

### 2.3. Sample preparation

Aqueous protein solutions of IgG and BSA (10 μmol $L^{-1}$ each) were diluted tenfold in ammonium acetate (pH 7.4, 8.4, and 9.4, respectively) for the GEMMA experiments and twofold for the CE experiments. DMSO (1:8000 v/v final dilution) and benzoic acid (0.1 mmol $L^{-1}$ final concentration) were applied in CE–UV samples as EOF marker and internal standard, respectively. Proteins were either combined in a mixed solution or present as single component samples as indicated within figures. For *on-line* desalting experiments, sodium chloride was added at 5 mmol $L^{-1}$ final concentration to the GEMMA samples.

### 2.4. Instrumentation

The employed GEMMA system consisted of (i) a nano ES unit including a $^{210}$Po source (model 3480), (ii) a nano differential mobility analyzer (nano DMA, series 3080), and (iii) an ultrafine condensation particle counter (CPC, series 3025A). Samples were introduced into the nano ES unit *via* a 25 μm inner diameter and 26 cm long cone tipped fused silica capillary. The nano ES was operated with positive high voltage. All parts were from TSI Inc (Shoreview, MN, USA). For CE separations employing UV detection, an Agilent 3D CE (Waldbronn, Germany) was used. Electrophoresis was performed at 25 °C in positive polarity with a fused silica capillary of 50 μm inner diameter and $L_{total/effective}$ = 60.2/51.7 cm from Polymicro (Phoenix, AZ, USA). Samples were introduced by application of 25 mbar pressure for 10 s. Analytes were separated by application of 20 kV leading to an electric field strength of 33.2 kV $m^{-1}$. Detection was *via* assessment of UV absorption simultaneously at 200, 205, and 260 nm. Prior to each run, the capillary was equilibrated for 2 min with BGE and after each run it was washed for 1.5 min with sodium hydroxide solution followed by 2 min rinsing with water.

### 2.5. GEMMA analysis modes

The normal mode (NM) represents the conventional GEMMA setup used for analysis. For this, the sample is placed into the pressure chamber, and about 4 psid (approximately 0.3 bar) pressure and 2.6–2.8 kV are applied. This results typically in 300–500 nA current. The sheath flow in the nano ES unit is set to 1.1 Lpm (0.1 Lpm $CO_2$, 1.0 Lpm air), the sheath flow in the nano DMA is at 13.5 Lpm. The scanning process (variation of the applied field strength) begins when a steady state is reached, i.e., when the sample is continuously fed to the system (about 5 min after the sample has initially been introduced to the GEMMA instrument). The scan range covers particles with the EM diameter between 2 nm and 60 nm, however, also a shorter scan range can be set. For every analysis a number of scans ($n$ = 6) is taken with high repeatability and data from each scan is retrieved from the instrument. Subsequently (to correct for possibly occurring spikes), a resulting GEMMA spectrum is obtained as a median of these scans (individual scans are not depicted).

In the flushing mode (FM) the applied pressure in the nano ES unit is reduced to approx. 1 psid (approx. 70 mbar). Therefore, the impact of pressure gradient as driving force to move analytes through the capillary is greatly reduced. The voltage, sheath flow settings and the resulting current were as previously for NM. Furthermore, measurements are carried out not over a scan range but at a constant EM diameter value specific for a given analyte (determined *via* NM measurements at the peak apex of respective single charged analyte species – for BSA 7 nm, for IgG 9 nm EM diameter was set during FM, respectively). The time needed for analytes to pass through the capillary is determined. Measurements start immediately after immersion of the capillary end to the sample vial to allow for time determination of sample passage through the instrument and are terminated after a steady state (i.e., plateau of analyte detection) is reached.

For CE mode (CM) the same conditions (pressure, sheath flow, voltage) as in FM were applied. However, samples are injected to the system only for 2 s followed by the change of the sample tube to the respective electrolyte solution. This results in an analyte plug similar as for conventional CE setups. Additionally, in case of mixed samples (including BSA and IgG at 1 μmol $L^{-1}$ concentration, each), no longer a constant EM diameter was regarded as for FM, but a size range between 6 nm and 12 nm EM diameter was scanned to follow the separation of analytes (scan time at 18 s, time for detector reset between scans at 3 s).

For FM and CM the capillary was filled with analyte free buffer prior to immersion of the sample.

## 3. Results and discussion

The results presented in the following sections demonstrate that under certain conditions electrophoretic separation of analytes can be achieved in the liquid phase within the capillary part of the nano ES unit of a conventional, commercially available GEMMA instrument. This was done theoretically calculating

driving velocities in the nano ES capillary and their contribution to overall analyte migration. On the other hand, our theoretical considerations were verified experimentally. We monitored the separation of two proteins (BSA and IgG) as exemplary analytes in the nano ES capillary of the system. This finding opens up very interesting avenues like the *on-line* desalting of protein samples which we likewise demonstrated here. In the future, the CE separation of even nanoparticles prior to the GEMMA analysis by means of a standard GEMMA instrument seems to be easily feasible and an *on-line* hyphenation of a stand-alone CE to a GEMMA instrument appears highly interesting.

### 3.1. Theoretical considerations and experimental assessment of individual forces contributing to sample introduction to a GEMMA system via a nano ES process

Samples are introduced into the nano ES unit of the GEMMA system *via* a fused silica cone tipped capillary. During sample introduction the movement of the analytes can be calculated by taking four processes into account: (i) pressure is applied to the pressure chamber of the instrument ($\Delta p_{psid}$) to feed the sample containing electrolyte solution continuously to the nano ES capillary; (ii) upon application of electrolyte solutions in the basic pH range, electroosmosis occurs – the EOF ($v_{EOF} = E \times \mu_{EOF}$) is directed to the cathode of the instrument, i.e., to the capillary tip (nano ES process operated with positive high voltage); (iii) the analytes electrophoretic net mobility $\mu_i^{eff}$ has to be regarded as well; (iv) finally, a mixed sheath flow of $CO_2$ and air is applied at the capillary tip in order to transport droplets of the nano ES process to the nano DMA which may have a small impact ($\Delta p_{sheath}$) on the pressure difference along the capillary. Fig. 1 gives an overview on respective contributions to analyte migration. Assessment of individual velocity contributions allows calculation of the overall time needed for analytes to pass through the GEMMA setup. The time needed for the analyte to pass through the nano DMA and to reach the CPC unit of the instrument is neglected as it is constant for all presented experiments. In doing so, the influence of $\Delta p_{psid}$ and $\Delta p_{sheath}$ on migration time of analytes can be calculated using Hagen–Poiseuille equation (capillary inner diameter, ID, $d$, 25 μm; in simplification the dynamic viscosity value of water, $\eta$, 1.002 mPa s, at 20 °C is used; length of capillary, $L$, 26 cm). The total movement of the analyte can be calculated with the following equation:

$$v = \frac{d^2 \times \left(\Delta p_{psid} + \Delta p_{sheath}\right)}{32 \times \eta \times L} + E \times \left(\mu_{EOF} - \mu_i^{eff}\right) \quad (1)$$

Calculated results for $\Delta p_{psid}$ are shown in Fig. 2(A); upon reduction of the applied pressure to the sample chamber, the time needed for analytes to pass through the nano ES capillary of the instrument is increased significantly.

Initially, $\Delta p_{sheath}$ was determined by measuring the time needed for water to pass an empty capillary by application of only this force at 2 Lpm. However, after 80 min still no solvent passing through the capillary was detected. Upon application of Hagen–Poiseuille equation the pressure difference to move the solvent through the capillary in 80 min was calculated. It was kept in mind that the time needed to fill an air filled capillary is only half the time needed to fill a previously solvent filled capillary (viscosity of air was neglected). Consequently, the sheath flow contribution was found to be smaller than 0.05 psid (approximately 3 mbar) and is hence negligible in comparison to $\Delta p_{psid}$.

$\mu_{EOF}$ and $\mu_i^{eff}$ were determined by application of a conventional CE–UV setup. Samples containing 0.5 μmol $L^{-1}$ BSA and IgG, respectively, in 25 mmol $L^{-1}$ ammonium acetate at different pH values were analyzed. $\mu_{EOF}$ and $\mu_i^{eff}$ were calculated according to

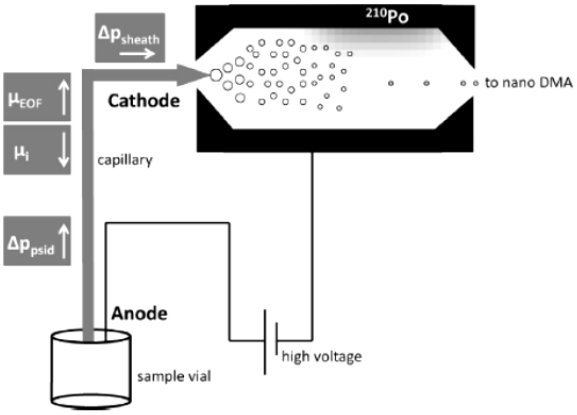


**Fig. 1.** Schematic drawing of the nano ES unit of a GEMMA instrument: a sample vial is placed into the pressure chamber. Pressure and an electric field are applied leading to different forces acting on analyte particles upon sample introduction to the nano ES process. The directions of forces acting on particles in the liquid phase during sample introduction to the nano ES are indicated by arrows.

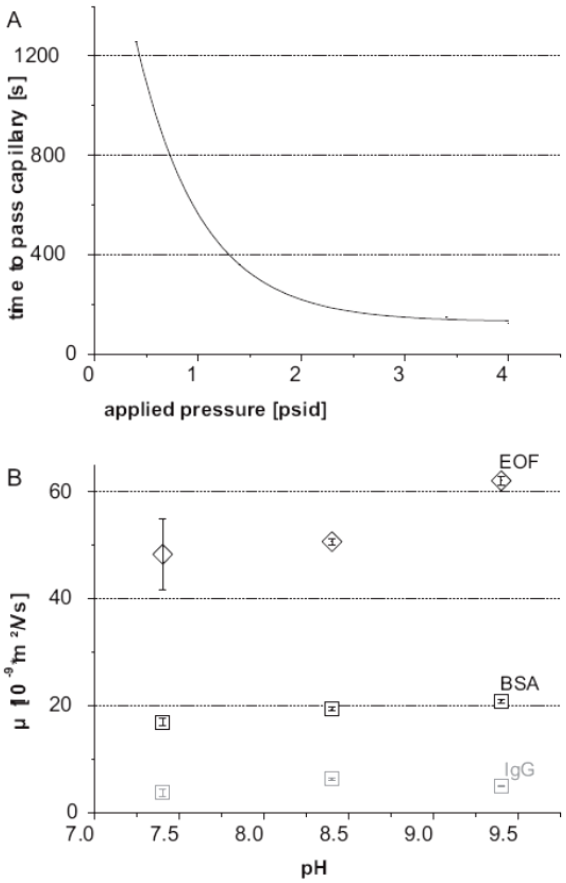


**Fig. 2.** Dependence of analyte migration time through the nano ES capillary on the applied pressure to the sample chamber (A): the migration time of analytes was calculated by Hagen–Poiseuille equation. Electrophoretic net mobilities of analytes under comparable conditions as during the nano ES process (B): the EOF mobility is increasing with increasing pH values, whereas the electrophoretic net mobilities of analytes do not change significantly.

standard protocols from the migration of a neutral marker. Results are shown in Fig. 2(B) (average and standard deviation values for $n = 4$ measurements each are plotted). As expected, increasing pH values of ammonium acetate lead to an increase in the observed EOF, whereas net mobilities of analytes did not change significantly.

For the operation of the nano ES unit, a high electric field strength at the tip of the capillary is necessary to form a stable Taylor cone. This field is produced by a high voltage applied *via* a platin wire immersed in the sample solution and a grounded counter electrode. However, due to this design there is not only a voltage drop between the tip of the capillary and the counter electrode but also along the capillary. The electric field E along the capillary can be calculated as follows:

$$E = \frac{4 \times I}{\kappa \times \pi \times d^2} \quad (2)$$

where $I$ is the electric current measured by the nano ES unit, ID of the capillary, $d$, $2.5 \times 10^{-5}$ m according to the manufacturing company and $\kappa$ is the conductivity of the employed electrolyte solution. For a 25 mmol $L^{-1}$ ammonium acetate solution at pH 9.4, $\kappa$ was calculated to be 0.259 S $m^{-1}$. As during the nano ES process an average current of 400 nA (see also experimental section) was recorded, $E$ could be assessed in the range of 3.1 kV $m^{-1}$. This is in the same order of magnitude as $E$ values typically employed for CE separations on standard instruments.

Initial CE experiments were carried out at pH 7.4, 8.4, and 9.4, respectively. However, stable electrophoresis conditions were found only at slightly basic pH values; therefore, pH 9.4 was further applied for the GEMMA experiments. For this pH value, the time needed for BSA and IgG to migrate across the capillary considering $\Delta p_{psid}$, $\mu_{EOF}$, $\mu_i^{eff}$ was calculated as detailed above. The estimated time to pass the capillary was about 370 s for IgG and about 400 s for BSA ($\Delta p = 1$ psid, $E = 3.1$ kV $m^{-1}$). The difference of migration times can be explained by different mobilities of respective proteins upon electrophoresis. Fig. 3 depicts corresponding spectra obtained in FM. The different time needed to pass a capillary for BSA (black) and IgG (grey) is clearly demonstrated. The migration time of IgG is about 30 s less than the migration time of BSA confirming theoretical calculations. However, it must be noted that the theoretically estimated migration times of analytes were approximately 80 s higher than measured values. A possible explanation for this observation might be found in uncertainties of the inner diameter of the used capillaries as well as in the pressure gauge of the instrument which is not designed for pressure determination with high precision. Differences between calculated and observed migration times can result from actual pressure values slightly deviating from read out values given by the instrument.

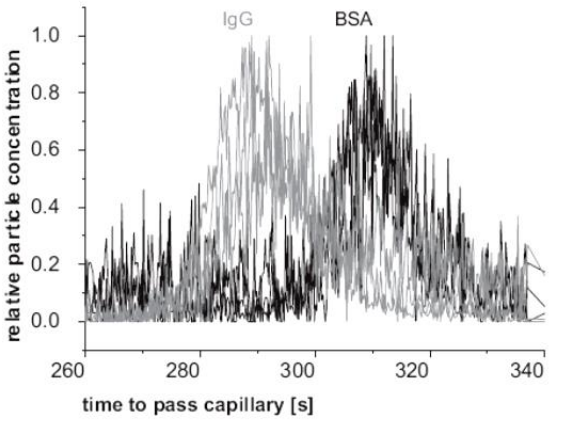


**Fig. 4.** Analyte migration through the capillary in CM: BSA (black) and IgG (grey) samples were investigated under conditions as given in Fig. 3. Again, differences in analyte migration are detectable.

### 3.2. Instrumental feasibility

In order to separate analytes electrophoretically in the nano ES capillary of a standard GEMMA instrument we reduced $\Delta p_{psid}$ and $\Delta p_{sheath}$ to lowest possible values. However, initial experiments demonstrated (data not shown) that at least 0.4 psid (approximately 30 mbar) are necessary to transport analytes through the capillary as the signal intensity decreases with decreasing pressure applied to the sample at the capillary inlet. Likewise, if the sheath flow is further reduced, loss of the analyte signal in corresponding spectra is observed. The latter effect is most probably caused by insufficient transport of aerosolized particles from the capillary tip

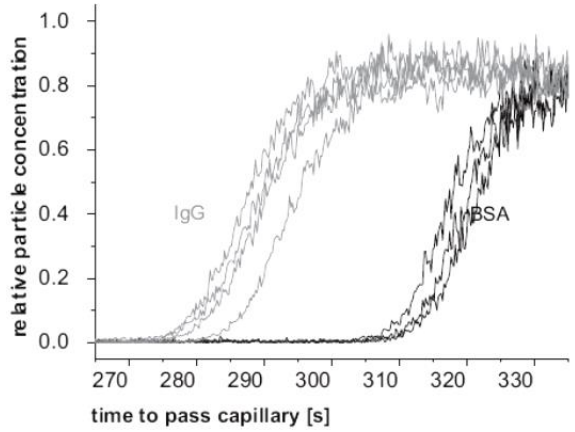


**Fig. 3.** Analyte migration through the nano ES capillary in FM: BSA (black) and IgG (grey) samples ($c = 1$ μmol $L^{-1}$ protein concentration, pH 9.4 ammonium acetate, respectively) were investigated. Measurements were performed at 1 psid (approximately 70 mbar) and 1.1 Lpm sheath flow at the capillary tip. Differences in BSA and IgG migration through the nano ES capillary are clearly detectable.

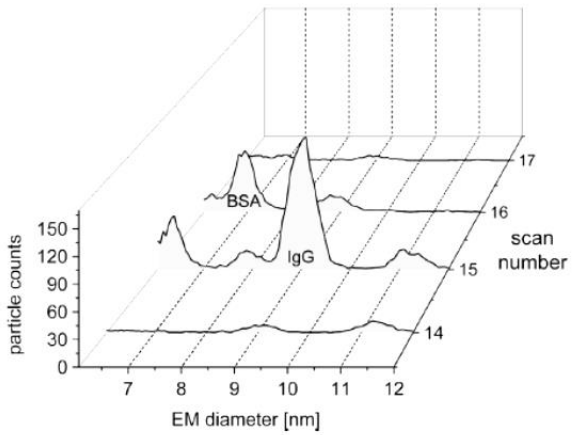


**Fig. 5.** CE separation of BSA and IgG in CM: the sample contained both analytes, BSA and IgG at $c = 1$ μmol $L^{-1}$ protein concentration and pH 9.4 ammonium acetate, respectively. Measurement conditions as in Fig. 3, median values from 6 individual measurements are shown. The IgG peak is detected in scan 15, BSA in scan 16. Hence, CE separation of analytes can be demonstrated.

through the nano DMA to the detector unit of the instrument. A threshold of 0.3 Lpm sheath flow was determined.

### 3.3. GEMMA measurements in CE mode

The measurements of BSA and IgG solutions in ammonium acetate in CM were taken to confirm the results described already for FM (one protein per respective sample). The corresponding signals of analytes after injection to the GEMMA instrument are shown in Fig. 4 ($n = 3$ measurements). The difference between the migration time of IgG (grey) and BSA (black) is about 20 s and the peak width for both analytes about 30 s. These results again demonstrate the CE separation potential within the nano ES capillary of the commercial GEMMA instrument.

In a next step we mixed both proteins in a single sample and tried to resolve the two analytes *via* electrophoresis in the liquid phase in CM. Fig. 5 shows consecutive single GEMMA scans demonstrating the separation of the two proteins, BSA and IgG, from such a mixed sample. A peak corresponding to IgG with significant height can be found just in scan 15. BSA is detected only in scan 16. Small traces of IgG can be observed in scans 14 and 16, respectively. This can be explained by a broadly distributed IgG peak resulting from analyte molecules retained on the capillary wall or tip. A corresponding blank (data not shown) only gives a baseline signal. Nevertheless, it can be concluded that analytes injected from a single sample to a commercially available, conventional GEMMA instrument can indeed be separated by CE in the nano ES capillary. A true CE–GEMMA hyphenation is given in CM.

### 3.4. On-line *desalting in the nano ES capillary through electrophoretic analyte separation*

Results from *on-line* desalting in the nano ES capillary of the GEMMA instrument (addition of 5 mmol $L^{-1}$ sodium chloride to a mixed BSA/IgG sample in ammonium acetate) are depicted in Fig. 6, together with results for the same sample obtained in NM. GEMMA experiments in NM exhibit results shown in Fig. 6(A) (for

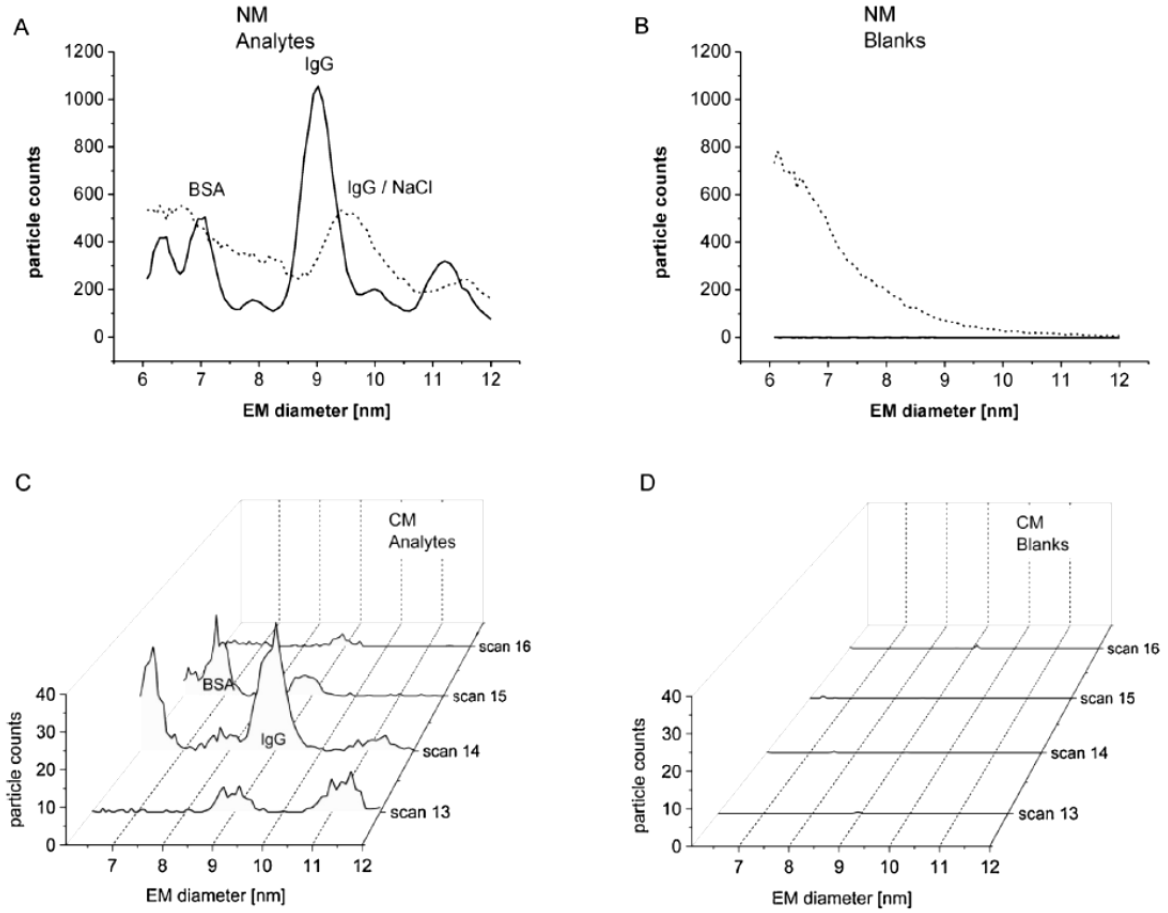


**Fig. 6.** Comparison of the GEMMA spectra obtained for a BSA and IgG containing sample with and without sodium chloride addition in NM and CM: samples containing both analytes, BSA and IgG at $c = 1\ \mu mol\ L^{-1}$ (pH 9.4 ammonium acetate) were measured in NM (A); solid lines represent samples without salt addition, dashed lines depict the samples with sodium chloride addition ($c = 5\ mmol\ L^{-1}$). The salt addition also increases the background signal for a sample containing no protein, i.e., plain ammonium acetate (B). Additionally, BSA can no longer be detected in the presence of sodium chloride, the EM diameter of IgG is shifted to higher values and the width of the IgG peak increases significantly. Samples containing both analytes at $c = 1\ \mu mol\ L^{-1}$ and sodium chloride at $c = 5\ mmol\ L^{-1}$ were measured in CM as well (C) as were buffer blanks (D). The EM diameter of BSA and IgG correlates with the values determined from samples without sodium chloride addition measured in NM (see Fig. 5). Analytes were separated from the contaminating salt. Measurement conditions as in Fig. 3.

samples) and Fig. 6(B) (for blanks), dashed lines, respectively. For comparison reasons also spectra recorded in the absence of sodium chloride (solid lines) are shown. Addition of sodium chloride leads to a massive increase in the background signal (Fig. 6(B)) due to salt aggregation in droplets generated by the nano ES process and their subsequent detection as residue particles. Concurrently, also aggregates between proteins and salt molecules are recorded. Whereas the IgG peak maximum shifts to higher EM diameter values by about 6% due to an unwanted salt crust formation around the protein, BSA can be no longer detected due to the increased background signal. Additionally, the IgG peak also increases in peak width as a result from heterogeneous protein/salt aggregates.

Taken together, these effects demonstrate well aggregation of proteinaceous analytes and sodium chloride for the GEMMA measurements: deposition of non-volatile salts on respective protein surfaces make the protein particles appear larger and more heterogeneous. However, GEMMA spectra in CM (analytes in Fig. 6(C), blanks in Fig. 6(D), respectively) demonstrate the feasibility of *on-line* desalting of samples. In contrast to spectra obtained in NM the EM diameter of BSA is again determined at 7 nm and for IgG at 9 nm. These values are in good accordance with values obtained for measurements of samples without salt addition (compare to Fig. 5). As was shown already in this previous figure, the proteins are again separated from each other.

It should be mentioned that 5 mmol $L^{-1}$ sodium chloride is of course a value far from physiological buffer conditions. However, at the same time this concentration is such that it can be easily obtained *via* dilution of a sample in a volatile electrolyte solution, when analytes were originally dissolved in a physiological buffer. This is even the case for reasonable dilution factors still offering the possibility of analyte detection despite its lower concentration after dilution. Hence, the chosen sodium chloride concentration is an exemplary value, however, with significance for the analysis of future samples.

## 4. Conclusions

With the current work we demonstrate the electrophoretic separation of two proteins within the 26 cm nano ES capillary of a standard GEMMA device based on theoretical considerations describing the contribution of forces acting on analytes. Additionally, we verify our calculations experimentally. We found (i) BSA and IgG, two exemplary analytes, each in a respective sample, to migrate differently through the nano ES capillary and (ii) components of a mixed IgG/BSA sample to be electrophoretically separable prior to electrophoresis in the gas-phase (i.e., nano DMA). In order to obtain these results, the main force transferring samples from the sample vial to the capillary tip, the pressure applied to the pressure chamber for continuous sample introduction to the system, had to be reduced to the lowest acceptable value.

Our results demonstrate that an *on-line* CE–GEMMA (CE–ES–DMA) combination (electrophoresis in the liquid and subsequently in the gas-phase at atmospheric pressure) is even feasible with a commercial GEMMA instrument not intended for electrophoretic applications in the liquid phase. The fact that the instrument is not intended for CE lead to several technical difficulties like for instance unstable pressure settings or unnecessary long detector reset times (3 s). Therefore, at the moment only a rough pre-separation of samples was carried out (which, however, leads already to significantly improved results for the GEMMA measurements) as a kind of feasibility study. We believe that future instrumental advancements (like coupling of an independent commercial CE instrument (which much longer separation capillary) to a GEMMA) will open up new highly interesting avenues in nanoparticle, virus, virus-like particle, recombinant antibody and protein/protein complex/protein assemblies analysis.

Electrophoretic zone separation of sample constituents in the capillary of the nano ES unit furthermore allowed *on-line* desalting of samples. High concentrations of non-volatile sample components (salts, sugars, detergents, etc.) lead to heterogeneous aggregates between these constituents and analytes, which can be concluded from observed higher EM diameters and broader EM diameter distributions. In the worst case an increase in the baseline signal even thwarts the EM diameter determination of analytes. However, electrophoretic separation of these low molecular weight sample contaminations (from e.g. employed physiological buffers) from analyte particles in the liquid phase again allows the EM diameter determination of analytes despite an increased salt concentration. We therefore expand the GEMMA also to the analysis of complex samples or samples with higher salt concentrations, eliminating the impact of undesired components and salts from the GEMMA spectra. A logical continuation of presented work will deal with further CE aspects and their impact on sample introduction to the GEMMA system, for instance the addition of detergents to electrolyte solutions or electrophoretic sample stacking.

## Author contributions

Idea and experimental design by MMD and VUW; experimental work by LK and VUW; guidance by MMD and VUW; physical background and calculations by PK and WWS; idea and supervision, instrumentation and funding by GA; all authors contributed to the manuscript writing.

## Acknowledgement

This project was supported by Austrian Science Foundation (FWF), grant No. TRP29 to WWS and GA.

## References

[1] W.H. De Jong, P.J. Borm, Drug delivery and nanoparticles: applications and hazards, Int. J. Nanomed. 3 (2008) 133–149.
[2] M.A. Maurer-Jones, K.C. Bantz, S.A. Love, B.J. Marquis, C.L. Haynes, Toxicity of therapeutic nanoparticles, Nanomedicine 4 (2009) 219–241.
[3] S.A. Love, M.A. Maurer-Jones, J.W. Thompson, Y.S. Lin, C.L. Haynes, Assessing nanoparticle toxicity, Ann. Rev. Anal. Chem. 5 (2012) 181–205.
[4] M.A. Maurer-Jones, C.L. Haynes, Toward correlation in in vivo and in vitro nanotoxicology studies, J. Law Med. Ethics 40 (2012) 795–801.
[5] F. Jian, Y. Zhang, J. Wang, K. Ba, R. Mao, W. Lai, Y. Lin, Toxicity of biodegradable nanoscale preparations, Curr. Drug Metab. 13 (2012) 440–446.
[6] M.A. Maurer-Jones, I.L. Gunsolus, C.J. Murphy, C.L. Haynes, Toxicity of engineered nanoparticles in the environment, Anal. Chem. 85 (2013) 3036–3049.
[7] K.S. Lin, K. Dehvari, Y.J. Liu, H. Kuo, P.J. Hsu, Synthesis and characterization of porous zero-valent iron nanoparticles for remediation of chromium-contaminated wastewater, J. Nanosci. Nanotechnol. 13 (2013) 2675–2681.
[8] E. Jurneczko, P.E. Barran, How useful is ion mobility mass spectrometry for structural biology? The relationship between protein crystal structures and their collision cross sections in the gas phase, Analyst 136 (2011) 20–28.
[9] S.L. Kaufman, J.W. Skogen, F.D. Dorman, F. Zarrin, K.C. Lewis, Macromolecule analysis based on electrophoretic mobility in air: globular proteins, Anal. Chem. 68 (1996) 1895–1904.
[10] S.L. Kaufman, A.R. Kuchumov, M. Kazakevich, S.N. Vinogradov, Analysis of a 3.6-MDa hexagonal bilayer hemoglobin from Lumbricus terrestris using a gas-phase electrophoretic mobility molecular analyzer, Anal. Biochem. 259 (1998) 195–202.
[11] S.L. Kaufman, Analysis of biomolecules using electrospray and nanoparticle methods: the gas-phase electrophoretic mobility molecular analyzer (GEMMA), J. Aerosol Sci. 29 (1998) 537–552.
[12] G. Bacher, W.W. Szymanski, S.L. Kaufman, P. Zoellner, D. Blaas, G. Allmaier, Charge-reduced nano electrospray ionization combined with differential mobility analysis of peptides, proteins, glycoproteins, noncovalent protein complexes and viruses, J. Mass Spectrom. 36 (2001) 1038–1052.
[13] E.A. Kapellios, S. Karamanou, M.F. Sardis, M. Aivaliotis, A. Economou, S.A. Pergantis, Using nanoelectrospray ion mobility spectrometry (GEMMA) to determine the size and relative molecular mass of proteins and protein assemblies: a comparison with MALLS and QELS, Anal. Bioanal. Chem. 399 (2011) 2421–2433.

[14] C.S. Kaddis, S.H. Lomeli, S. Yin, B. Berhane, M.I. Apostol, V.A. Kickhoefer, L.H. Rome, J.A. Loo, Sizing large proteins and protein complexes by electrospray ionization mass spectrometry and ion mobility, J. Am. Soc. Mass Spectrom. 18 (2007) 1206–1216.
[15] J. Kemptner, M. Marchetti-Deschmann, R. Muller, A. Ivens, P. Turecek, H.P. Schwarz, G. Allmaier, A comparison of nano-electrospray gas-phase electrophoretic mobility macromolecular analysis and matrix-assisted laser desorption/ionization linear time-of-flight mass spectrometry for the characterization of the recombinant coagulation glycoprotein von Willebrand factor, Rapid Commun. Mass Spectrom. 24 (2010) 761–767.
[16] V.U. Weiss, X. Subirats, A. Pickl-Herk, G. Bilek, W. Winkler, M. Kumar, G. Allmaier, D. Blaas, E. Kenndler, Characterization of rhinovirus subviral A particles via capillary electrophoresis, electron microscopy and gas-phase electrophoretic mobility molecular analysis: part I, Electrophoresis 33 (2012) 1833–1841.
[17] P. Kallinger, V.U. Weiss, A. Lehner, G. Allmaier, W.W. Szymanski, Analysis and handling of bio-nanoparticles and environmental nanoparticles using electrostatic aerosol mobility, Particuology 11 (2013) 14–19.
[18] J. Kemptner, M. Marchetti-Deschmann, J. Siekmann, P.L. Turecek, H.P. Schwarz, G. Allmaier, GEMMA and MALDI-TOF MS of reactive PEGs for pharmaceutical applications, J. Pharm. Biomed. Anal. 52 (2010) 432–437.
[19] L. Malm, U. Hellman, G. Larsson, Size determination of hyaluronan using a gas-phase electrophoretic mobility molecular analysis, Glycobiology 22 (2012) 7–11.
[20] J.M. López-Herrera, A.M. Ganán-Calvo, A note on charged capillary jet breakup of conducting liquids: experimental validation of a viscous one-dimensional model, J. Fluid Mech. 501 (2004) 303–326.
[21] N.A. Fuchs, On the stationary charge distribution on aerosol particles in a bipolar ionic atmosphere, Geofis. Pura Appl. 56 (1963) 185–193.
[22] W.A. Hoppel, G.M. Frick, Ion–aerosol attachment coefficients and the steady-state charge distribution on aerosols in a bipolar ion environment, Aerosol Sci. Technol. 5 (1986) 1–21.
[23] R. Flagan, History of electrical aerosol measurements, Aerosol Sci. Technol. 28 (1998) 301–380.
[24] P. Intra, N. Tippayawong, An overview of differential mobility analyzers for size classification of nanometer-sized aerosol particles, Songklanakarin J. Sci. Technol. 30 (2008) 243–256.
[25] J.A. Koropchak, S. Sadain, X. Yang, L.E. Magnusson, M. Heybroek, M. Anisimov, S.L. Kaufman, Nanoparticle detection technology for chemical analysis, Anal. Chem. 71 (1999) 386A–394A.
[26] J.A. Loo, B. Berhane, C.S. Kaddis, K.M. Wooding, Y. Xie, S.L. Kaufman, I.V. Chernushevich, Electrospray ionization mass spectrometry and ion mobility analysis of the 20S proteasome complex, J. Am. Soc. Mass Spectrom. 16 (2005) 998–1008.
[27] G. Allmaier, C. Laschober, W.W. Szymanski, Nano ES GEMMA and PDMA, new tools for the analysis of nanobioparticles–protein complexes, lipoparticles, and viruses, J. Am. Soc. Mass Spectrom. 19 (2008) 1062–1068.
[28] K.D. Cole, L.F. Pease 3rd, D.H. Tsai, T. Singh, S. Lute, K.A. Brorson, L. Wang, Particle concentration measurement of virus samples using electrospray differential mobility analysis and quantitative amino acid analysis, J. Chromatogr. A 1216 (2009) 5715–5722.
[29] L.F. Pease 3rd, D.I. Lipin, D.H. Tsai, M.R. Zachariah, L.H. Lua, M.J. Tarlov, A.P. Middelberg, Quantitative characterization of virus-like particles by asymmetrical flow field flow fractionation, electrospray differential mobility analysis, and transmission electron microscopy, Biotechnol. Bioeng. 102 (2009) 845–855.
[30] M. Havlik, M. Marchetti-Deschmann, G. Friedbacher, P. Messner, W. Winkler, L. Perez-Burgos, C. Tauer, G. Allmaier, Development of a bio-analytical strategy for characterization of vaccine particles combining SEC and nanoES GEMMA, Analyst 139 (2014) 1412–1419.
[31] C. Laschober, J. Wruss, D. Blaas, W.W. Szymanski, G. Allmaier, Gas-phase electrophoretic molecular mobility analysis of size and stoichiometry of complexes of a common cold virus with antibody and soluble receptor molecules, Anal. Chem. 80 (2008) 2261–2264.
[32] D.H. Tsai, L.F. Pease 3rd, R.A. Zangmeister, M.J. Tarlov, M.R. Zachariah, Aggregation kinetics of colloidal particles measured by gas-phase differential mobility analysis, Langmuir 25 (2009) 140–146.
[33] L.F. Pease 3rd, D.H. Tsai, J.L. Hertz, R.A. Zangmeister, M.R. Zachariah, M.J. Tarlov, Packing and size determination of colloidal nanoclusters, Langmuir 26 (2010) 11384–11390.
[34] H. Hinterwirth, S.K. Wiedmer, M. Moilanen, A. Lehner, G. Allmaier, T. Waitz, W. Lindner, M. Laemmerhofer, Comparative method evaluation for size and size-distribution analysis of gold nanoparticles, J. Sep. Sci. 36 (2013) 2952–2961.
[35] V.U. Weiss, A. Lehner, L. Kerul, R. Grombe, M. Kratzmeier, M. Marchetti-Deschmann, G. Allmaier, Characterization of crosslinked gelatin nanoparticles by electrophoretic techniques in the liquid and the gas phase, Electrophoresis 34 (2013) 3267–3276.
[36] L.F. Pease 3rd, D.H. Tsai, J.A. Fagan, B.J. Bauer, R.A. Zangmeister, M.J. Tarlov, M.R. Zachariah, Length distribution of single-walled carbon nanotubes in aqueous suspension measured by electrospray differential mobility analysis, Small 5 (2009) 2894–2901.
[37] A. Jouyban, E. Kenndler, Theoretical and empirical approaches to express the mobility of small ions in capillary electrophoresis, Electrophoresis 27 (2006) 992–1005.
[38] K. Kleparnik, P. Bocek, Theoretical background for clinical and biomedical applications of electromigration techniques, J. Chromatogr. 569 (1991) 3–42.
[39] K.C. Lewis, J.W. Jorgenson, S.L. Kaufman, Capillary zone electrophoresis with electrospray condensation particle counting detection, J. Capillary Electrophor. 3 (1996) 229–235.
[40] T. Ma, Y. Fung, Hyphenating capillary isoelectric focusing with gas-phase electrophoretic mobility molecular analyzer for determination of proteins in human tear fluids, ECS Meeting Abstracts, MA2012-02, 2012, pp. 2773.
[41] S. Pihlasalo, L. Auranen, P. Hanninen, H. Harma, Method for estimation of protein isoelectric point, Anal. Chem. 84 (2012) 8253–8258.

## 3.2 CE-GEMMA measurements with vsvg- and m-Cherry vaults

As GEMMA offers the possibility to detect, quantify and characterize nanoparticles up to the size of several 100 nm (actual values are depending on the applied DMA), it is perfectly fitted to analyze larger protein assemblies. In the case of my analyses, ribonucleoproteins forming nanoobjects so-called vaults, which may be potentially used as drug delivery nanodevices and are thus of great biotechnological interest, were investigated. To date there is only limited information on such nanobioparticles, especially on their ability to deliver drugs to infected cells.

My research work included setup of the GEMMA instrument, checking of the instrument with BSA and IgG, analysis of protein complexes, sample preparation and isolation concerning ribonucleoprotein vaults as well as the analysis of vaults in NM and CM. Measurements were done at the Department of Chemistry and Biochemistry, UCLA in the research group of Prof. Joseph Loo.

### 3.2.1 Instrumentation

The GEMMA system used at UCLA consisted of (i) a nano ES unit including a $^{210}$Po source (model 3480), (ii) a nano differential mobility analyzer (nano DMA, series 3080) including a nano DMA and (iii) ultrafine condensation particle counter (CPC, series 3025A). Samples were introduced to the nano ES via a 25 µm inner diameter cone tipped fused silica capillary. All parts were from TSI Inc (Shoreview, MN, USA). Since the experiments done in CM do not follow the standard procedure of GEMMA (= NM) the results were not normalized to dw/dlogDp units but they are evaluated directly in raw counts. The measurements in NM are evaluated in dw/dlogDp. Further measurement conditions are given with individual figures.

### 3.2.2 Chemicals

Following chemicals were used for experiments discussed in 3.2:

| Chemical | Product No. | Company |
|---|---|---|
| Albumine Bovine (BSA) | A-0281 | Sigma (St.Louis, MO, USA) |
| Albumine from chicken | A-2512 | Sigma (St.Louis, MO, USA) |
| Ammonium Acetate | 0011155B | Merck (Darmstadt, Germany) |
| Ammonium Hydroxide | AX1303-6 | EMD Millipore (Billerica, MA, USA) |
| apo Transferrin | T-1428 | Sigma (St.Louis, MO, USA) |
| Methanol | 67-56-1 | Sigma (St.Louis, MO, USA) |

### 3.2.3 Samples

The analyzed sample stock solutions are given below:

| Sample | Concentration | Buffer, concentration |
|---|---|---|
| BSA | 1 µM | $NH_4OAc$ (20 mM, pH 7.4) |
| Didemnin B | 9 mM | $NH_4OAc$ (20 mM, pH 7.4) |
| Hemoglobin | 40 µM | $NH_4OAc$ (20 mM, pH 7.4) |
| Mmm1-D5-Fusion Complex | 70 µM | $NH_4OAc$ (20 mM, pH 7.4) |
| N2N3 Receptor | 40 µM | $NH_4OAc$ (20 mM, pH 7.4) |
| Ovalbumin | 1 µM | $NH_4OAc$ (20 mM, pH 7.4) |
| apo Transferrin | 1 µM | $NH_4OAc$ (20 mM, pH 7.4) |
| TriC | 5.5 µM | $NH_4OAc$ (20 mM, pH 7.4) |
| m-Cherry Vaults | 40%, Interphase 40% - 45%, 45% phases from Sucrose Gradient | MES (50 mM, pH 6.5) |

| | | |
|---|---|---|
| mix | 40%, Interphase 40% - 45%, 45%, 50% phases from Sucrose Gradient | MES (50 mM, pH 6.5) |

### 3.2.4 Sample preparation

Volatility of buffer is important for the formation of single charged analyte particles for GEMMA analysis. Therefore, $NH_4OAc$ was employed as electrolyte solution and it was necessary to exchange the buffer of vault stock solutions by Microcon desalting. The stock solutions of other analytes were simply diluted with $NH_4OAc$ (pH = 7.4) to concentration appropriate for GEMMA analysis (usually ~1 µM, for the exact concentration see respective figure description). The final volume of analyte solutions needed for measurements was 20 µL.

For vault samples, Microcon desalting was necessary prior GEMMA analysis. Vault molecules were generated in sf9 recombinant baculovirus cells. The recombinant baculovirus cells contained rat major vault protein (MVP) and m-Cherry protein. The whole procedure is described in [26].

Samples were obtained from Jan Mrazek (Rome Group, UCLA). The concentration of vsvg is expected to be 10 times higher than the concentration of m-Cherry because of different expression levels in cells. Vsvg and m-Cherry were finally separated from other sample components using sucrose density gradient centrifugation (stepwise gradient). The samples from 40%, Interphase 40% - 45%, 45% and 50% [w/w] sucrose were used for further GEMMA measurements. To purify the vaults from ill soluble components of these fractions centrifugation at 20 000 g followed the initial gradient purification. 30 µL from the supernatant and 470 µL of ammonium acetate were pipetted on the Microcon YM 30 centrifugal tubes to change the sample buffer to ammonium acetate. The solution was centrifuged at 10 000 g for 10 minutes. The filtrate was removed and 370µL $NH_4OAc$ was added to the solution on the filter. The whole process was repeated three times. The retentate (vault solution) on the upper part of Microcon tube was analyzed via GEMMA.

### 3.2.5 Checking instrument setup with standard proteins in NM

After the change of the $^{210}$Po-source and the restart of the GEMMA at UCLA, Transferrin (as a protein standard) was measured to check the instrument performance. The results are depicted in Figure 3.1.

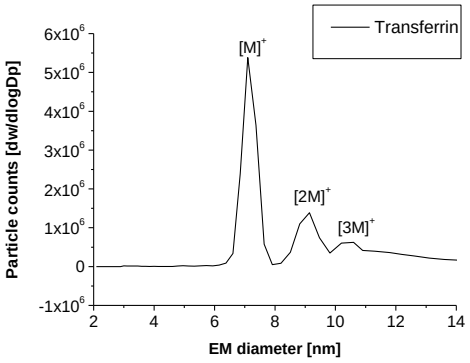


**Figure 3.1: GEMMA spectrum of Transferrin**

| | | |
|---|---|---|
| Electrolyte: 20 mM $NH_4OAc$, pH 7.4 | Voltage: 1.7 kV | Sheath flow: 15 lpm |
| Sample: Transferrin | Current: 300 – 400 nA | Pressure: 4 psid |
| Concentration: 1 µM | $CO_2$: 0.1 lpm | Median of 6 spectra |
| Capillary: 25 µm id | Air: 2 lpm | mode: NM |

The results of Transferrin measurements via GEMMA are characteristic for the instrument: a single charged monomer peak (at 7.1 nm) can be found. Also dimer and oligomer peaks with higher EM diameter can be recognized. Nevertheless the monomer peak exhibits the highest signal. Therefore, the instrument at UCLA seems to be in good shape.

In the next step Ovalbumin and BSA were measured to compare the GEMMA spectra obtained from the instrument at UCLA and TUVIE. Ovalbumin and BSA are suitable analytes for GEMMA, their analysis was already successful performed [10]. The spectra of Ovalbumin as well as BSA (Figure 3.2) measured at UCLA and TUVIE depicting absolute and relative values are shown on the following page.

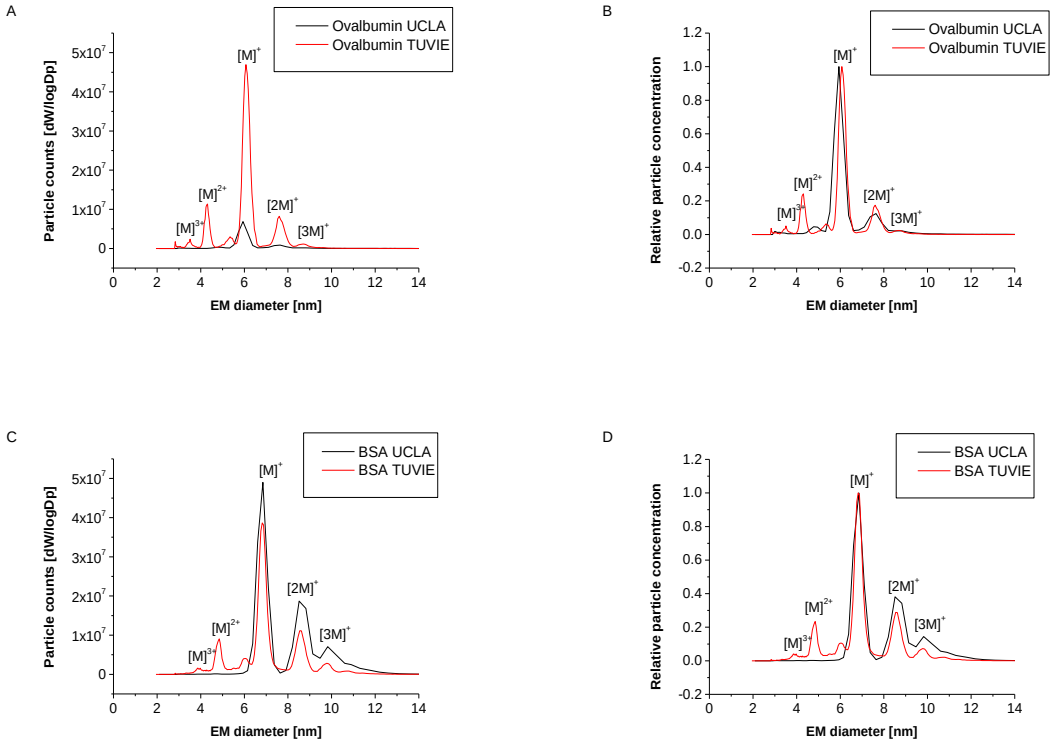


**Figure 3.2: Comparison of GEMMA spectra obtained at UCLA and TUVIE for Ovalbumin (A,B) and BSA (C,D). Absolute (A,C) and relative (B,D) values are plotted**

| | | |
|---|---|---|
| Electrolyte: 20 mM $NH_4OAc$, pH 7.4 | Voltage: 1.7 kV – 2.7 kV | Sheath flow: 15 lpm |
| Sample: BSA, Ovalbumin | Current: 300 – 400 nA | Pressure: 3 - 4 psid |
| Concentration: 1 µM | $CO_2$: 0.1 lpm | Median of 6 spectra |
| Capillary: 25 µm id | Air: 1 -2 lpm | mode: NM |

The EM diameter of analytes was determined at the peak apex: for Ovalbumin 6.0 nm EM diameter (EM diameter in literature at 6.3 nm [10]) and for BSA 6.9 nm EM diameter was determined (EM diameter in literature at 7.1nm:[10]). Small deviations between instruments are common as usually no calibration is carried out between instruments.

There is a difference in the double charged monomer peak of Ovalbumin (~4.2 nm) and BSA (~4.9 nm) in spectra obtained at TUVIE and UCLA: There is no visible double charged monomer peak in the GEMMA spectra from UCLA the reason being that the $^{210}$Po-Source in the instrument at UCLA was installed just a few days before the measurements were taken (the $^{210}$Po-source at TUVIE on the other hand exceeded already several half-lives). Hence, a more efficient charge reduction occurred in the UCLA instrument. The other peaks

show accordance in the EM diameter values, in the case of BSA even the particle counts are comparable.

### 3.2.6 Standard GEMMA measurements: Hemoglobin – N2N3 Receptor Complex

Hemoglobin belongs to class of conjugated proteins – hem-proteins that possess iron-porphyrin prosthetic groups united with protein [27]. Hemoglobin transports oxygen in red blood cells of all vertebrates except of fish family fish family Channichthyidae [28]. *S. aureus* acquires heme-iron from human hemoglobin (molecular weight 64.7 kDa, consisting of two subunits alpha and two subunits beta as well as four hem units with iron, see the amino acid sequence in 5.2) using the N2N3 receptor (molecular weight 38.8 kDa, see the amino acid sequence in 5.2) [29]. In previous experiments (not published yet) was shown that Hemoglobin and N2N3 form complex in molar ratio 1:1 or 1:2 at higher receptor concentrations. To observe if the complex of Hemoglobin and N2N3 is also formed *in vitro*, GEMMA analysis were carried out. Results are shown in Figures 3.3 – 3.9.

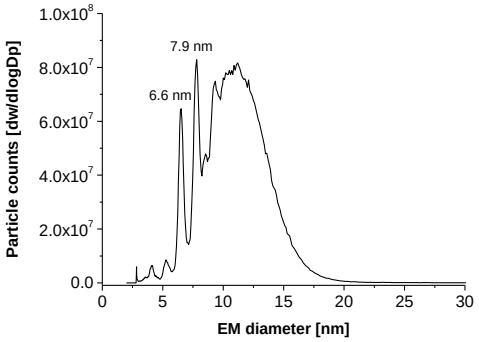


**Figure 3.3: GEMMA spectra for Hemoglobin (16 µM) and N2N3 Receptor (4 µM)**

| | | |
|---|---|---|
| Electrolyte: 20 mM $NH_4OAc$, pH 7.4 | Voltage: 2.1 kV | Sheath flow: 15 lpm |
| Sample: Hemoglobin & N2N3 Receptor | Current: 300 nA | Pressure: 4.5 psid |
| Concentration: Hem 16 µM, N2N3 4 µM | $CO_2$: 0.1 lpm | Median of 6 spectra |

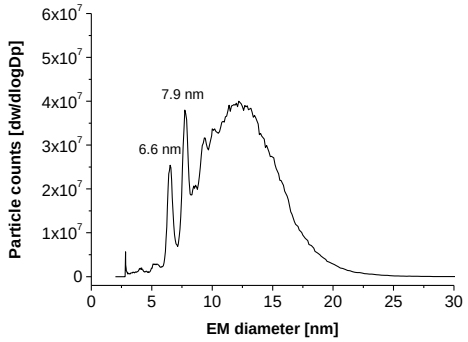


**Figure 3.4: GEMMA spectra for Hemoglobin (8 µM) and N2N3 Receptor (2 µM)**

| | | |
|---|---|---|
| Electrolyte: 20 mM $NH_4OAc$, pH 7.4 | Voltage: 2.6 kV | Sheath flow: 15 lpm |
| Sample: Hemoglobin & N2N3 Receptor | Current: 130 nA | Pressure: 5 psid |
| Concentration: Hem 8 µM, N2N3 2 µM | $CO_2$: 0.1 lpm | Median of 6 spectra |
| Capillary: 25 µm id | Air: 1 lpm | mode: NM |

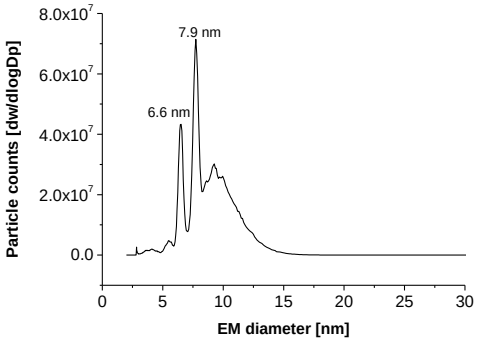


**Figure 3.5: GEMMA spectra for Hemoglobin (4 µM) and N2N3 Receptor (1 µM)**

| | | |
|---|---|---|
| Electrolyte: 20 mM $NH_4OAc$, pH 7.4 | Voltage: 1.8 kV | Sheath flow: 15 lpm |
| Sample: Hemoglobin & N2N3 Receptor | Current: 300 nA | Pressure: 4 psid |
| Concentration: Hem 4 µM, N2N3 1 µM | $CO_2$: 0.1 lpm | Median of 6 spectra |

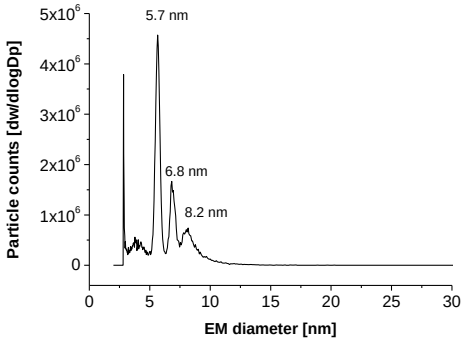


**Figure 3.6: GEMMA spectra for Hemoglobin (0.4 µM) and N2N3 Receptor (0.1µM)**

| | | |
|---|---|---|
| Electrolyte: 20 mM $NH_4OAc$, pH 7.4 | Voltage: 1.9 kV | Sheath flow: 15 lpm |
| Sample: Hemoglobin & N2N3 Receptor | Current: 300 nA | Pressure: 4 psid |
| Concentration: Hem 0.4 µM,N2N3 0.1 µM | $CO_2$: 0.1 lpm | Median of 6 spectra |
| Capillary: 25 µm id | Air: 1 lpm | mode: NM |

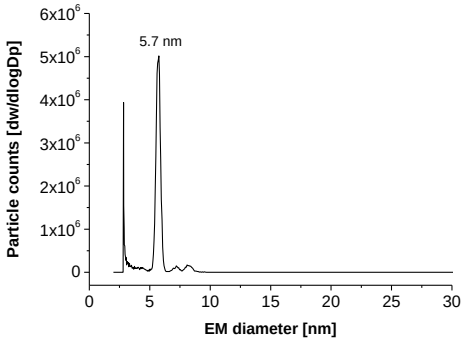


**Figure 3.7: GEMMA spectra for Hemoglobin (0.4 µM) and N2N3 Receptor (0.2 µM)**

| | | |
|---|---|---|
| Electrolyte: 20 mM $NH_4OAc$, pH 7.4 | Voltage: 1.9 kV | Sheath flow: 15 lpm |
| Sample: Hemoglobin & N2N3 Receptor | Current: 300 nA | Pressure: 4 psid |
| Concentration: Hem 0.4 µM,N2N3 0.2 µM | $CO_2$: 0.1 lpm | Median of 6 spectra |
| Capillary: 25 µm id | Air: 1 lpm | mode: NM |

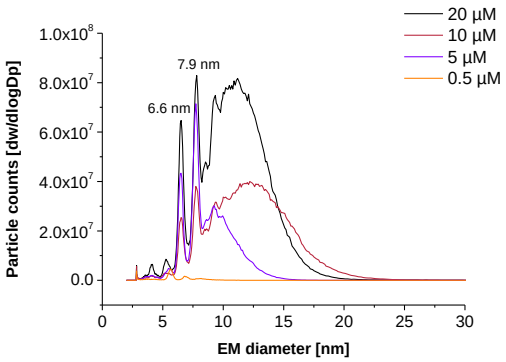


**Figure 3.8: Comparison of GEMMA spectra for Hemoglobin (16 µM, 8 µM, 4 µM and 0.4 µM) and N2N3 Receptor (4 µM, 2 µM, 1 µM, 0.1 µM)**

| | | |
|---|---|---|
| Electrolyte: 20 mM $NH_4OAc$, pH 7.4 | Voltage: 1.9 kV | Sheath flow: 15 lpm |
| Sample: Hemoglobin & N2N3 Receptor | Current: 300 nA | Pressure: 4 psid |
| Concentration: molar ratio of Hemoglobin and Receptor = 4:1, sum of concentration is given in the legend | $CO_2$: 0.1 lpm | Median of 6 spectra |
| Capillary: 25 µm id | Air: 1 lpm | mode: NM |

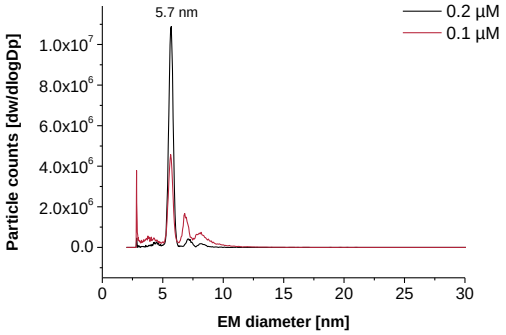


**Figure 3.9: Comparison of GEMMA spectra for Hemoglobin and N2N3 Receptor**

| | | |
|---|---|---|
| Electrolyte: 20 mM $NH_4OAc$, pH 7.4 | Voltage: 1.9 kV | Sheath flow: 15 lpm |
| Sample: Hemoglobin & N2N3 Receptor | Current: 300 nA | Pressure: 4 psid |
| Concentration: Hemoglobin: 0.4 µM, Receptor 0.2 µM (blue), 0.1 µM (red) | $CO_2$: 0.1 lpm | Median of 6 spectra |
| Capillary: 25 µm id | Air: 1 lpm | mode: NM |

At concentrations lower than 1µM the receptor peak can be recognized at 5.7 nm corresponding to approx. 34 kDa (according to the regression curve presented in [10]). For instance, in Figure 3.7 the receptor peak is significant bigger than other peaks. The determined molecular weight value is in good accordance with the value given in literature describing N2N3 Receptor at 39 kDa [29]. There are many aggregates formed at higher concentrations (Figures 3.3 - 3.5 and 3.8) detected at 11 – 13 nm. Hemoglobin tetramer

(monomer 16.2 kDa, tetramer 64.7 kDa, according to [30]) is detected at 6.6 nm (EM diameter in literature at 6.9 nm [10]) in samples with concentration of Hemoglobin higher than 0.4 µM. In Figures 3.3 - 3.5 and 3.8 a peak at 7.9 nm is detected that may correspond to Hemoglobin - N2N3 complex formed of Hemoglobin tetramer and one N2N3 molecule (corresponds to approx. 89 kDa according to [10]). The Hemoglobin - N2N3 complex was detected in samples with concentration of Hemoglobin higher than 0.4 µM. However many unspecific aggregates can be seen in these samples as well. There were no dilutions of these samples analyzed by GEMMA allowing a better understanding of the aggregate formation.

### 3.2.7 Standard GEMMA measurements: Mmm1-D5-Fusion Complex

Mmm1 protein is a molecular tether between endoplasmic reticulum and mitochondria in eukaryotic cells. In previous experiments (not published yet) it was shown that Mmm1 and D5 form a complex in molar ratio 1:1. The stability of the Mmm1-D5-Fusion Complex (molecular weight 31.2 kDa, see the amino acid sequence in 5.2) in solutions containing up to 30% v/v MeOH was investigated as necessary prerequisite for future ESI MS work. The results are depicted in Figure 3.10A (absolute values) and 3.10B (relative values).

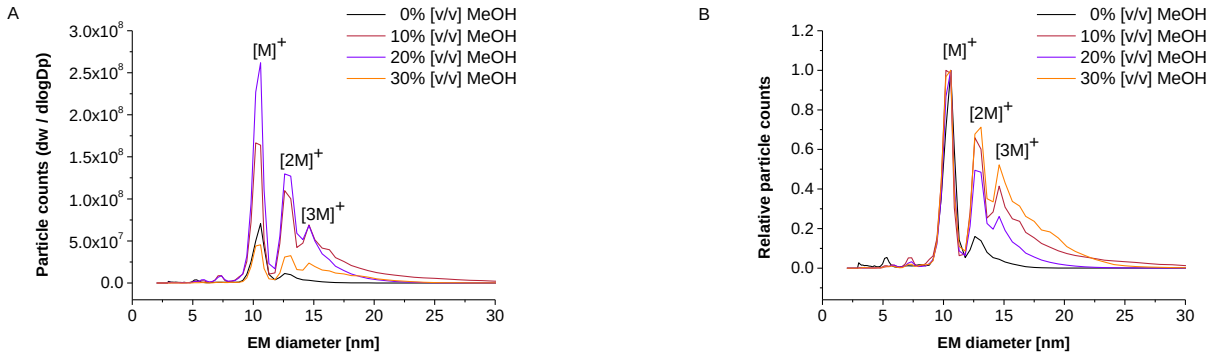


**Figure 3.10: Stability of mmm1-D5-Fusion Complex depending on the MeOH content, GEMMA spectra depicted as absolute (A) or as relative particle counts (B)**

| | | |
|---|---|---|
| Electrolyte: 20 mM $NH_4OAc$, pH 7.4 | Voltage: 1.8 - 2 kV | Sheath flow: 15 lpm |
| Sample: mmm1-D5-Fusion Complex & Methanol | Current: 100 - 300 nA | Pressure: 4 - 5 psid |
| Concentration: Fusion Complex, c = 7µM (0% v/v MeOH), c = 12µM (10%, 20%, 30% v/v MeOH) | $CO_2$: 0.1 lpm | Median of 6 spectra |
| Capillary: 25 µm id | Air: 1 lpm | mode: NM |

In Figure 3.10 the single charged monomer peak at 11 nm can be recognized. There is also a single charged dimer peak at 13 nm present in all GEMMA spectra. The lower absolute analyte signal in the sample without any MeOH addition is due to a lower concentration of the Mmm1-D5-Fusion Complex (7µM) relative to samples with the higher MeOH concentration (12µM). The complex can be detected in samples at all MeOH concentrations, its EM diameter is constant, its counts are increasing until 20% v/v MeOH, then a signal decline can be observed.

### 3.2.8 Standard GEMMA measurements: TriC

TriC is a chaperonin that uses ATP cycling to facilitate folding of approximately 10% of the eukaryotic proteome. TriC consists of two stacked rings of eight paralogous subunits each. ([31]) The GEMMA analysis of TriC (919.2 kDa, see the amino acid sequence of TriC subunits in 5.2) was performed. Additionally, the drug DB (Didemnin B, 1112 Da) was added to the solution to determine the binding of DB to TriC complex. It is expected that TriC and DB form a complex in molar ratio 1:1. The resulting GEMMA spectra are shown in Figures 3.11 – 3.13:

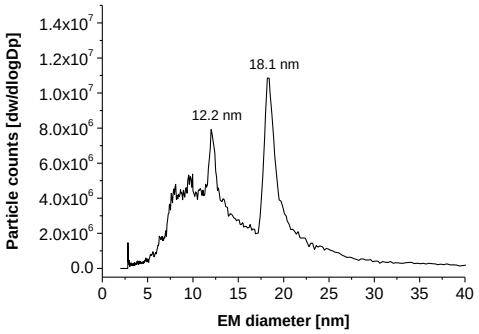


**Figure 3.11: GEMMA spectra of TriC**

| | | |
|---|---|---|
| Electrolyte: 20 mM $NH_4OAc$, pH 7.4 | Voltage: 1.7 kV | Sheath flow: 15 lpm |
| Sample: TriC | Current: 700 nA | Pressure: 4 psid |
| Concentration: 1 µM | $CO_2$: 0.1 lpm | Median of 6 spectra |
| Capillary: 25 µm id | Air: 1 lpm | mode: NM |

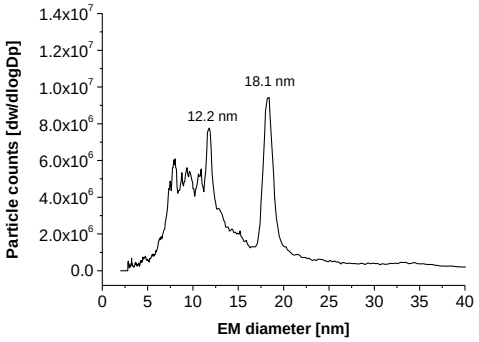


**Figure 3.12: GEMMA spectra of TriC and DB**

| | | |
|---|---|---|
| Electrolyte: 20 mM $NH_4OAc$, pH 7.4 | Voltage: 1.7 kV | Sheath flow: 15 lpm |
| Sample: TriC & DB | Current: 700 nA | Pressure: 4 psid |
| Concentration: TriC 1 µM, DB 90 µM | $CO_2$: 0.1 lpm | Median of 6 spectra |
| Capillary: 25 µm id | Air: 1 lpm | mode: NM |

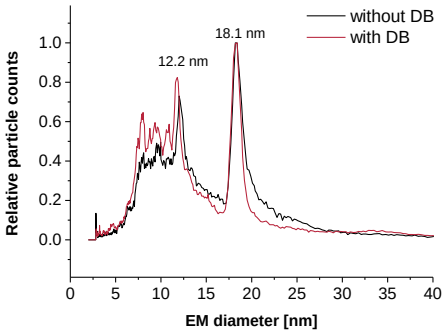


**Figure 3.13: Comparison of GEMMA spectra of TriC with and without DB, relative values**

| | | |
|---|---|---|
| Electrolyte: 20 mM $NH_4OAc$, pH 7.4 | Voltage: 1.7 kV | Sheath flow: 15 lpm |
| Sample: TriC & DB | Current: 700 nA | Pressure: 4 psid |
| Concentration: TriC 1 µM, (without DB: red) DB 90 µM (with DB: blue) | $CO_2$: 0.1 lpm | Median of 6 spectra |
| Capillary: 25 µm id | Air: 1 lpm | mode: NM |

There are 2 peaks detected in the GEMMA spectrum of TriC (Figure 3.11): a molecule fragment at 12.2 nm ~ 329 kDa (consistent with previous MS measurements, molecular weight of the fragment was calculated with [10]) and the molecular peak at 18.1 nm ~1.1 MDa (calculated with [10]). In Figure 3.12 binding of DB to TriC was not seen, there is no change in the GEMMA spectrum. The problem is the low molecular weight of DB (~1 kDa) relative to TriC (~1 MDa). The binding of one DB molecule to TriC would not change the molecular

weight of the complex significantly. Additionally, the binding mechanism of DB on TriC (whether surface binding or binding to the bulk) is unknown. However, the site of drug binding influences the EM diameter change as well. Therefore, the analysis of complex formation cannot be performed with the current GEMMA setup due to limitations in resolving power.

### 3.2.9 Standard GEMMA measurements: Vaults, samples stored in solution for two months

Vaults are the largest known ribonucleoid particles found in eukaryotic cells so far. The dimensions of vaults are 40 × 40 × 70 nm [25] forming a barrel-shaped hollow particle [19]. The molecular weight of vaults from rat liver was estimated to be 12.9 MDa ± 0.1 MDa. (examined by scanning transmission electron microscopy) [20] . *In vivo*, vaults are composed of 3 kinds of proteins: a major vault protein (MVP), Vault Poly (ADP-Ribose) Polymerase **(**VPARP) and Telomerase/Vault-Associated Protein (TEP1) [32]. Lately, the expression of recombinant vaults using MVP with additional amino acids fused at the N- and C-termini was carried out. Recombinant vault particles can be assembled from expression of either MVP alone, or from MVP with one or two of other small vault proteins [33]. Vaults can be expressed by a baculovirus expression system and heterologous proteins (e.g. fluorescent proteins, enzymes, proteinaceous drugs) can be encapsulated inside of these recombinant particles using a protein-targeting domain termed INT for vault INTeraction [21].

The fusion of membrane lytic peptide derived from adenovirus protein VI (pVI) to the N-terminus of the major vault protein led to directed targeting and better delivery of vaults to the cytoplasm[22]. It was also shown that vaults can collapse at the particle waist and reassemble back into whole vaults (half-vault/vault equilibrium) [34] [35]. The vault structure is an opened system that allows the incorporation of the VPARP and TEP1 proteins into the vault interior due to half-vault/vault equilibrium [34a]. In this work, the analysis of vsvg and m-Cherry expressed in one system was carried out with GEMMA. The expression process of vaults is examined. Without mixing MVPs, the assembly of vaults may be conducted by a ribosomal complex or a similar cellular mechanism. However, if mixing occurs, vault formation might be a spontaneous process in the cytosol. Therefore, it was supposed that GEMMA results would lead to a better understanding of assembly of large ribonucleoid

particles. Upon detection of 2 separate peaks two vault species are formed. Vaults are formed immediately after expression of respective MVP building blocks, no mixing of building blocks occurs.

The EM diameter of m-Cherry- (10 MDa – 12 MDa) and vsvg- (8 MDa – 9MDa) vaults was determined in this work using regression curve for monomers from [10] ($y = -4.287 + 2.225 * x - 0.348 * x^2 + 0.197 * x^3$, y stands for molecular weight and x for EM diameter), EM diameter for m-Cherry vaults was estimated in range 38 nm – 40 nm and for vsvg vaults in range 35 nm – 36 nm.

The distance of channels in the given GEMMA instrument in that EM diameter range is about 1.1 – 1.5 nm, which makes the recognition of m-Cherry and vsvg peaks difficult.

To determine the EM diameter of vsvg- and mCherry vaults mix samples (sample preparation described in 3.2.4) were analyzed in NM of GEMMA. For the very first analysis attempt, mix samples were measured after being stored for 2 months at 4°C. Further experiments were carried out with fresh vault samples. First results are depicted in Figure 3.14. The absolute values are depicted in Figure 3.14A, the relative values in Figure 3.14B.

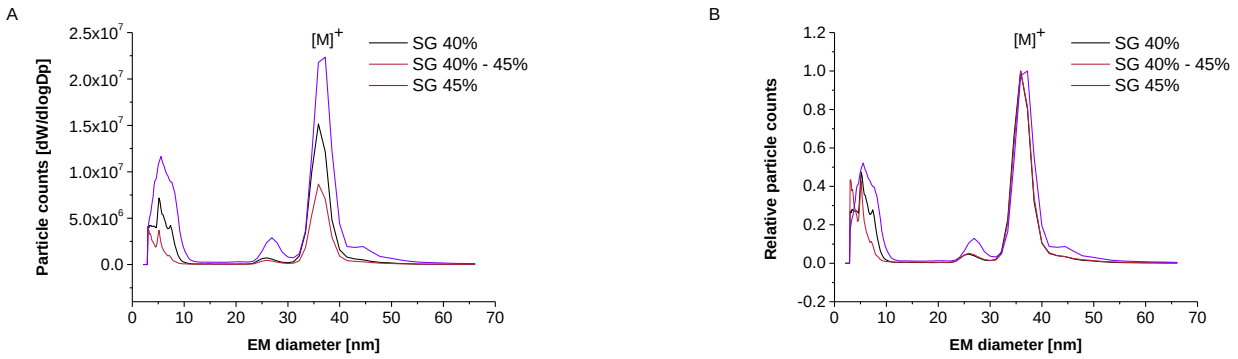


**Figure 3.14: GEMMA spectra of mix from 40% [w/w] (black), 40% - 45% [w/w] (Interphase) (red), 45% [w/w] (purple) analyte concentration of sucrose gradient, A depicted as absolute particle counts, B depicted as relative particle counts**

| | | |
|---|---|---|
| Electrolyte: 20 mM $NH_4OAc$, pH 7.4 | Voltage: 1.9 kV | Sheath flow: 15 lpm |
| Sample: mix: 40% (black), Interphase 40% - 45% (red), 45% (purple) phase of sucrose gradient | Current: 300 nA | Pressure: 4 psid |
| Concentration: not diluted | $CO_2$: 0.1 lpm | Median of 6 spectra |
| Capillary: 25 µm id | Air: 2 lpm | mode: NM |

From Figure 3.14 EM diameters of mix components can be determined. The EM diameter of the main peak of samples 2 (40 w/w% sucrose) and 3 (40 - 45 w/w% sucrose) is at 35.9 nm, for sample 4 (45 w/w% sucrose) the determined EM diameter is at 37.2 nm. There can be just one main peak recognized in the GEMMA spectra, the difference in EM diameter of vsvg and m-Cherry might be too small for GEMMA analysis. A peak around 26 nm EM diameter and detected with a relative low particle count number was suggested to result from a vault artifact with about a half molecular weight of vault.

### 3.2.10 Standard GEMMA measurements: Vaults, diluted samples

In order to exclude analyte concentration dependent artifacts during GEMMA measurements, a mix sample was diluted 1:10 with ammonium acetate to observe changes in GEMMA spectra in accordance to the vault concentration. Results are shown in Figure 3.15.

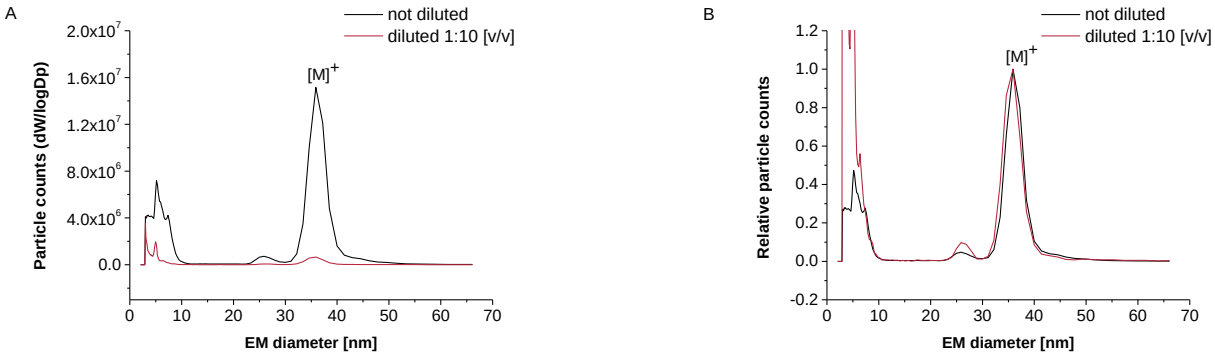


**Figure 3.15: Comparison of GEMMA spectra of mix obtained from 40% [w/w] analyte concentration phases of sucrose gradient, A depicted as absolute particle counts, B depicted as relative particle counts**

| | | |
|---|---|---|
| Electrolyte: 20 mM $NH_4OAc$, pH 7.4 | Voltage: 2.1 kV | Sheath flow: 15 lpm |
| Sample: mix: 40% phase of sucrose gradient | Current: 300 nA | Pressure: 4 psid |
| Concentration: not diluted (black), diluted 1:10 (red) | $CO_2$: 0.1 lpm | Median of 6 spectra |
| Capillary: 25 µm id | Air: 1 lpm | mode: NM |

The peak signal of vaults particle decreased significantly with dilution, the signal of particles with EM diameter under 10 nm that also include buffer molecules increased relative to the vault peak. Additionally, no changes in EM diameter for vault particles were detected.

However, a slight increase of the relative intensity of vault artifacts (at 26 nm EM diameter) could be seen possibly due to lower analyte stability in buffers of lower ionic strength.

### 3.2.11 Standard GEMMA measurements: Vaults, stability at – 20°C

Further measurements were performed with mix. To observe the stability of the vault particles a sample aliquot of sample 3 (40 - 45 w/w% sucrose) was frozen to -20°C for 48 hours. The results are depicted in Figure 3.16.

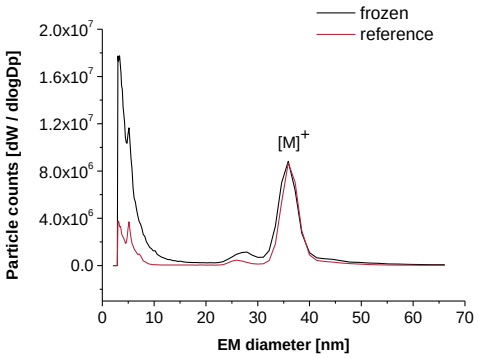


**Figure 3.16: Comparison of GEMMA spectra of mix obtained from 40% - 45% [w/w] analyte concentration of sucrose gradient before and after storage at -20°C (48 hours)**

| | | |
|---|---|---|
| Electrolyte: 20 mM $NH_4OAc$, pH 7.4 | Voltage: 1.9 kV | Sheath flow: 15 lpm |
| Sample: mix: Interphase 40% - 45% of sucrose gradient | Current: 300 nA | Pressure: 4 psid |
| Concentration: not diluted | $CO_2$: 0.1 lpm | Median of 6 spectra |
| Capillary: 25 µm id | Air: 2 lpm | sample frozen (-20 °C) for 48 hours (black), reference spectrum (red) |

As can be learned from Figure 3.16 the majority of vault particles do not collapse after being frozen. The vaults appear stable after being exposed -20°C. An increase of low molecular weight material might be due to molecules released from the interior of vaults during the freezing and thawing process. A slight increase of vault artifacts (at 26 nm EM diameter) could be due to partial analyte instability under the given conditions.

### 3.2.12 Standard GEMMA measurements: Vaults, impact of Microcon desalting

Further experiments were performed to compare the GEMMA spectra of mix before and after Microcon desalting. Results are depicted in Figures 3.17.

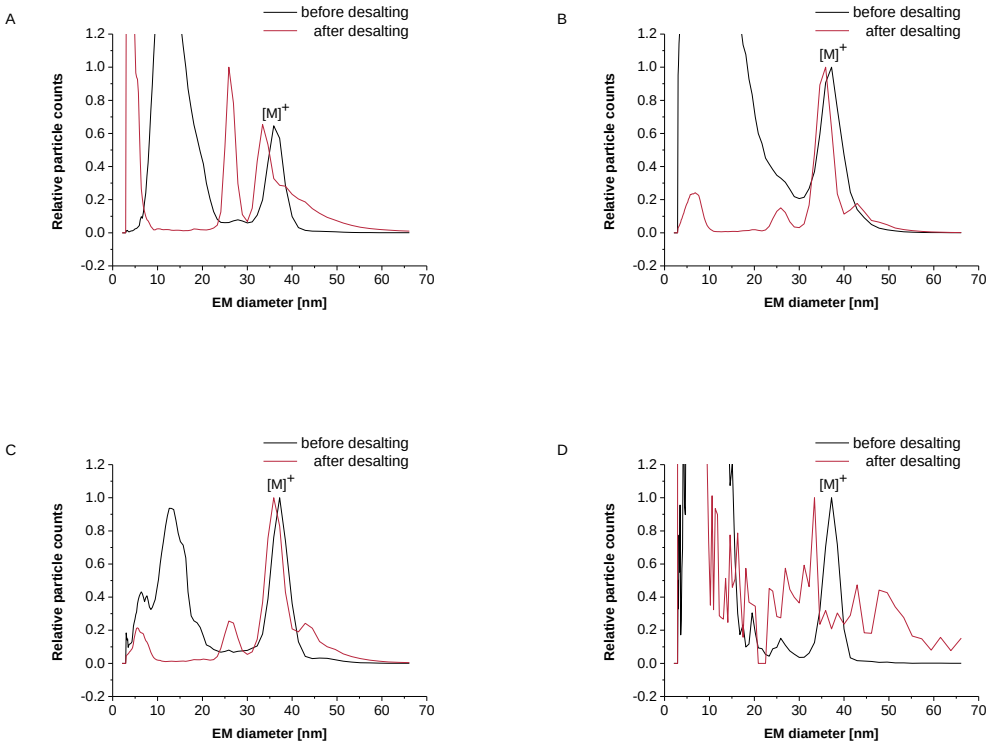


**Figure 3.17: Comparison of GEMMA results for mix before desalting (black) and after desalting (red) from 40% [w/w] (Figure A), Interphase 40 % - 45% [w/w] (Figure B), 45% [w/w] (Figure C), 50% [w/w] (Figure D) phases of sucrose gradient**

| | | |
|---|---|---|
| Electrolyte: 20 mM $NH_4OAc$, pH 7.4 | Voltage: 1.9 kV | Sheath flow: 15 lpm |
| Sample: mix: 40% (Fig. A), Interphase 40% - 45% (Fig.B), 45% (Fig.C), 50% (Fig. D) phase of sucrose gradient | Current: 300 nA | Pressure: 4 psid |
| Concentration: not diluted | $CO_2$: 0.1 lpm | Median of 3-6 spectra |
| Capillary: 25 µm id | Air: 1 lpm | mode: NM, samples measured before desalting (black) and after desalting (red) |

Figure 3.17 shows the relative increase of the vault peak after Microcon desalting in comparison to the peak representing the low molecular weight material in case of 40%-, 45% and Interphase 40% - 45% [w/w] fractions of the sucrose gradient. The vault concentration of the 50% [w/w] sucrose fraction is low relative to low weight material. The peak apexes of

single charged molecular vault peaks after Microcon desalting are shifted to 1 – 4 nm smaller EM diameters values relative to the peak apexes of single charged molecular vault peaks before Microcon desalting due to decrease of concentration of salts that aggregate on vault molecules.

The peak at 26 nm corresponds to a vault artifact with about the half molecular weight of complete particles. The intensity of this vault artifact increases after the microcon desalting step. There is also a smaller peak at 44.5 nm in Interphase 40% - 45% and 45% fraction after Microcon desalting. This peak could correspond to a dimer vault that could be seen in samples with higher concentrations. For this reason the Interphase 40% - 45% sample was diluted in $NH_4OAc$, the results are shown in section 3.2.13.

### 3.2.13 Standard GEMMA measurements: Vaults, dilutions after Microcon desalting

Further experiments with mix samples from 40% - 45% Interphase were necessary to be able to discuss the peaks found in GEMMA spectra of mix from 40% - 45% Interphase as shown in section 3.2.12. The results are shown in Figures 3.18 (absolute values) and 3.19 (relative values).

The peak at 44.5 nm is no longer visible in diluted samples. Therefore it is likely that this peak corresponds to a single charged dimer of vaults (monomer seen at 36 nm). The 26 nm artifact of vaults (in the Figure denoted as $[M/2]^+$) is significantly bigger to the vault particle peak at 36 nm in sample diluted 1:25 with ammonium acetate. To confirm this observation, one more analysis of this sample was done with lowered Sheath flow in the Nano ES unit (0.3 lpm). Results are depicted in 3.20.

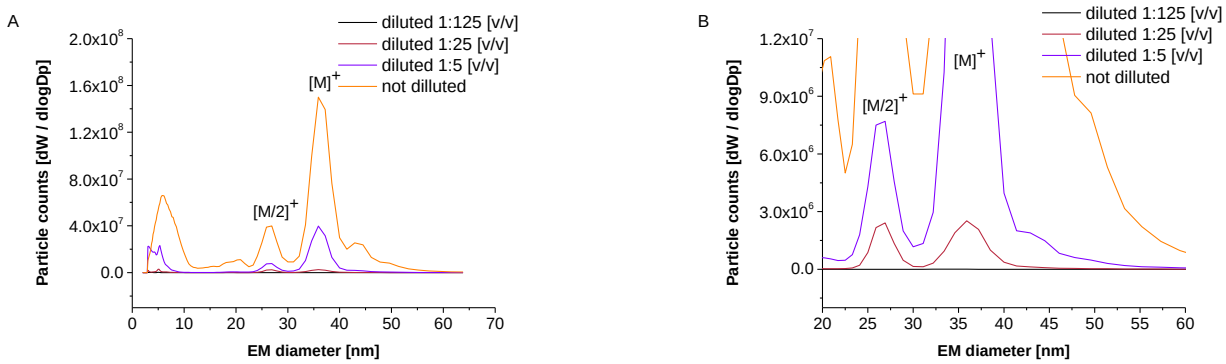


**Figure 3.18: GEMMA results of mix from 40% - 45% [w/w] (Interphase) of sucrose gradient at different analyte concentration**

| | | |
|---|---|---|
| Electrolyte: 20 mM $NH_4OAc$, pH 7.4 | Voltage: 1.9 – 2.3 kV | Sheath flow: 15 lpm |
| Sample: mix: Interphase 40% - 45% of sucrose gradient | Current: 300 - 400 nA | Pressure: 4 psid |
| Concentration: not diluted (orange) & diluted 1:5 (purple), 1:25 (red), 1:125 (black) | $CO_2$: 0.1 lpm | Median of 3-6 spectra |
| Capillary: 25 µm id | Air: 1 lpm | mode: NM |

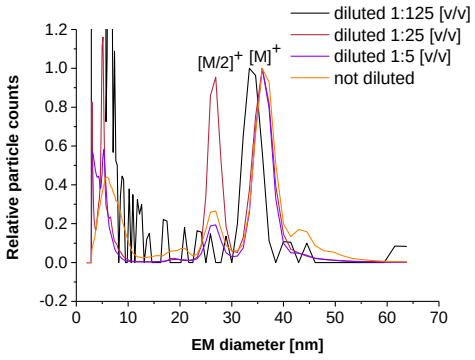


**Figure 3.19: Results from Figure 3.18 depicted as relative particle counts**

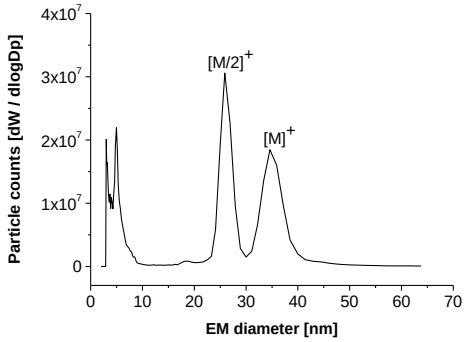


**Figure 3.20: GEMMA results of mix vaults from 40% - 45% [w/w] (Interphase) of sucrose gradient at lower Sheath flow in the nano ES unit**

| | | |
|---|---|---|
| Electrolyte: 20 mM $NH_4OAc$, pH 7.4 | Voltage: 1.9 – 2.3 kV | Sheath flow: 15 lpm |
| Sample: mix: Interphase 40% - 45% of sucrose gradient | Current: 300 - 400 nA | Pressure: 4 psid |
| Concentration: diluted 1:25 | $CO_2$: 0.1 lpm | Median of 6 spectra |
| Capillary: 25 µm id | Air: 0.3 lpm | mode: NM |

Figure 3.20 again shows a significantly higher 26 nm vault artifact peak (in the Figure denoted as $[M/2]^+$). Therefore, vault molecules tend to dissociate to half vaults at lower analyte concentrations. The reason could be the instability of vaults at lower concentrations in ammonium acetate (due to likewise dilution of an additionally stabilizing compound) or equilibrium dependant dissociation due to lower vault concentration.

### 3.2.14 Standard GEMMA measurements, m-Cherry vaults

As no distinct peak for m-Cherry can be recognized in mixtures with vsvg (mix), GEMMA analysis of m-Cherry alone in comparison to mix as reference took part. The results are depicted in Figure 3.21.

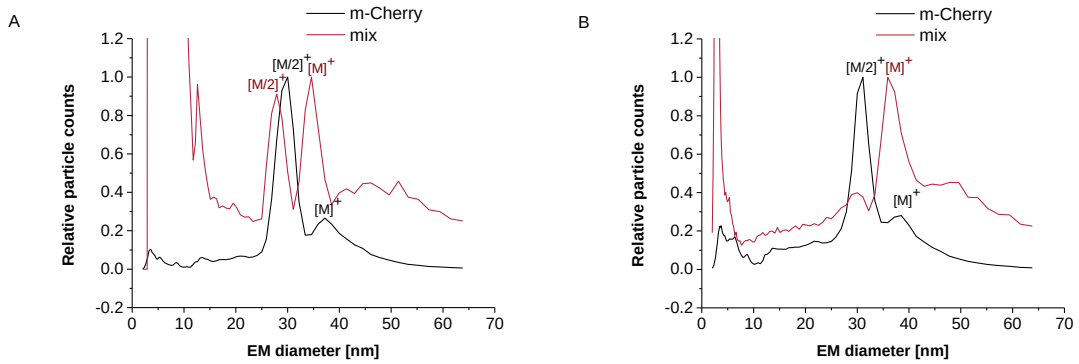


**Figure 3.21: Comparison of GEMMA spectra for m-Cherry vaults and mix from 40% [w/w] sucrose gradient (A) and 45% [w/w] sucrose gradient (B)**

| | | |
|---|---|---|
| Electrolyte: 20 mM $NH_4OAc$, pH 7.4 | Voltage: 1.9 kV | Sheath flow: 15 lpm |
| Sample: m-Cherry vaults (blue), mix (red) | Current: 300 nA | Pressure: 4 psid |
| Concentration: not diluted | $CO_2$: 0.1 lpm | Median of 6 spectra |
| Capillary: 25 µm id | Air: 1 lpm | mode: NM |

From Figure 3.21 a difference in spectra recorded for m-Cherry vaults and a mix of both vault species can be detected (it is of note that the concentration of vsvg is about 10 times higher than that of m-Cherry in mix samples as a result of analyte preparation in cells). Because of that the detected EM diameter in mix samples is assumed to represent the signal of vsvg vaults. The EM diameter of single charged monomer peak of m-Cherry is about 37 – 38 nm, the EM diameter of the single charged monomer peak of vsvg is about 35 – 36 nm. For m-Cherry the vault artifact with about half molecular weight of the whole vault particle is relative more intense than in mix samples. This leads to an assumption of bigger instability of m-Cherry than vsvg vaults. The EM diameter of 'half vault particles' (in the Figure denoted as $[M/2]^+$) of m-Cherry is about 30 – 31 nm, 'half vault particles' of vsvg are about 26 – 28 nm in diameter (see also Figures 3.18 - 3.20). Therefore, the difference of EM diameter of m-Cherry and vsvg vaults is about 2 nm, the width of the peaks is more than 5 nm at half peak height. However, the distance of channels analyzing EM diameters in the given GEMMA instrument in that EM diameter range is about 1.1 – 1.5 nm. Additionally, the concentration of m-Cherry is ten times less the concentration of vsvg. Thus, the differentiation of the two vault types is very difficult. In the presence of m-Cherry the vsvg peak is not resolved from the m-Cherry peak. Therefore, I tried to analyze these samples in the CM of GEMMA.

### 3.2.15 CM experiments with mixed vault/protein samples

CM is a new method for GEMMA analysis (as described in this work). Therefore, the optimization of this method for more analytes is necessary. CM has already been successfully employed for protein separation (BSA and IgG). In this part the application of this method to separate particles with a big difference in molecular weight and EM diameter was performed. Ovalbumin (EM diameter = 6 nm), Transferrin (EM diameter = 7.2 nm) and vsvg / m-Cherry vaults (EM diameter = 35 – 36 nm) were analyzed. First experiments were performed with all three analytes, Ovalbumin and Transferrin were 4 µM, vaults were 1:5 diluted after Microcon desalting (Interphase 40% - 45% was used). Exemplary GEMMA spectra are shown in Figure 3.22. The experiment was repeated n = 5 times in total.

A separation of proteins and vaults can be observed, the vault peak is detected in one scan (scan 9) before the proteins (Ovalbumin ~ 6 nm and Transferrin ~ 7.2 nm) pass the system (scan 10). However, in the scan detecting proteins (scan 10) as well vaults can be seen (however, at lower concentrations than with the previous spectrum). In the following scan there is none of these analytes detected. Therefore, the separation of vaults from Ovalbumin and Transferrin was just partial. The problem is the peak broadness probably because of (i) the pressure application leading to parabolic flow profile inside the capillary, (ii) a long injection time (5 s injection time was necessary to detect analytes), (iii) attachment of analytes to surface and (iv) diffusion of analytes. The next sample plugs were performed with 4.5 µM Ovalbumin and vault samples (mix taken from Interphase 40% - 45% of sucrose gradient) diluted 1:9 with ammonium acetate after the Microcon desalting. The results are depicted in Figure 3.23.

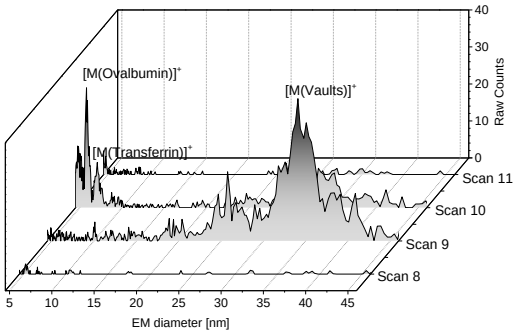


**Figure 3.22: Separation of Ovalbumin, Transferrin and mix from 40% - 45% [w/w] (Interphase) of sucrose gradient in CM**

| | | |
|---|---|---|
| Electrolyte: 20 mM $NH_4OAc$, pH 7.4 | Voltage: 1.9 kV | Sheath flow: 15 lpm |
| Sample: Ovalbumin, Transferrin, mix | Current: 300 nA | Pressure: 1.4 psid |
| Concentration: Ovalbumin & Transferrin 4 µM, mix diluted 1:5 | $CO_2$: 0.1 lpm | individual measurements |
| Capillary: 25 µm id | Air: 1 lpm | mode: CM, 5 s plug |

In the measurements depicted in Figure 3.23 the partial separation of vaults from Ovalbumin took part. The vaults can be seen in two scans, Ovalbumin is only detected in the second scan together with vaults. Better separation of analytes can possible been reached at lower pressure (in this measurement 2.4 psid) but at lower pressure, no stable electrospray in the system could be maintained). The partial separation at higher pressure could be observed because of short scan times (16 seconds per one scan).

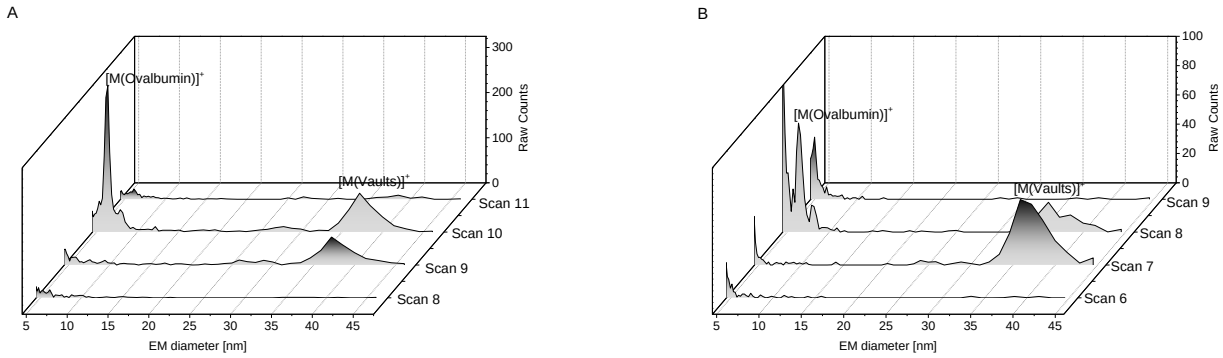


**Figure 3.23: Separation of Ovalbumin and mix from 40% - 45% [w/w] (Interphase) of sucrose gradient in CM, 2 experiments (A & B)**

| | | |
|---|---|---|
| Electrolyte: 20 mM $NH_4OAc$, pH 7.4 | Voltage: 1.8 kV | Sheath flow: 15 lpm |
| Sample: Ovalbumin, mix: 45% Phase of sucrose gradient | Current: 200 - 300 nA | Pressure: 2.4 psid |
| Concentration: Ovalbumin 4µM, mix diluted 1:5 | $CO_2$: 0.1 lpm | individual measurements |
| Capillary: 25 µm id | Air: 0.5 lpm | mode: CM, 5 s plug |

### 3.2.16 CM with vaults, longer capillary

The length of the capillary for all previous measurements was 25 cm. In the CM system the CE separation is disturbed by an applied pressure difference in the capillary (hydrodynamic flow profile leads to peak broadening). To see if the CE separation would be better in the system with a longer separation distance the next CM experiments were done with a 75 cm long capillary. One exemplary spectrum is depicted in Figures 3.24. The experiment was carried out n = 10 times.

From Figure 3.24 it can be seen that the separation of Ovalbumin and mix (Interphase 40% - 45% from sucrose gradient) in a 75 cm long capillary was even worse than in a 25 cm long capillary. The vaults can be detected in a few scans before and after Ovalbumin can be seen (vaults can be detected in scans 10 – 17, Ovalbumin in scans 12 – 15). In a next step to decrease the sample amount injected to the system in CM, the concentration of sample was diluted 1:10 with ammonium acetate the final Ovalbumin concentration was 0.45 µM, vaults were diluted 1:90 after Microcon desalting. However, there was no improvement observed.

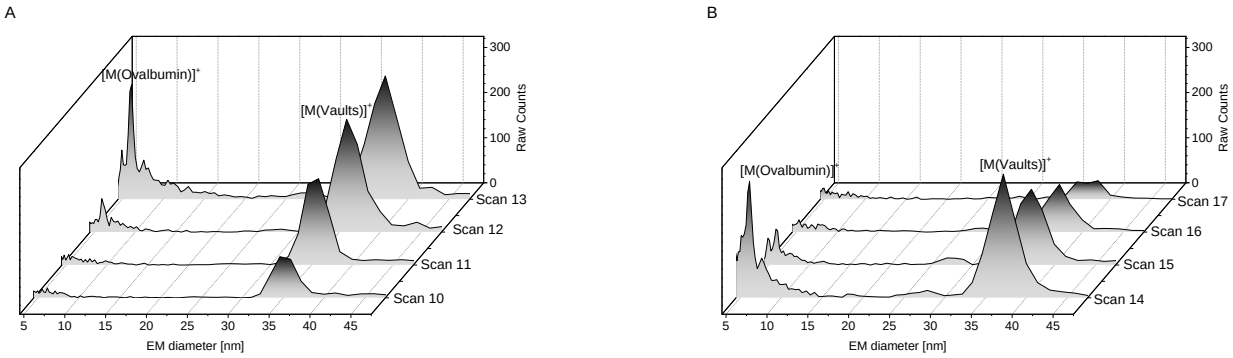


**Figure 3.24: Separation of Ovalbumin and mix from 40% - 45% [w/w] (Interphase) of sucrose gradient in CM (with 75 cm capillary), one experiment, scans 10 – 13 (A), scans 14 -17 (B)**

| | | |
|---|---|---|
| Electrolyte: 20 mM $NH_4OAc$, pH 7.4 | Voltage: 1.8 kV | Sheath flow: 15 lpm |
| Sample: Ovalbumin, mix: 45% Phase of sucrose gradient | Current: 200 - 300 nA | Pressure: 1 psid |
| Concentration: Ovalbumin 2.5µM, vaults diluted 1:8 | $CO_2$: 0.1 lpm | individual measurements |
| Capillary: 25 µm id | Air: 1.5 lpm | mode: CM, 5 s plug |

The problem is the peak broadness because of the pressure application leading to parabolic flow profile, long injection time (5 s injection time was necessary to detect analytes), attachment of analytes to surface and diffusion of analytes, that is more intense to observe in the 75 cm long capillary. The handling with 25 cm capillary is easier. The 25 cm capillary is more appropriate for separation of proteins and vaults in CM. Additionally, the preparation of tipped capillaries is a problem: Capillaries of 25 cm length and prepared with a tip can be purchased. For longer capillaries, the tip has to be prepared in-house (which often leads to a bad reproducibility) to obtain a stable Taylor conus.

### 3.2.17 CM with vault samples

Despite problems to separate vault particles from proteinaceous standards as reported in the previous section, it was tried to analyze mix in CM to separate these two analytes from each other. One exemplary result from three CM runs is depicted in Figure 3.25.

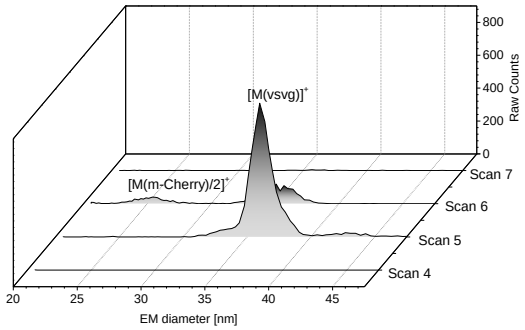


**Figure 3.25: Separation of m-Cherry and vsvg from mix from 40% - 45% [w/w] (Interphase) of sucrose gradient in CM**

| | | |
|---|---|---|
| Electrolyte: 20 mM $NH_4OAc$, pH 7.4 | Voltage: 1.9 kV | Sheath flow: 20 lpm |
| Sample: mix: Interphase 40% - 45% Phase of sucrose gradient | Current: 300 nA | Pressure: 2.4 psid |
| Concentration: not diluted | $CO_2$: 0.1 lpm | individual measurement |
| Capillary: 25 µm id | Air: 0.7 lpm | mode: CM, 5 s plug |

Vaults are present mainly in two scans of CM, there is a peak at 35-36 nm that corresponds to vsvg (mainly in scan 5, it is also found in scan 6 in Figure behind vsvg peak in scan 5). The artifact of vaults may be seen at 25.9 nm in scan 6. The m-Cherry artifact with about half molecular weight of the whole vault particle is relative more intense as in the case of vsvg, because of the higher instability of m-Cherry particles (see section 3.2.14). Possibly, the partial separation of vault artifact and complete particle was achieved in CM.

### 3.2.18 Stability of vaults in MeOH

The following experiments were performed to determine the stability of vaults in solutions containing MeOH as necessary prerequisite for future ESI MS work. The mix from 40% - 45% Interphase of sucrose gradient were analyzed at 0%, 10%, 20% and 30% [v/v] MeOH content in NM GEMMA. The results are shown in Figure 3.26. The absolute values are shown in Figure 3.26A, the relative values in Figure 3.26B.

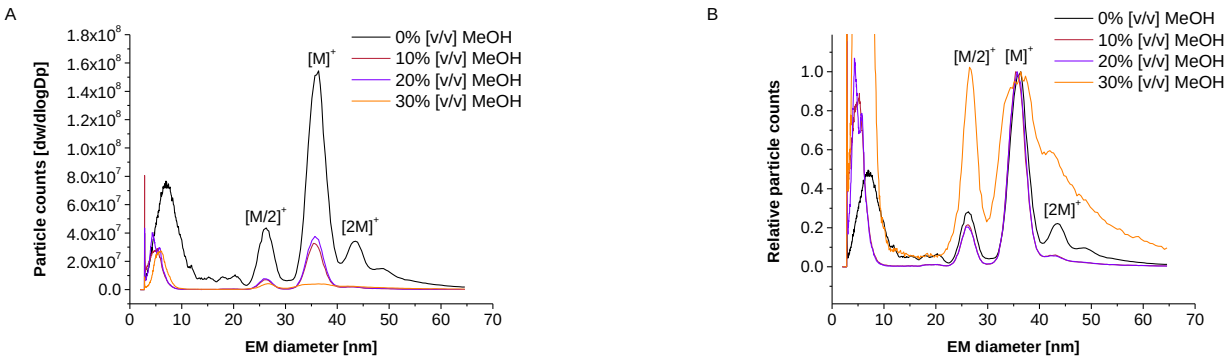


**Figure 3.26: GEMMA results of mix stability in MeOH**

| | | |
|---|---|---|
| Electrolyte: 20 mM $NH_4OAc$, pH 7.4 | Voltage: 1.9 kV | Sheath flow: 15 lpm |
| Sample: mix: 45% Phase of sucrose gradient | Current: 300 nA | Pressure: 1 psid |
| Concentration: vaults diluted 1:6, Methanol 0-, 10-, 20- & 30% [v/v] | $CO_2$: 0.1 lpm | median of 6 spectra |
| Capillary: 25 µm id | Air: 1.0 lpm | mode: NM |

From Figure 3.26 the stability of vaults up to 20% MeOH content in the sample can be observed (although upon MeOH addition particle counts are diminished). In 30% MeOH, the peak of vaults decreases significantly. Concomitantly, more unspecific aggregates as well as vault artifacts are detected. Vault particles are seemingly no longer stable at 30% MeOH content.

# 4 Conclusions and Outlook

In this work the electrophoretic separation of standard proteins in the liquid phase (nano ES capillary) of a standard, commercially available GEMMA was performed. Theoretical considerations gave basics for the understanding of force distribution in the nano ES capillary. The optimization of applied pressure, sheath flow in the nano ES unit as well as the pH of the employed buffer, the concentration of sample as well as the plug time for CM was carried out. The separation of BSA and IgG with different migration times was observed. The reduction of pressure was necessary in order to enable the separation of analytes, however at least 0.4 psid (= 0.03 bar) is needed for providing stable aerosol. Furthermore, the new developed method enabled the analysis of samples with higher salt concentration (up to 2 mM) due to online desalting. When the reference conditions of GEMMA (= NM) are applied, the analytes are covered with salt molecules upon drying of droplets resulting in heterogeneous EM diameter distributions, making the determination of EM diameters of analytes difficult if not even impossible. In our results the online desalting of sample was shown, resulting EM diameter corresponded to the EM diameter determined from the sample without any salt content. The next step in application of this new method can be analysis of samples containing detergents as well as electrophoretic sample stacking.

The new developed method for electrophoretic separation was also applied for real biological samples. Vaults sample were analyzed at UCLA, for the setup of the instrument the $^{210}$Po-source was exchanged, the instrument was checked by analysis of a standard protein. The results of GEMMA spectra of BSA and Ovalbumin were compared to spectra obtained at TUVIE. The results showed accordance in the EM diameter for both proteins and in the case of BSA even the particle counts were comparable.

The analysis of mix sample of two different vault particles in NM detected only one main peak in the GEMMA spectrum. However, analysis of individual particles demonstrated that there is a difference of EM diameter of the single charged monomer peaks of individual species. The EM diameter of m-Cherry was found at about 37 – 38 nm, the EM diameter of vsvg was found at about 35 – 36 nm. Furthermore it was shown that vaults are stable also after being exposed -20°C (for 48 hours). Additionally, CM experiments were carried out with vault sample as well as with samples containing vaults and Ovalbumin. Partial separation of vaults from Ovalbumin was observed in CM. These experiments were done also in 75 cm long capillary, but the better results were achieved in 25 cm capillary. CM was applied for the

separation of vault mix as well. The artifact peak that may correspond to m-Cherry-MVP vault artifact and vsvg-MVP vault molecular peak are detected in different scans.

The analysis of vaults in solutions with MeOH content showed that the vaults are no longer stable at 30% v/v MeOH, for lower MeOH concentrations at least partial analyte stability is given.

Additionally, preliminary measurements of Hemoglobin-N2N3 Receptor Complex, TriC-Drug Complex were performed. Furthermore, the stability of Mmm1-D5-Fusion Complex in solutions containing up to 30% v/v MeOH was investigated.

# 5 Appendix

Additional results that were not given in sections 3.1 and 3.2 are summed up in the following part.

To optimize the CM it was necessary to check several parameters: pH of solution, the lowest possible pressure in the pressure chamber and the lowest possible Air- and $CO_2$ sheath flow in the nano ES unit. This was done in NM, FM as well as in CM. The influence of the plug time in CM was investigated as well. Additional results of online desalting at lower sodium chloride concentration are shown as well. The migration times of analytes were calculated from results of CE. All these experiments are described in section 5.1.

The amino acid sequences of analyzed proteins and protein complexes are listed in section 5.2.

# 5.1 Additional experiments to investigation of electrophoretic effects during sample introduction to a GEMMA instrument via a nano electrospray setup in more detail

## 5.1.1 GEMMA measurements of Ovalbumin, BSA and IgG in NM

GEMMA measurements of proteins (Ovalbumin, BSA and IgG) were done under reference conditions (=NM) to track changes in spectra obtained under different conditions and modes of GEMMA. The results are depicted in Figure 5.1.

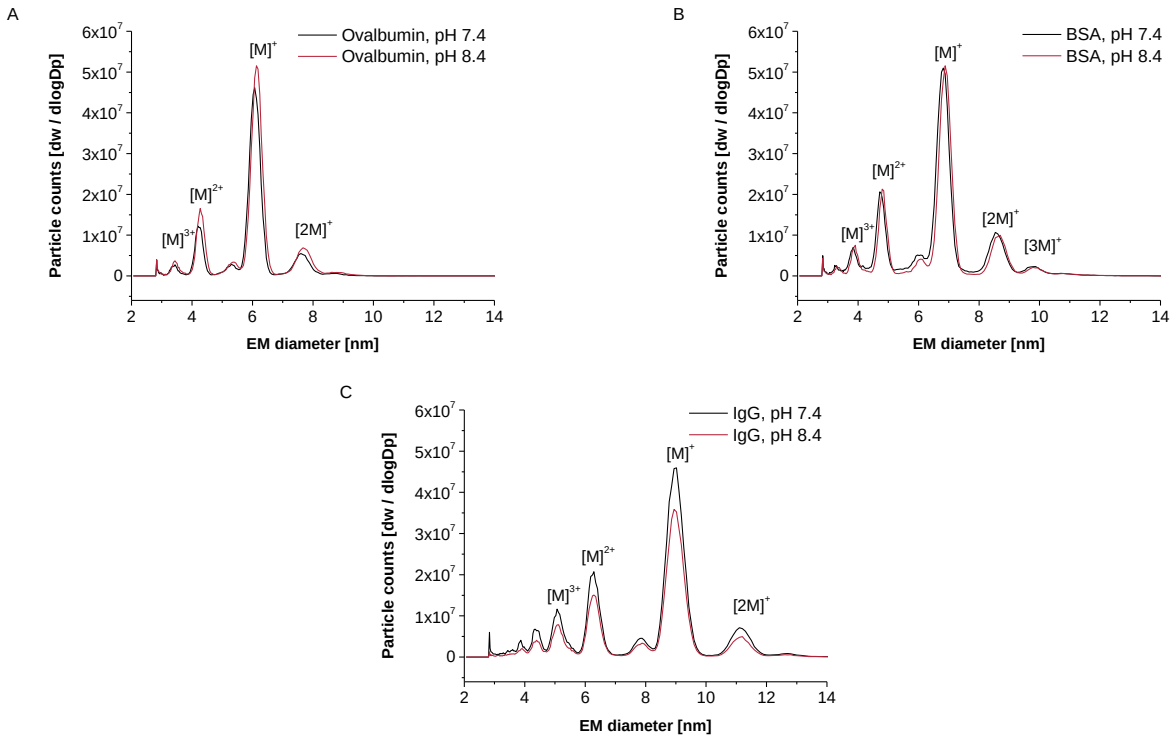


**Figure 5.1: GEMMA results for Ovalbumin (A), BSA (B) and IgG (C)**

| | | |
|---|---|---|
| Electrolyte: 20 mM $NH_4OAc$, pH 7.4 (red) & 8.4 (blue) | Voltage: 2.4 kV | Sheath flow: 15 lpm |
| Sample: Ovalbumin, BSA, IgG | Current: 300 nA | Pressure: 4 psid |
| Concentration: 1 µM | $CO_2$: 0.1 lpm | Median of 6 spectra |
| Capillary: 25 µm id | Air: 1 lpm | mode: NM |

The major peak detected respectively corresponds to the single charged protein monomer. Ovalbumin is detected at an EM diameter of 6.1 nm (EM diameter in literature 6.3 nm: [10]), BSA at an EM diameter of 6.9 nm (7.1nm: [10]) and IgG at an EM diameter of 8.9 nm (9.3 nm: [10, 36]), respectively. The results correlate with the diameters described in literature. Small deviations are probably due to measurements carried out (according to the manufacturer) without instrument calibration. Other peaks at lower EM diameter values correspond to multiple charged monomer peaks. They were detected because of the age of the employed $^{210}$Po source. Peaks with higher EM diameter result from single charged dimer and multimer particles as already described in literature [10]. Variation of pH had no influence on the EM diameters of peaks and the ratio of detected species under investigated conditions.

### 5.1.2 GEMMA spectra at lower psid values in the sample chamber

The pressure applied in the pressure chamber accelerates analytes towards the capillary tip and make the electrophoretic separation of analytes more difficult (as the resulting force is directed against the electrophoretic mobility of analytes and additionally peak broadening occurs). Because of that, it was the intention to carry out GEMMA measurements in CM at as low pressure values as possible. To observe the impact of pressure applied on the sample chamber on the migration of analytes through the capillary and on the resulting spectra and to determine the minimum pressure needed for particles transport through the electrospray unit, the analytes were analyzed at various pressure values: 3.4 psid, 1.4 psid, 0.4 psid and 0 psid. The Figures 5.2 – 5.3 show the GEMMA spectra of Ovalbumin, BSA and IgG recorded under different pressure levels applied to the pressure chamber. For all analytes, spectra at pH 7.4 and pH 8.4 were recorded. However, as these do not differ significantly at these two pH values, only results at pH 7.4 are shown. To enable a better comparison the spectra were normalized, the single charged monomer peak was set as 100% (except for Figure 5.2)

The influence of the pressure applied to the sample chamber can be determined from Figures 5.2 – 5.3. The spectra at 1.4 psid and 3.4 psid show a similar peak form and EM diameter for the investigated analyte. On the other hand, the results at 0.4 psid show the limits of the instrument at lower psid values. The signal intensity decreases tremendously. If there is no pressure applied, seemingly the amount of analyte reaching the ES tip is too low, resulting in no recorded signal.

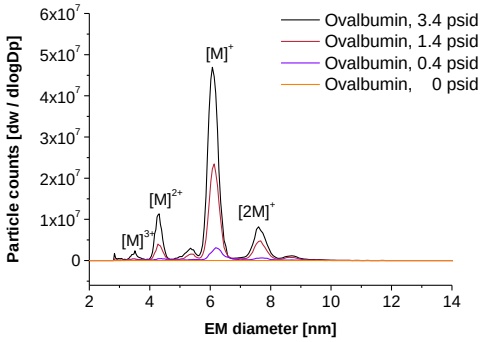


**Figure 5.2: Comparison of GEMMA results for Ovalbumin recorded under different pressure levels applied to pressure chamber**

| | | |
|---|---|---|
| Electrolyte: 20 mM $NH_4OAc$, pH 7.4 | Voltage: 2.8 kV | Sheath flow: 15 lpm |
| Sample: Ovalbumin | Current: 300 – 400 nA | Pressure: 0 – 3.4 psid |
| Concentration: 1 µM | $CO_2$: 0.1 lpm | Median of 6 spectra |
| Capillary: 25 µm id | Air: 1 lpm | mode: NM |

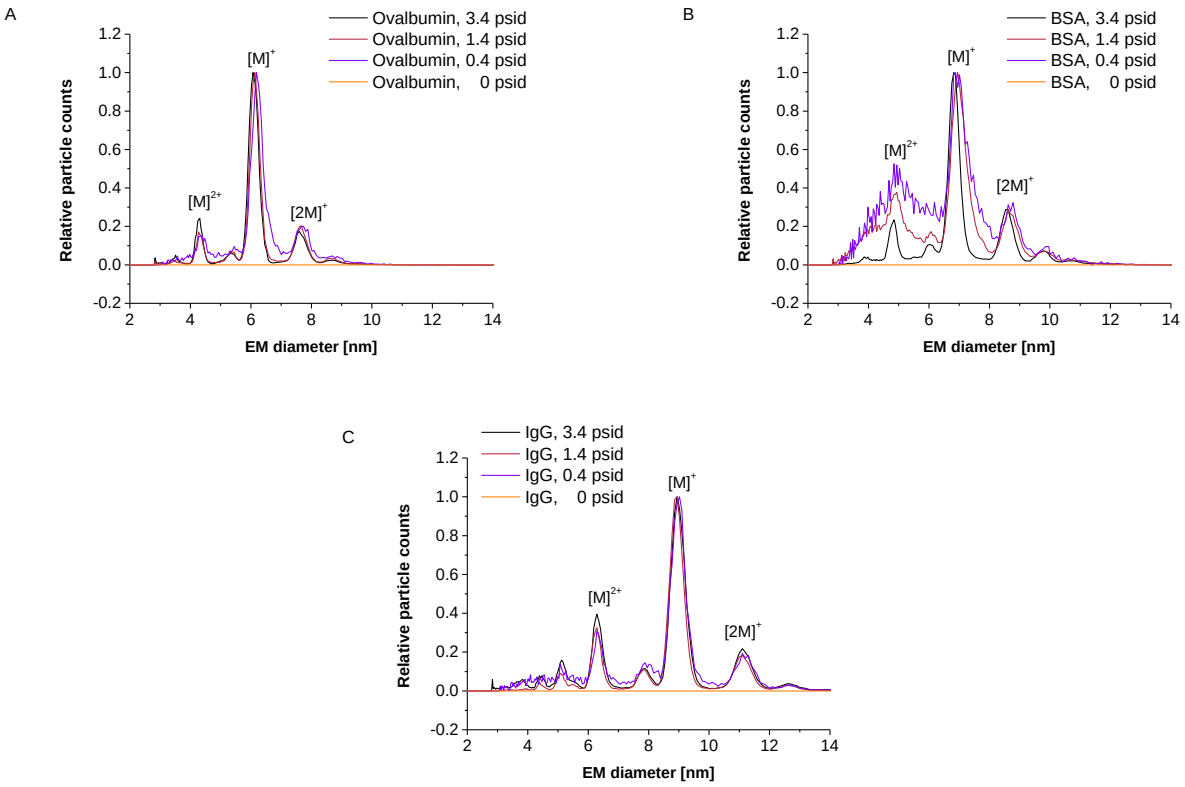


**Figure 5.3: Comparison of GEMMA results for Ovalbumin (A), BSA (B), IgG (C) recorded under different pressure levels applied to pressure chamber, depicted as relative particle counts**

| | | |
|---|---|---|
| Electrolyte: 20 mM $NH_4OAc$, pH 7.4 | Voltage: 2.8 kV | Sheath flow: 15 lpm |
| Sample: Ovalbumin, BSA, IgG | Current: 300 – 400 nA | Pressure: 0 – 3.4 psid |
| Concentration: 1 µM | $CO_2$: 0.1 lpm | Median of 6 spectra |
| Capillary: 25 µm id | Air: 1 lpm | mode: NM |

As it was our intention to reduce the pressure applied to the sample chamber as much as possible and at the same time still record spectra at stable conditions 1.4 psid (= 0.1 bar) was chosen, because of stable results provided at this pressure level.

### 5.1.3 GEMMA spectra at lower Air and $CO_2$ sheath flow values in the electrospray unit

Another factor that influences the migration of analytes in the GEMMA capillary is the air and $CO_2$ sheath flow acting at the capillary tip. To see if it is possible to reduce these flows

and hence their influence on the analyte migration through the capillary, the GEMMA analysis of Ovalbumin, BSA and IgG at lower air and $CO_2$ flows was carried out.

Proteins were analyzed at combinations between 0 and 0.1 lpm $CO_2$ and 0, 0.2, 0.5 and 1 lpm Air sheath flow. The sheath flow in DMA was set to 15 lpm for a good resolution of peaks, at Macrolon (Macrolon = sum of $CO_2$ and Air sheath flow) ≤ 0.1 lpm the sheath flow in the DMA was at 13.5 lpm because of a limitation of the instrument. (The pump of the DMA unit is not able to produce high flow value exceeding approximately 14 lpm and hence 15 lpm could not be reached under certain conditions.) Figure 5.4 shows the spectra of Ovalbumin, BSA and IgG at different Air and $CO_2$ sheath flow levels in the electrospray unit. Again spectra are recorded at pH 7.4 and 8.4, respectively. As there was no significant change between pH values, only results at pH 7.4 are shown.

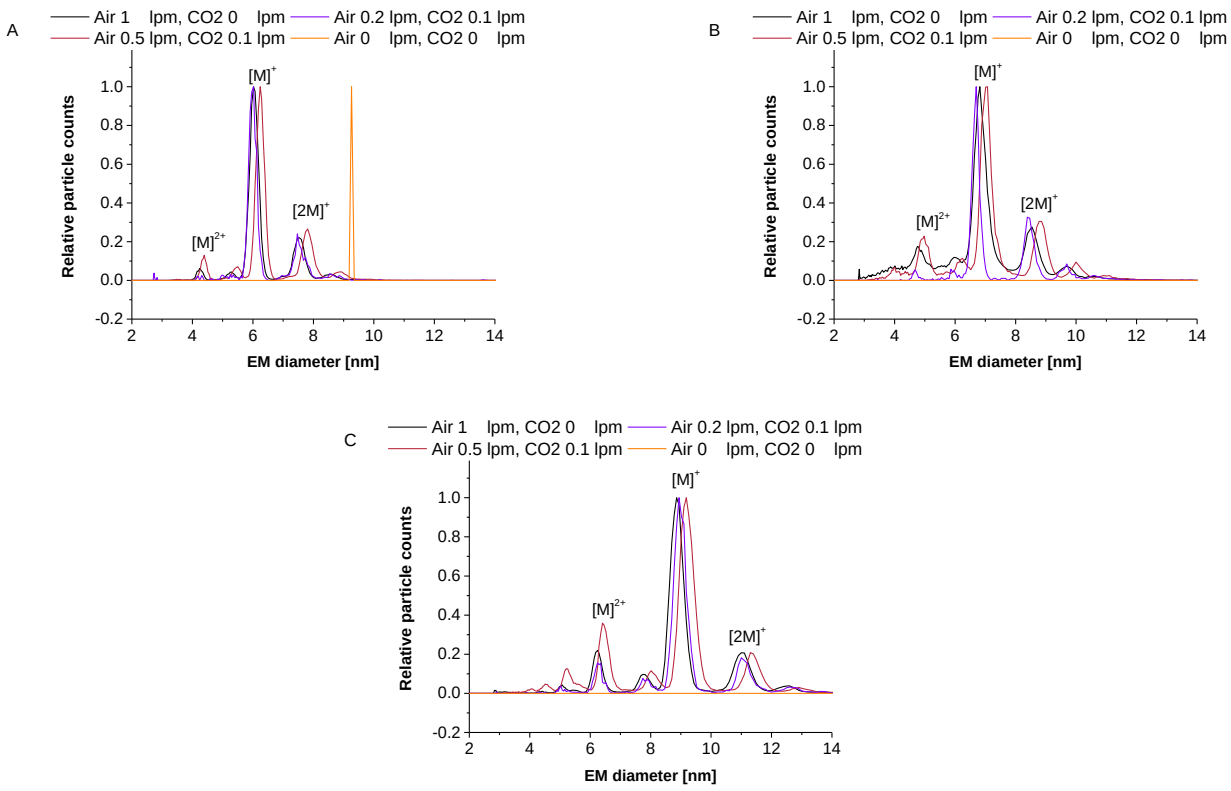


**Figure 5.4: Comparison of GEMMA results for Ovalbumin (A), BSA (B), IgG (C) recorded at different Air and $CO_2$ sheath flow levels in electrospray unit, depicted as relative particle counts**

| | | |
|---|---|---|
| Electrolyte: 20 mM $NH_4OAc$, pH 7.4 | Voltage: 2.8 – 3.0 kV | Sheath flow: 13.5 lpm |
| Sample: Ovalbumin, BSA, IgG | Current: 400 – 500 nA | Pressure: 4 psid |
| Concentration: 1 µM | $CO_2$: 0 - 0.1 lpm | Median of 6 spectra |
| Capillary: 25 µm id | Air: 0 - 1 lpm | mode: NM |

Figure 5.4 shows the impact of different Macrolon values on recorded spectra: without Macrolon, particles are not transported from the electrospray chamber to the DMA and hence cannot be detected. Results of measurements at Macrolon 0.3 lpm (Air 0.2 lpm, $CO_2$ 0.1 lpm) demonstrate these sheath flows as sufficient for GEMMA analysis of proteins. The EM diameters of the peaks remain stable more or less at all conditions. From these measurements it can be concluded that at least Macrolon 0.3 lpm is necessary for GEMMA analysis.

### 5.1.4 CE experiments for investigation of electrophoretic effects during sample introduction to a GEMMA instrument

CE experiments of Ovalbumin, BSA and IgG samples were carried out to estimate the EOF ($\mu_{EOF}$) and mobility of analytes ($\mu_{app}$) in GEMMA. The measurements were carried out with a fused silica capillary (diameter 25µm) on a standard 3D CE instrument (Agilent). The preparation of samples and analysis were described in 3.1. In this section the calculation of EOF and mobility of analytes will be described in detail.

The EOF mobility ($\mu_{EOF}$) and the apparent mobility ($\mu_{app}$) of analytes can be calculated from:

$$\mu_{EOF} = \frac{L_{effective}}{U}\frac{L_{total}}{t_{EOF}} \quad (1)$$

$$\mu_{app} = \frac{L_{effective}}{U}\frac{L_{total}}{t_{app}} \quad (2)$$

$L_{effective}$ is the effective length of the capillary (= 51.7 cm) and $L_{total}$ the total length of the capillary (= 60.2 cm). The migration times ($t_{EOF}$ and $t_{app}$) can be read from the electropherograms, $t_{EOF}$ from DMSO migration (n= 8), $t_{app}$ from protein migration (n=4). The effective mobility $\mu_{eff}$ (independent from EOF) can be determined as:

$$\mu_{eff} = \mu_{EOF} - \mu_{app} \quad (3)$$

Results are part of section 3.1. The product of the electric field E (=3.2 $kVm^{-1}$, the value was obtained as described in 3.1) in GEMMA capillary and $\mu_{eff}$ leads to the analyte velocity $v_{CE}$

$$v_{CE} = E * \mu_{eff} \quad (4)$$

and finally the calculation of the migration time needed to pass the capillary considering the length of the capillary L (= 26cm):

$$t_{CE} = L / v_{CE} \quad (5)$$

Results in table 5.1 show that the biggest differences of migration times of analytes considering EOF and $\mu_{eff}$ are at the lower pH levels (7.4 and 8.4).

**Table 5.1** Migration time of analytes $t_{CE}$ considering EOF and $\mu_{eff}$

| | BSA [s] | Ovalbumin [s] | IgG [s] |
|---|---|---|---|
| pH 7.4 | 259 | 244 | 182 |
| pH 8.4 | 259 | 245 | 183 |
| pH 9.4 | 197 | 184 | 142 |

The reproducibility of CE analysis is better at higher pH, because of that pH 9.4 was used for further experiments.

### 5.1.5 Calculation of analyte migration

To estimate the migration time of analytes $F_{psid}$ (pressure applied to the sample chamber) has to be considered as well. The influence of $F_{psid}$ on migration time of analytes can be calculated using Hagen–Poiseuille equation:

$$Q = \frac{\Delta P * \pi\, d^4}{128 \mu * L} \qquad (6)$$

Q is the volumetric flow rate, ΔP the pressure difference (ΔP=1psid in CM), d is the inner diameter of the capillary (= 25µm), µ is the dynamic viscosity (calculated as water = 0.001 Pa·s at 20°C), L is the length of the capillary (L = 26 cm). The linear flow rate $v_{psid}$ is then calculated as described in equation 7.

$$v_{psid} = Q / A \qquad (7)$$

A is the cross sectional area of the capillary ($A = \pi * d^2/4 = 4.9 * 10^{-10}$ $m^2$). The resulting linear flow rate is the sum of $v_{psid}$ and $v_{CE}$ (both of the flow rates are directed towards the capillary tip):

$$v = v_{psid} + v_{CE} \qquad (8)$$

The final migration time of analytes can be calculated from v and L:

$$t = L / v \qquad (9)$$

Results for Ovalbumin, BSA and IgG at different pH and ΔP = 1psid are depicted in Table 5.2:

**Table 5.2** Migration time of analytes considering EOF, $\mu_{eff}$ as well as $F_{psid}$ :

| | BSA [s] | Ovalbumin [s] | IgG [s] |
|---|---|---|---|
| pH 7.4 | 171 | 164 | 134 |
| pH 8.4 | 171 | 165 | 134 |
| pH 9.4 | 142 | 135 | 111 |

From table 5.2 the differences of analyte migration times considering EOF, $\mu_{eff}$ as well as $F_{psid}$ (the sheath flow at the capillary tip does not have impact on migration time, as already shown in 3.1) can be recognized. This is a theoretical base for separation of analytes in CE-GEMMA.

### 5.1.6 Additional GEMMA measurements in FM

Additional GEMMA measurements in FM were necessary for the optimization of the FM and a successful setup of CM. A constant EM diameter value for each analyte was tracked over time, Ovalbumin was analyzed at 6.0 nm, BSA at 7.0 nm, IgG at 9.0 nm.

The first measurements (Figure 5.5) were taken at 3.4 psid in the pressure chamber, 1 lpm Air and 0.1 lpm $CO_2$ flow in the ES unit. These conditions were similar to the standard conditions in NM and were useful for comparison of analysis modes.

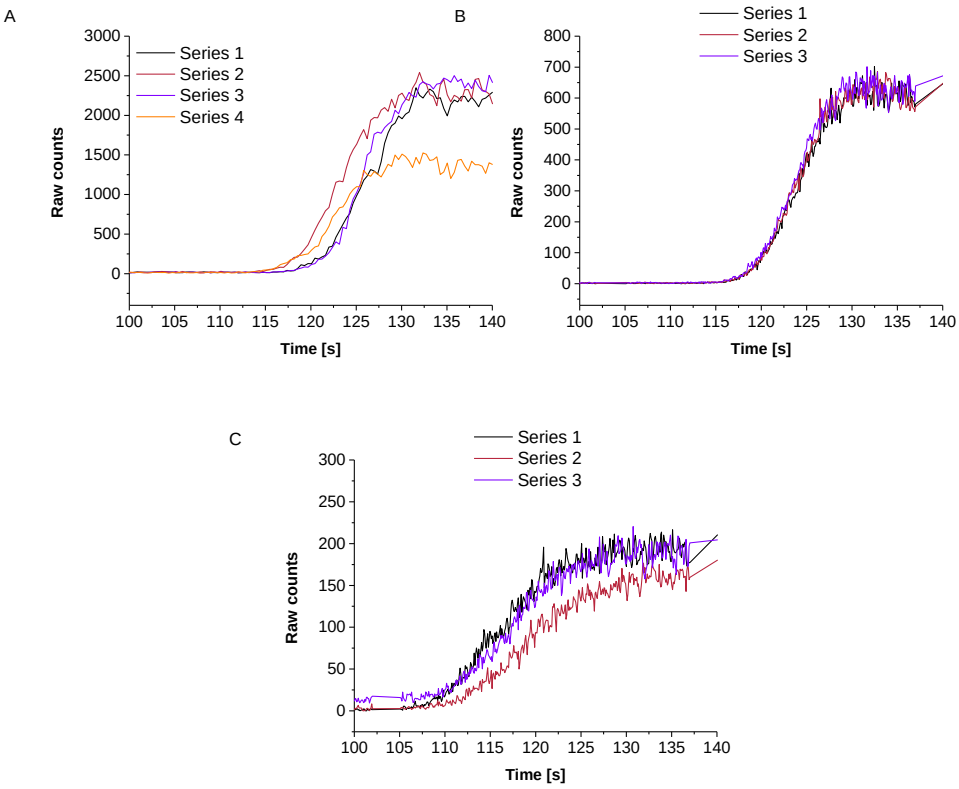


**Figure 5.5: Comparison of GEMMA results for Ovalbumin (A), BSA (B), IgG (C) in FM**

| | | |
|---|---|---|
| Electrolyte: 20 mM $NH_4OAc$, pH 7.4 | Voltage: 2.7 kV | Sheath flow: 13.5 lpm |
| Sample: Ovalbumin, BSA, IgG | Current: 300-400 nA | Pressure: 3.4 psid |
| Concentration: 1 µM | $CO_2$: 0.1 lpm | individual measurements |
| Capillary: 25 µm id | Air: 1 lpm | mode: FM |

There are differences in migration times of proteins at same conditions caused by a different electrophoretical mobility of these proteins in the capillary of GEMMA. IgG starts to be detected 110 seconds after being placed into the pressure chamber, BSA and Ovalbumin after 115 seconds. This correlates also with the theoretical considerations described in 5.1.5: IgG has the smallest mobility and should pass the system at the first place of these three analytes.

Next measurements (Figure 5.6) were done under decreased pressure in the pressure chamber $\Delta p$ = 1.4 psid and pH 7.4 and 8.4, respectively.

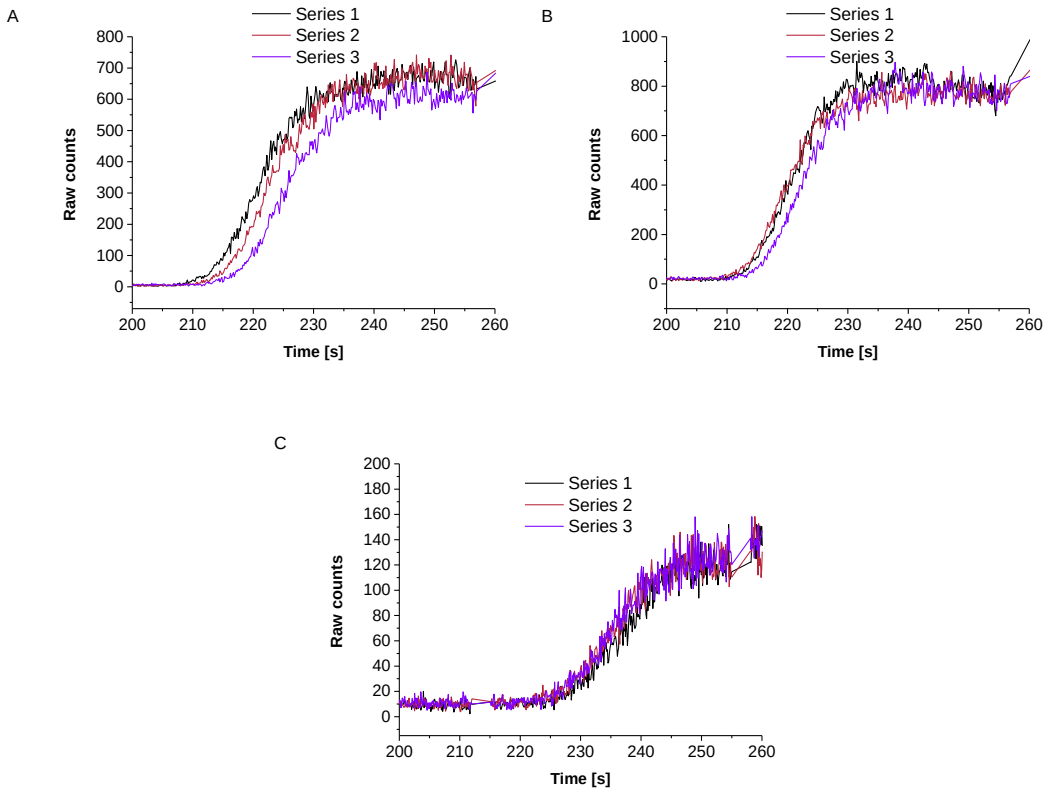


**Figure 5.6: Comparison of GEMMA results for Ovalbumin (A), BSA (B), IgG (C) in FM**

| | | |
|---|---|---|
| Electrolyte: 20 mM $NH_4OAc$, pH 7.4 | Voltage: 2.7 kV | Sheath flow: 13.5 lpm |
| Sample: Ovalbumin, BSA, IgG | Current: 300-400 nA | Pressure: 1.4 psid |
| Concentration: 1 µM | $CO_2$: 0.1 lpm | individual measurements |
| Capillary: 25 µm id | Air: 1 lpm | mode: FM |

The samples at pH 8.4 were also analyzed under these conditions (1.4 psid in pressure chamber, 1 lpm Air- and 0.1 $CO_2$ sheath flow in electrospray unit). The spectra are depicted in Figure 5.7:

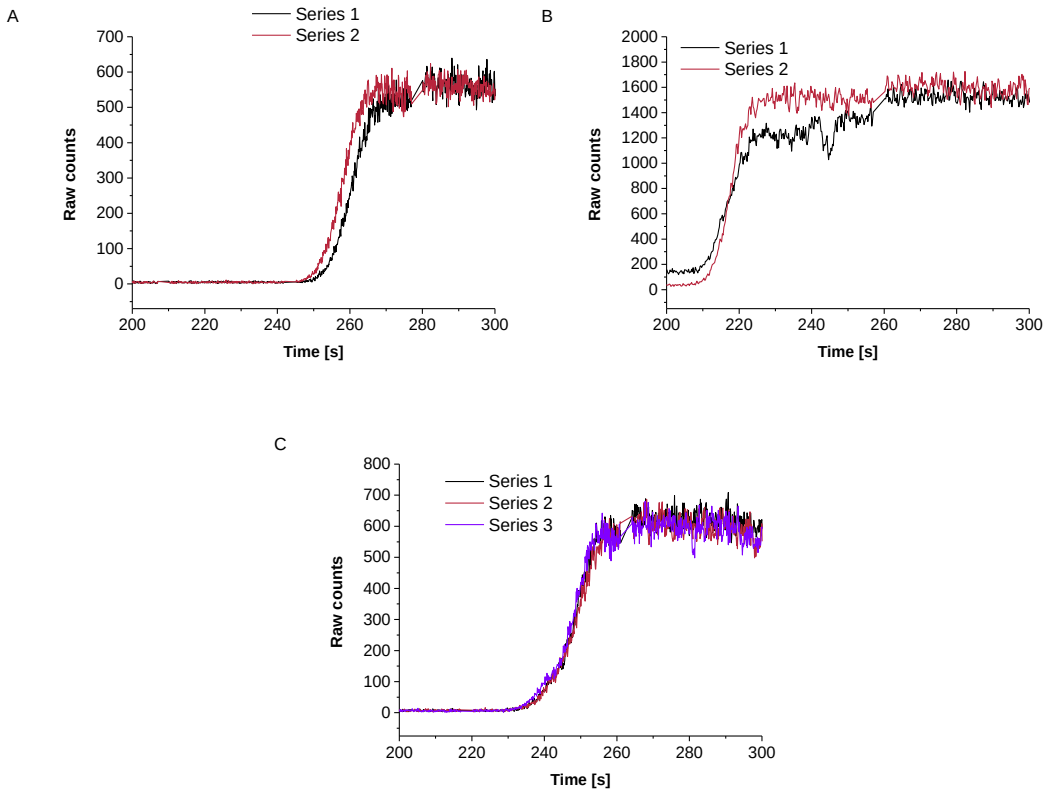


**Figure 5.7: Comparison of GEMMA results for Ovalbumin (A), BSA (B), IgG (C) in FM**

| | | |
|---|---|---|
| Electrolyte: 20 mM $NH_4OAc$, pH 8.4 | Voltage: 2.7 kV | Sheath flow: 13.5 lpm |
| Sample: Ovalbumin, BSA, IgG | Current: 300-400 nA | Pressure: 1.4 psid |
| Concentration: 1 µM | $CO_2$: 0.1 lpm | individual measurements |
| Capillary: 25 µm id | Air: 1 lpm | mode: FM |

The migration time of BSA and IgG at pH 8.4 does not differ significantly from the results at pH 7.4. On the other hand the migration time of Ovalbumin increased from 210 seconds to 250 seconds with increasing pH. The explanation for this increase could be the inaccurate pressure adjustment for that particular analysis, because of the stable migration time of other two proteins. The procedure of measurements at lower psid levels was optimized later: for the results shown above pressure was adjusted for every measurement, in later runs all analytes were measured consecutively without manipulation of pressure (washing with $NH_4OAc$ was also performed under corresponding conditions).

The following GEMMA measurements were carried out reducing the pressure in the pressure chamber even further to $\Delta p = 0.8$ psid. The resulting GEMMA spectra may be seen in Figures 5.8 – 5.10. Results for pH 7.4, 8.4 and 9.4 are shown, respectively.

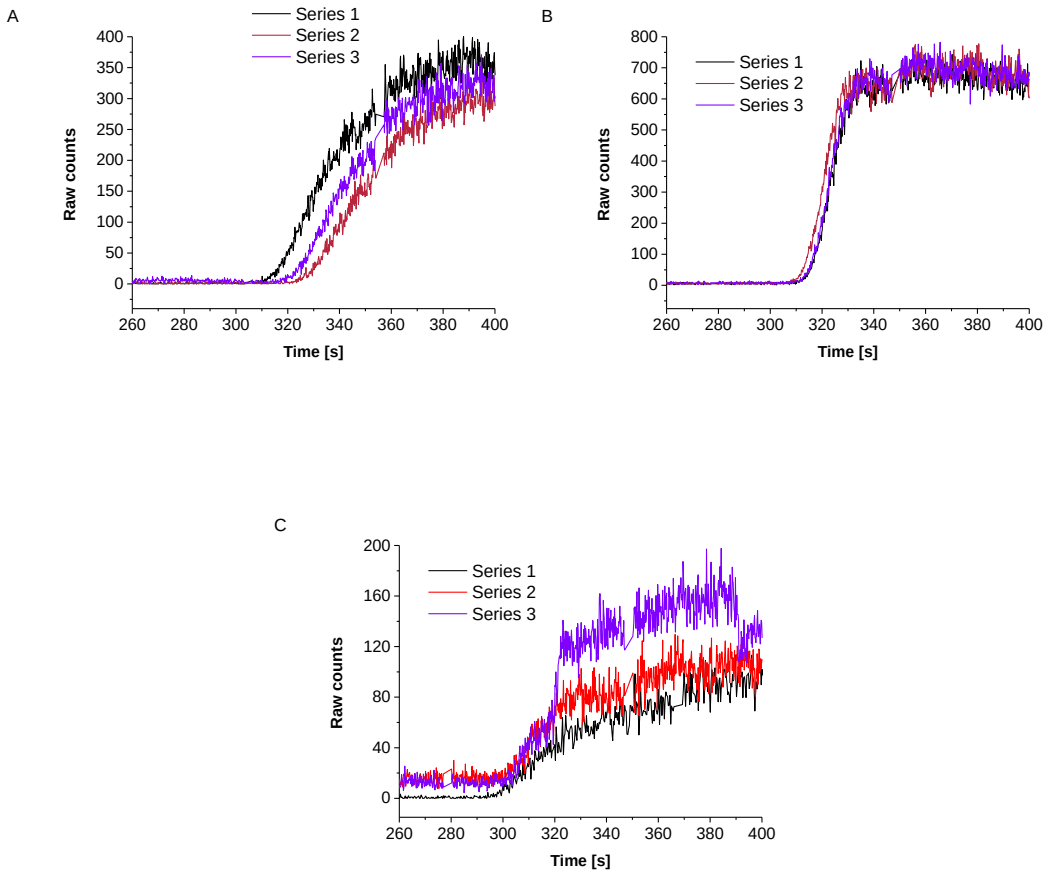


**Figure 5.8: Comparison of GEMMA results for Ovalbumin (A), BSA (B), IgG (C) in FM**

| | | |
|---|---|---|
| Electrolyte: 20 mM $NH_4OAc$, pH 7.4 | Voltage: 2.7 kV | Sheath flow: 13.5 lpm |
| Sample: Ovalbumin, BSA, IgG | Current: 300-400 nA | Pressure: 0.8 psid |
| Concentration: 1 µM | $CO_2$: 0.1 lpm | individual measurements |
| Capillary: 25 µm id | Air: 1 lpm | mode: FM |

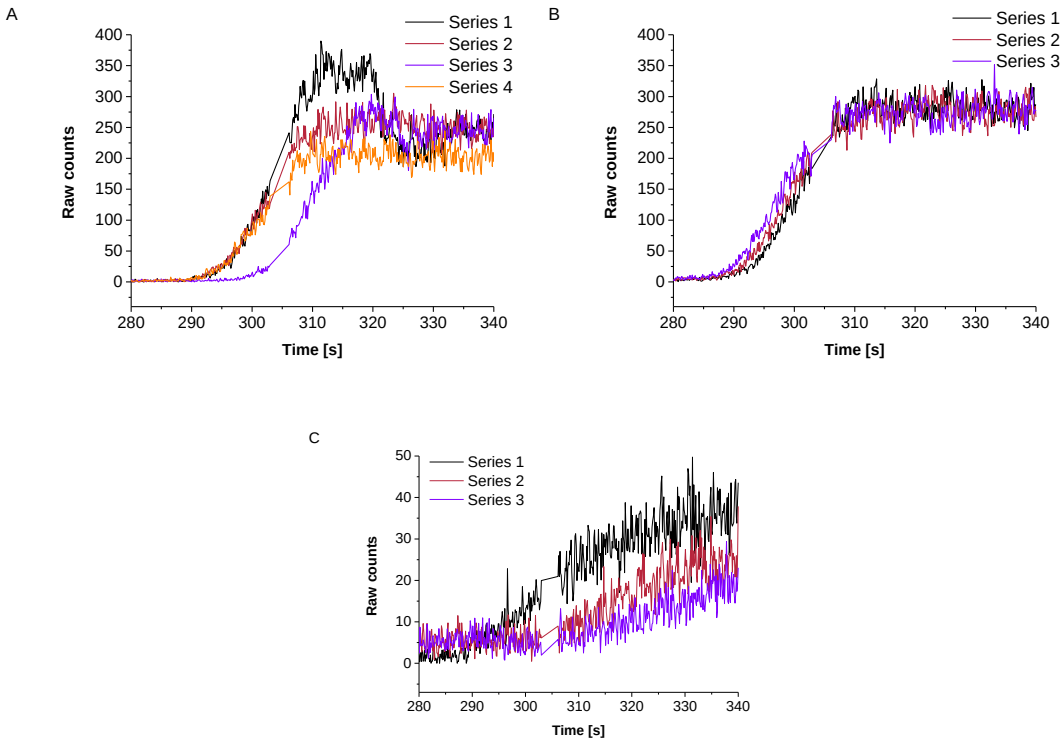


**Figure 5.9: Comparison of GEMMA results for Ovalbumin (A), BSA (B), IgG (C) in FM**

| | | |
|---|---|---|
| Electrolyte: 20 mM $NH_4OAc$, pH 8.4 | Voltage: 2.7 kV | Sheath flow: 13.5 lpm |
| Sample: Ovalbumin, BSA, IgG | Current: 300-400 nA | Pressure: 0.8 psid |
| Concentration: 1 µM | $CO_2$: 0.1 lpm | individual measurements |
| Capillary: 25 µm id | Air: 1 lpm | mode: FM |

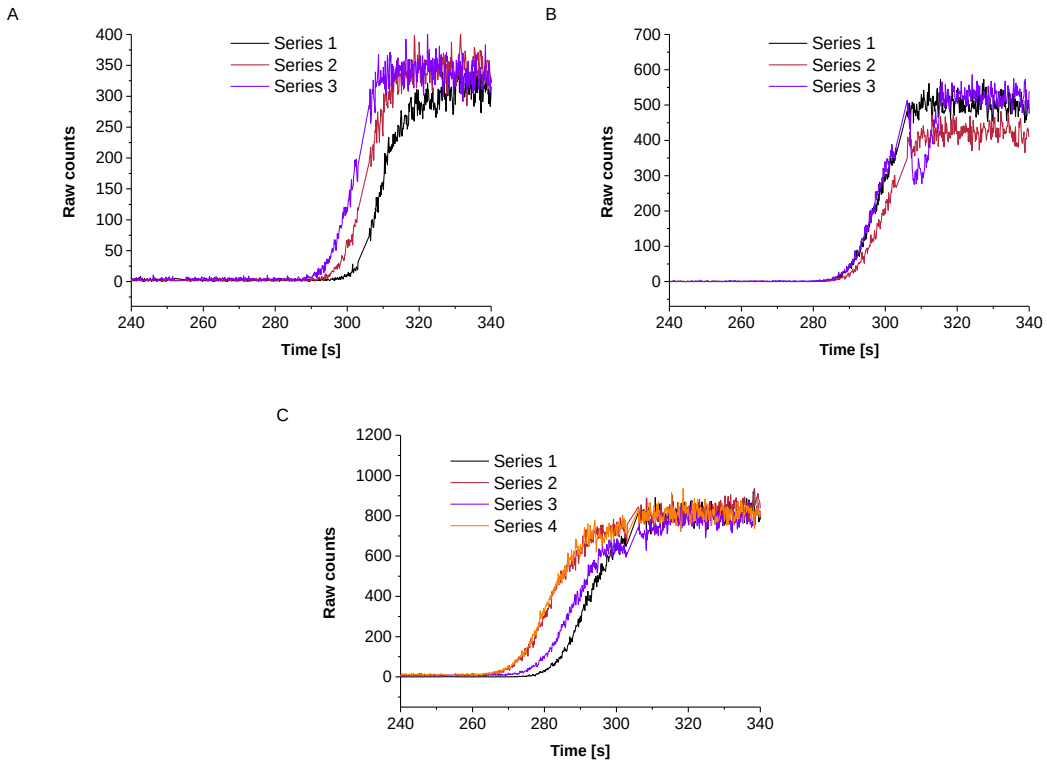


**Figure 5.10: Comparison of GEMMA results for Ovalbumin (A), BSA (B), IgG (C) in FM**

| | | |
|---|---|---|
| Electrolyte: 20 mM $NH_4OAc$, pH 9.4 | Voltage: 2.7 kV | Sheath flow: 13.5 lpm |
| Sample: Ovalbumin, BSA, IgG | Current: 300-400 nA | Pressure: 0.8 psid |
| Concentration: 1 µM | $CO_2$: 0.1 lpm | individual measurements |
| Capillary: 25 µm id | Air: 1 lpm | mode: FM |

The migration time of analytes is increasing with a decreasing pressure in the pressure chamber, as deduced already from in Hagen- Poiseuille equation. The other effect caused by a decreased pressure is the decreasing signal of analytes (i.e. Figures 5.5A, 5.6A, 5.8A: Ovalbumin 3.4 psid 1500 - 2500 raw counts, 1.4 psid: 600-700 raw counts, 0.8 psid: 300-400 raw counts).

The results of analysis of IgG at pH 8.4 is not considered as reliable, the signal is very low, there is a low signal to noise ratio. It is difficult to recognize the time when IgG molecules reach the detector. The possible reason may be the quality of sample. The later results were performed with new stock, the obtained results showed significantly higher signal of analytes.

At pH 7.4 Ovalbumin is the analyte with the longest migration time (~320s), following by BSA (~310s) and IgG (~300s). At pH 8.4 (without regarding results of IgG) is the migration time of Ovalbumin (~290s) also longer than that of BSA (~285s). Results at pH 9.4 show also Ovalbumin as the slowest analyte (~295s), BSA (~290s) and IgG (~275s) are faster. IgG has the smallest mobility (mobility is directed against EOF away from the capillary tip) and because of that appears as first analyte at the detector. BSA should pass the capillary later than Ovalbumin because of its higher mobility, but in the experiments, the migration time of Ovalbumin is about 5 seconds shorter than the migration time of BSA. However, a 5 seconds difference between analytes was not regarded to be significant as it might result from handling of the instrument. A point to discuss is a big difference of migration time of the same analytes at pH 7.4, 8.4 and 9.4. Following the knowledge that EOF is increasing with pH (mobility of ions is increasing just slightly) the migration of analytes at pH 9.4 should be faster than at lower pH. This is not the case in the results shown above (i.e. Ovalbumin pH 8.4 ~290s, pH 9.4 ~295s). The difference of migration times among analytes can be also caused by an inaccurate pressure setting.

Measurements at lower sheath flows (in the electrospray unit) were also performed. Protein analysis in FM at 0.8 psid, 0.6 lpm Air, 0.1 lpm $CO_2$ and pH levels 7.4, 8.4, 9.4 was possible. Migration times of analytes are still obtainable under these conditions. However, reproducibility problems appeared, as the same sample vial was used for repeated injections. Buffer electrolysis may occur influencing the mobility of analytes.

Additionally, it appears that the comparison of migration times in this set of measurements is difficult due to insufficiently precise pressure adjustment with a standard, commercially available GEMMA instrument. For the optimization of FM settings more measurements were needed.

Figure 5.11 show the results of the migration times (only Ovalbumin and BSA, there were problems with IgG sample, stable signal could not be observed, as already mentioned in results showed in Figure 5.9C) in FM at lower Macrolon: 3.4 psid, 0.2 lpm Air, 0.1 lpm $CO_2$, pH 8.4 and higher pressure values in the sample chamber.

Figure 5.11 demonstrates that there is a good signal/noise ratio even at lower Macrolon values, the information about migration time of analytes can be determined also at 0.2 lpm Air and 0.1 lpm $CO_2$. The migration times of Ovalbumin and BSA do not differ, the high pressure (3.4 psid) is the main force rendering other forces in the capillary negligible.

Next measurements were performed at 1.4 psid, 0.2 lpm Air, 0.1 lpm $CO_2$, pH 7.4 and 8.4. The GEMMA spectra of Ovalbumin, BSA, IgG are depicted in Figures 5.12 – 5.14.

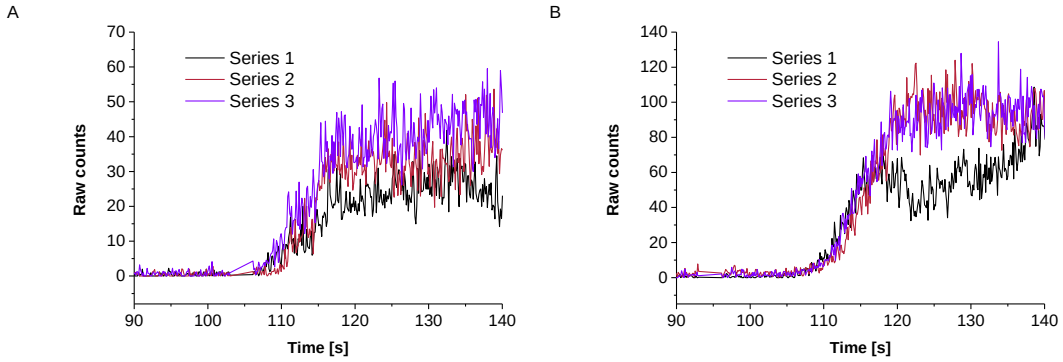


**Figure 5.11 Comparison of GEMMA results for Ovalbumin (A), BSA (B) in FM**

| | | |
|---|---|---|
| Electrolyte: 20 mM $NH_4OAc$, pH 8.4 | Voltage: 2.7 kV | Sheath flow: 13.5 lpm |
| Sample: Ovalbumin, BSA | Current: 300-400 nA | Pressure: 3.4 psid |
| Concentration: 1 µM | $CO_2$: 0.1 lpm | individual measurements |
| Capillary: 25 µm id | Air: 0.2 lpm | mode: FM |

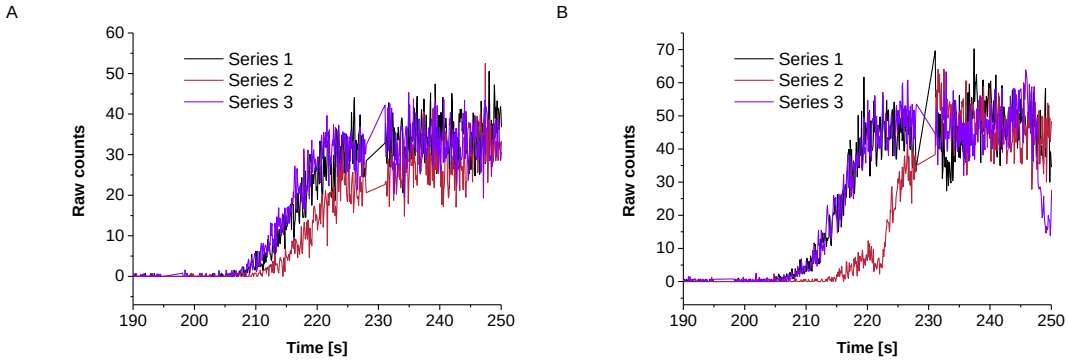


**Figure 5.12: Comparison of GEMMA results for Ovalbumin at pH 7.4 (A) and pH 8.4 (B) in FM**

| | | |
|---|---|---|
| Electrolyte: 20 mM $NH_4OAc$, pH 7.4 & 8.4 | Voltage: 2.7 kV | Sheath flow: 13.5 lpm |
| Sample: Ovalbumin | Current: 300-400 nA | Pressure: 1.4 psid |
| Concentration: 1 µM | $CO_2$: 0.1 lpm | individual measurements |
| Capillary: 25 µm id | Air: 0.2 lpm | mode: FM |

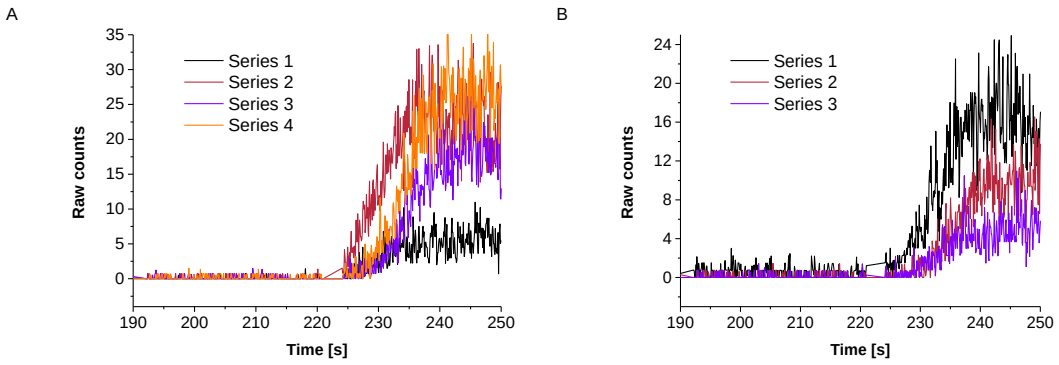


**Figure 5.13: Comparison of GEMMA results for BSA at pH 7.4 (A) and pH 8.4 (B) in FM**

| | | |
|---|---|---|
| Electrolyte: 20 mM $NH_4OAc$, pH 7.4 | Voltage: 2.7 kV | Sheath flow: 13.5 lpm |
| Sample: BSA | Current: 300-400 nA | Pressure: 1.4 psid |
| Concentration: 1 µM | $CO_2$: 0.1 lpm | individual measurements |
| Capillary: 25 µm id | Air: 0.2 lpm | mode: FM |

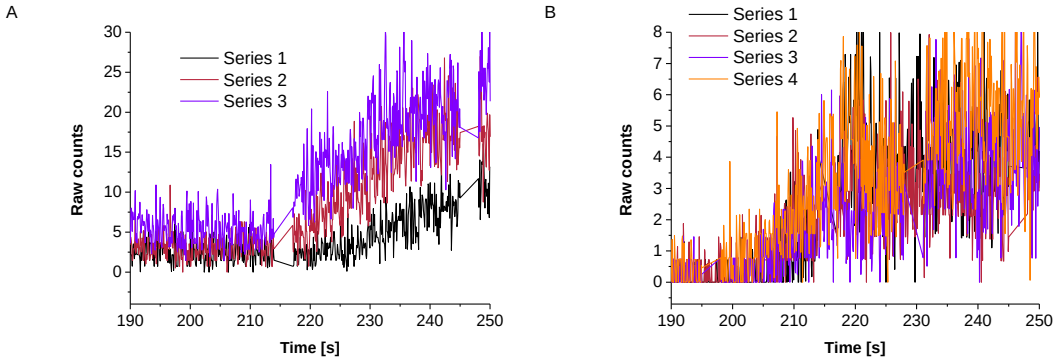


**Figure 5.14: Comparison of GEMMA results for IgG at pH 7.4 (A) and pH 8.4 (B) in FM**

| | | |
|---|---|---|
| Electrolyte: 20 mM $NH_4OAc$, pH 7.4 & 8.4 | Voltage: 2.7 kV | Sheath flow: 13.5 lpm |
| Sample: IgG | Current: 300-400 nA | Pressure: 1.4 psid |
| Concentration: 1 µM | $CO_2$: 0.1 lpm | individual measurements |
| Capillary: 25 µm id | Air: 0.2 lpm | mode: FM |

Figures 5.12 – 5.14 demonstrate the migration times of analytes at 1.4 psid and 0.3 lpm Macrolon. The migration time of BSA is the longest one at pH 7.4 (~ 225 s) as well as at pH 8.4 (~ 225 s) which correlates with theory described in section 5.1.6. IgG passes the capillary at 210 s at pH 7.4 or in 200 s at pH 8.4. This is the shortest migration time from the

three investigated analytes, confirmed also by theoretical considerations given in section 5.1.5. The mobility of Ovalbumin is smaller than BSA what makes the migration time shorter at pH 7.4 (~ 205 s) as well as at pH 8.4 (~ 205 s).

As already mentioned, the inaccurate pressure adjustment and manipulation with pressure after each run lead to significant pressure variation. To determine the lowest pressure with these Macrolon settings (0.2 lpm Air, 0.1 lpm $CO_2$) where the migration time is still possible to determine, the pressure was lowered to 0.8 psid and FM measurements were carried out. The results are depicted in Figure 5.15:

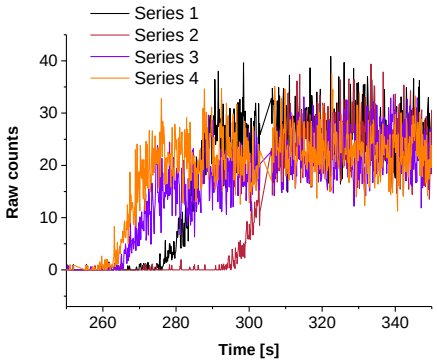


**Figure 5.15: GEMMA results of Ovalbumin at low Macrolon and low pressure difference in the pressure chamber (FM)**

| | | |
|---|---|---|
| Electrolyte: 20 mM $NH_4OAc$, pH 8.4 | Voltage: 2.7 kV | Sheath flow: 13.5 lpm |
| Sample: Ovalbumin | Current: 300-400 nA | Pressure: 0.8 psid |
| Concentration: 1 µM | $CO_2$: 0.1 lpm | individual measurements |
| Capillary: 25 µm id | Air: 0.2 lpm | mode: FM |

Measurements of BSA and IgG at 0.8 psid, 0.2 lpm Air, 0.1 lpm $CO_2$ could not be performed successfully, because of an instable electrospray generated by the low pressure and Macrolon. Results obtained for Ovalbumin also show noise present in the spectrum and due to this reason these low Macrolon conditions appear not to be suitable for FM of analytes.

In general, migration times determined at lower pressure are not as reproducible as values obtained at higher pressure applied in the pressure chamber. On the other hand, differences of the migration times of proteins are increasing with a decreasing pressure. Because of that these conditions are more suitable for CM. The reproducibility of results was increased with a new procedure used for CM: the pressure for all of measurements done in one day was set at the beginning of the measurement series. No pressure manipulation was

carried out between samples. Such, constant conditions for all analyses taken place in one day (the set of measurements with same conditions measured was preferably analyzed in one day) were obtained. Additionally, injections were only carried out once for each vial to reduce any electrolysis effects.

The other parameter that could possibly be optimized for analyte separation is the electrolyte pH. Differences of analytes` migration times at same pressure and different pH are not significantly (i.e. Figures 5.8 – 5.10, mostly 5 seconds difference between analytes). Therefore the influence of the pH can be neglected.

At higher pH levels the silanol groups of the fused silica capillary are deprotonated, stable CE conditions in the capillary are ensured. Measurements at pH 9.4 showed a reproducible FM profile in all runs. The reduction of the sheath flow at the capillary tip did not influence the migration time of analytes (theoretically discussed in 3.1). Because of that finding a higher sheath flow level with a higher signal/noise ratio was chosen.

### 5.1.7 Additional GEMMA measurements in CM

There were more experiments in CM necessary to obtain stable measurement conditions as described in 3.1. In the beginning the plug time as well as the concentration of the sample had to be optimized. There were 0.5 µM and 1 µM single protein samples (Ovalbumin, BSA or IgG) at pH 8.4 and pH 9.4 analyzed. The EM diameter measured in the detector remained constant over time. Ovalbumin was analyzed at 6.0 nm, BSA at 7.0 nm, IgG at 9.0 nm. The plug time was set 1 s – 5 s as indicated. The results are depicted in Figures 5.16 and 5.17.

Figure 5.16

| c = 1 µM; 5s plug time | c = 1 µM; 2s plug time | c = 0.5 µM; 5 s plug time | c = 0.5 µM, 1 s plug time |
|---|---|---|---|

Ovalbumin

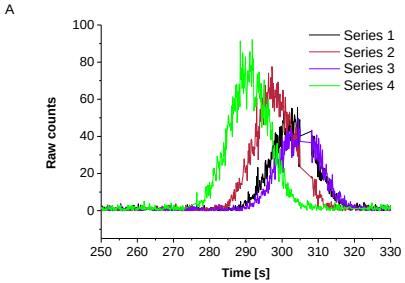


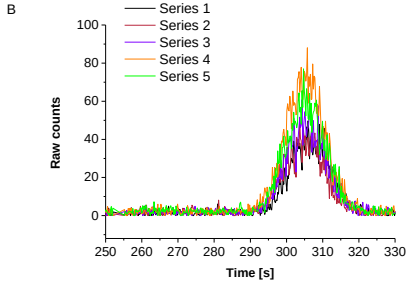


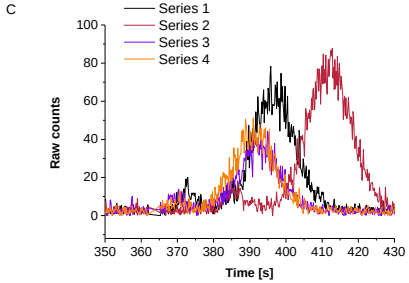


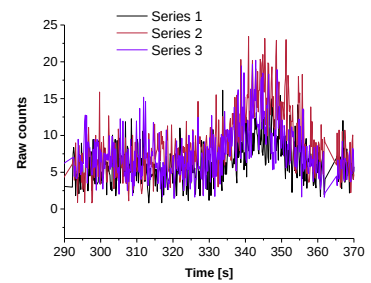


BSA

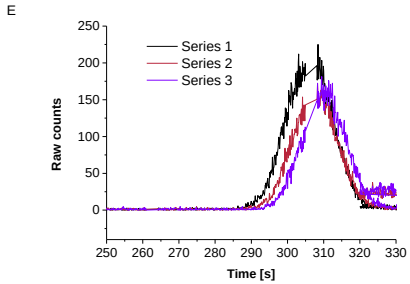


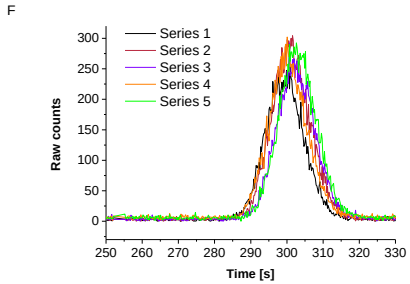


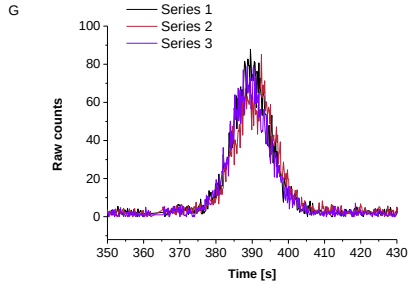


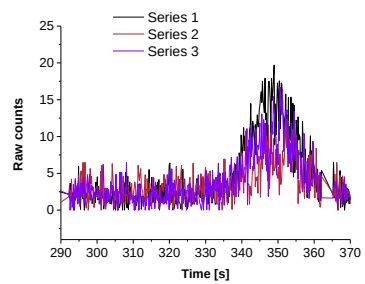


IgG

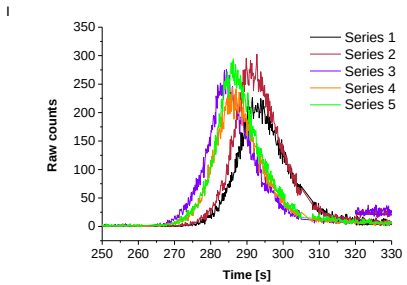


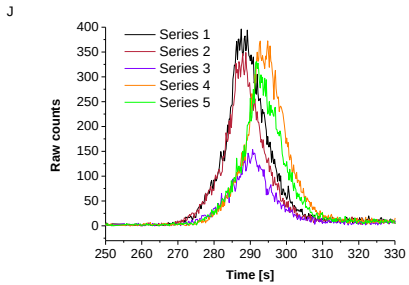


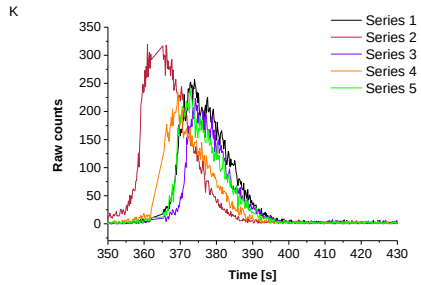


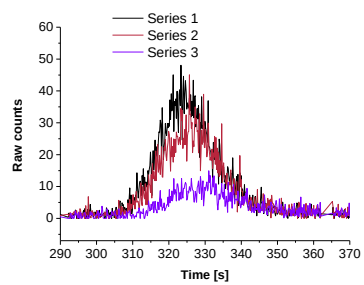

**Figure 5.16: Comparison of GEMMA results for Ovalbumin, BSA and IgG respectively at pH 9.4 in CM**

| | | | | | |
|---|---|---|---|---|---|
| Electrolyte: 20 mM $NH_4OAc$, pH 9.4 | Voltage: 2.7 kV | Sheath flow: 13.5 lpm | Concentration: 0.5 µM & 1 µM | $CO_2$: 0.1 lpm | individual measurements |
| Sample: Ovalbumin, BSA, IgG | Current: 300-400 nA | Pressure: 0.8 psid | Capillary: 25 µm id | Air: 0.6lpm | mode: CM, 1 s – 5 s plug |

Figure 5.17

| | Δp = 0.8psid; c = 0.5 µM | Δp = 1.4 psid; c = 1 µM |
|---|---|---|
| Ovalbumin | A 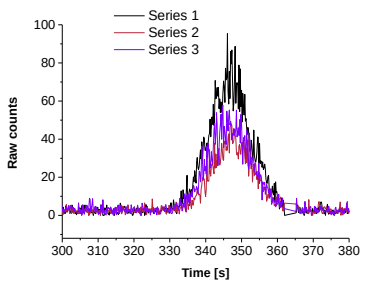 | B 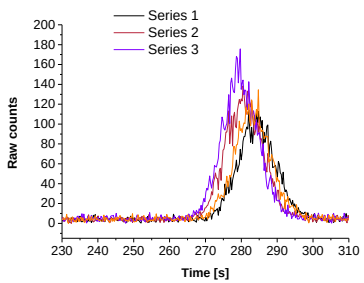 |
| BSA | C 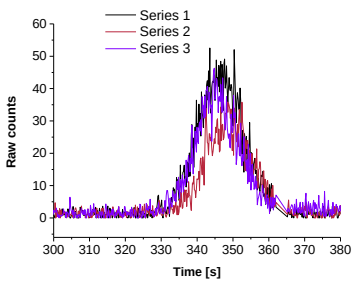 | D 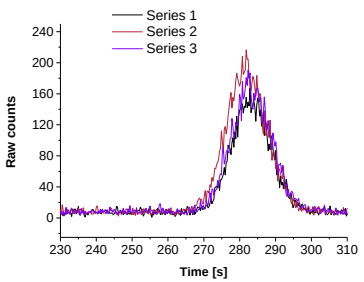 |

IgG


**Figure 5.17: Comparison of GEMMA results for Ovalbumin, BSA and IgG respectively at pH 8.4 in CM**

| | | | | | |
|---|---|---|---|---|---|
| Electrolyte: 20 mM $NH_4OAc$, pH 8.4 | Voltage: 2.7 kV | Sheath flow: 13.5 lpm | Concentration: 0.5 µM & 1 µM | $CO_2$: 0.1 lpm | individual measurements |
| Sample: Ovalbumin, BSA, IgG | Current: 300-400 nA | Pressure: 0.8 psid (A,C,E) & 1.4 psid (B.D,F) | Capillary: 25 µm id | Air: 0.6lpm | mode: CM, 5 s plug |

In Figure 5.16 the plugs of Ovalbumin, BSA and IgG are visible in all cases, the difference of time profile between BSA and Ovalbumin is small under every condition (Ovalbumin results in 5.16A and 5.16C are not stable and were not considered). The instability of results may be caused by the inaccurate pressure adjustment as already mentioned in section 5.1.6. The procedure of measurements at lower psid levels was optimized later, for Figure 5.16 the pressure was adjusted for every measurement.

IgG is detected about 20 seconds sooner than BSA under all conditions. The peak width for both proteins is about 30 – 40 s at the basis. Considering results presented above, the best separation of these analytes would take place at c = 0.5 µM and a plug time 1 s. The smaller amount of analyte fed to the capillary is responsible for the smaller width and height of the peaks. Analytes could be separated from each other. On the other hand the signal noise ratio is worse. Additionally, the 1 s plugs are also not reproducible because of the time needed for changing of vials in the pressure chamber in just one second. Because of that 2 s plug were preferred for the further experiments.

The smaller concentration of the sample did not change the quality of results significantly. For further experiments, samples with c = 1µM were preferred because of the higher sample signal obtained at this concentration.

The reproducibility of the experiments as shown in Figure 5.17 increased significantly, the experiments were done in one day without manipulation of the pressure between samples. The pressure was kept constant even when the capillary was washed with ammonium acetate. At 0.8 psid, c = 0.5 µM, 5 s plug, the differences of migration times among analytes are similar at both pH levels. Therefore, both pH levels are suitable for CM.

Results at increased pressure (1.4 psid, see Figures 5.17B, 5.17D, 5.17F) show that the difference of time profiles of IgG and BSA disappears under these conditions, the pressure in nano ES has to be held at lower levels to enable the separation of analytes.

In the next step IgG (c = 1µM) and BSA (c = 1µM), pH 9.4 were mixed together and the separation of these analytes was investigated (Figure 5.18). To detect both analytes, the EM diameter range between 6 nm and 12 nm was scanned in a sequence of consecutive runs.

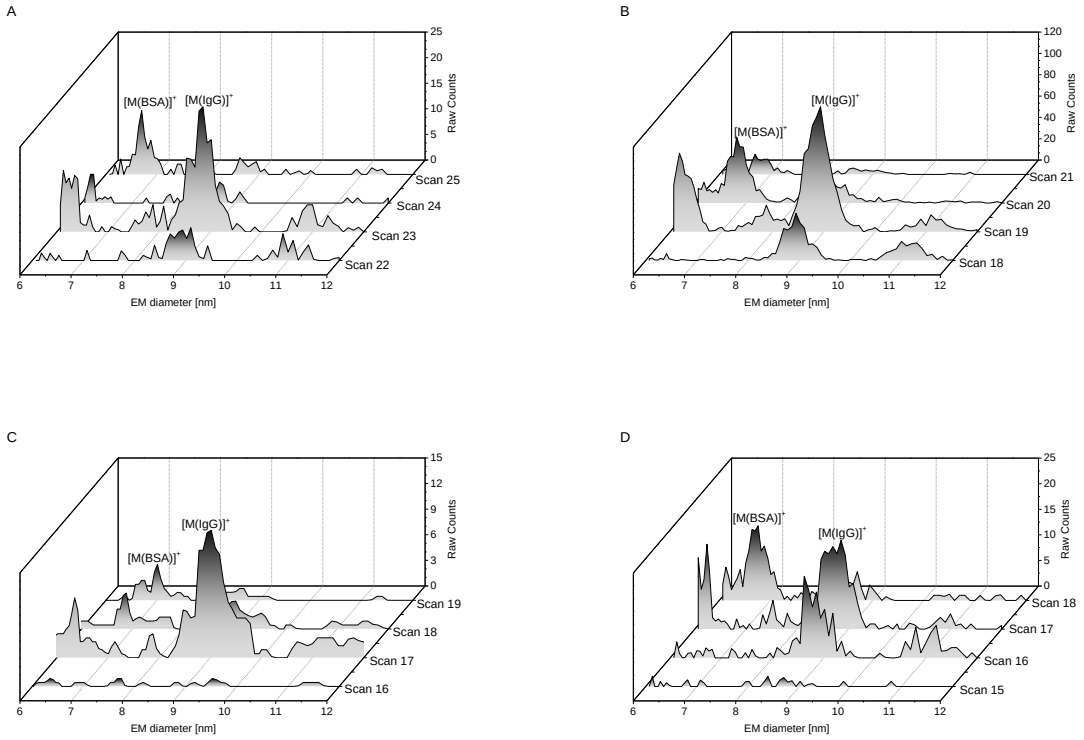


**Figure 5.18: Separation of BSA and IgG in CM, comparison of pressure and plug time, A: 0.6 psid, 3 s plug time; B: 0.8 psid, 2 s plug time, C: 0.9 psid, 1 s plug time, D: 1 psid, 2 s plug time**

| | | |
|---|---|---|
| Electrolyte: 20 mM $NH_4OAc$, pH 9.4 | Voltage: 2.7 kV | Sheath flow: 13.5 lpm |
| Sample: BSA & IgG | Current: 300-400 nA | Pressure: 0.6 psid - 1psid |
| Concentration: 1 µM | $CO_2$: 0.1 lpm | individual measurements |
| Capillary: 25 µm id | Air: 1 lpm | mode: CM, 1 s – 3 s plug |

From Figure 5.18 it can be concluded that the separation of samples containing BSA & IgG in CM was achieved. For almost all sequences, in one of the scans the IgG peak at 9 nm can be recognized (i.e. scan 19 in 5.18B), in the following scan BSA peak (~ 7 nm) can be detected (i.e. scan 20 in 5.18B). The results at pressure 0.6 psid in pressure chamber (Figure 5.18A) show a very low signal. Spectra recorded with 1 s plug (Figure 5.18C) yielded comparable results. Therefore, the CM measurements should be taken at least under 1 psid pressure in pressure chamber and 2 s plug time (see Figure 5 in 3.1). The same conditions as in results shown in Figure 5 in 3.1 were applied for the analysis of sample with pH 8.4 (see Figure 5.19 for median of 6 CM runs). To sum up the separation of BSA and IgG in CM was successful, 1 psid in the pressure chamber is necessary for sufficient signal of analytes, the separation worked better at pH 9.4 than 8.4.

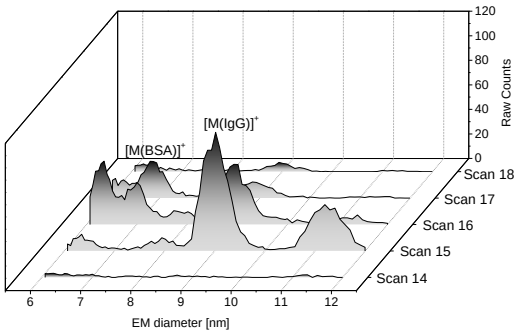


**Figure 5.19: GEMMA results for IgG and BSA sample in CM at pH 8.4**

| | | |
|---|---|---|
| Electrolyte: 20 mM $NH_4OAc$, pH 8.4 | Voltage: 2.7 kV | Sheath flow: 13.5 lpm |
| Sample: BSA & IgG | Current: 300-400 nA | Pressure: 1 psid |
| Concentration: 1 µM | $CO_2$: 0.1 lpm | median of 6 measurements |
| Capillary: 25 µm id | Air: 1 lpm | mode: CM, 2 s plug |

In Figure 5.19 the separation of BSA and IgG can be observed, IgG (EM diameter 9 nm) can be found in scans 15 and 16, BSA (EM diameter 7 nm) can be found in scans 16 and 17, however the separation at pH 9.4 went better, the IgG can be basically found only in peak 15 and BSA only in scan 16.

### 5.1.8 Additional online desalting experiments in the nano ES capillary through electrophoretic analyte separation

In 5.1.8 the online desalting of protein samples in CM is demonstrated. This is the first application of the new developed CM. The online desalting experiments were performed with samples containing BSA (c = 1 µM), IgG (c = 1 µM) and NaCl (0.5 mM – 5 mM, the results of 5 mM are shown in Figure 6 in 3.1). Measurements were done in NM as well as in CM. The particle counts of CM scans were normalized to allow the comparison of spectra. NM measurements were normalized as well. The results are depicted in Figures 5.20 – 5.21. The corresponding blanks are depicted in Figures 5.22 – 5.25.

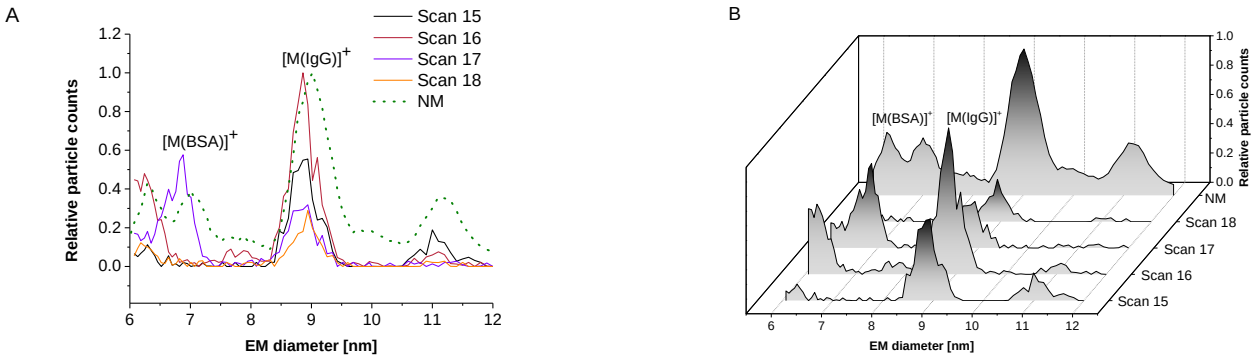


**Figure 5.20: Comparison of GEMMA spectra obtained for a BSA and IgG containing sample with sodium chloride addition (0.5 mM) in NM and CM depicted in 2D (A) and 3D (B)**

| | | |
|---|---|---|
| Electrolyte: 20 mM $NH_4OAc$, pH 9.4 | Voltage: 2.7 kV | Sheath flow: 13.5 lpm |
| Sample: BSA, IgG & NaCl | Current: 300-400 nA | Pressure: 1 psid |
| Concentration: BSA & IgG: 1 µM; NaCl : 0.5 mM | $CO_2$: 0.1 lpm | median of 6 measurements |
| Capillary: 25 µm id | Air: 1 lpm | 2 s plug (CM) as well NM ("NM") |

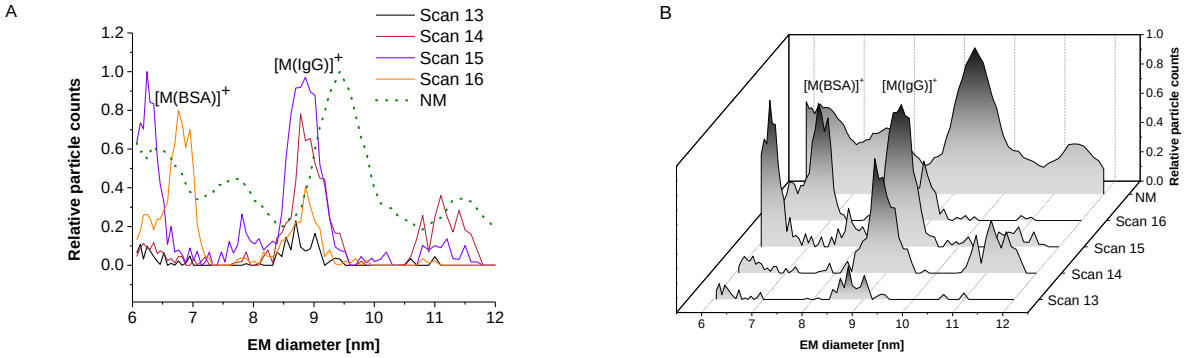


**Figure 5.21: Comparison of GEMMA spectra obtained for a BSA and IgG containing sample with sodium chloride addition (2 mM) in NM and CM depicted in 2D (A) and 3D (B)**

| | | |
|---|---|---|
| Electrolyte: 20 mM $NH_4OAc$, pH 9.4 | Voltage: 2.7 kV | Sheath flow: 13.5 lpm |
| Sample: BSA, IgG & NaCl | Current: 300-400 nA | Pressure: 1 psid |
| Concentration: BSA & IgG: 1 µM; NaCl : 2 mM | $CO_2$: 0.1 lpm | median of 6 measurements |
| Capillary: 25 µm id | Air: 1 lpm | 2 s plug (CM) as well NM ("NM") |

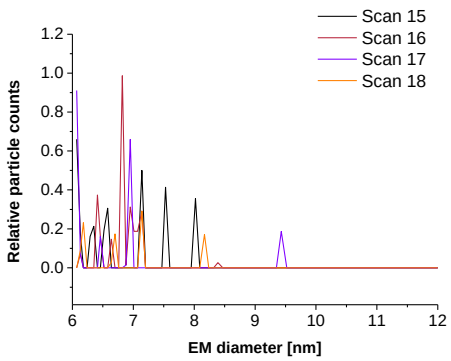


**Figure 5.22: GEMMA spectra obtained for blanks corresponding to Figure 5.20 (sample with sodium chloride 0.5 mM) in CM**

| | | |
|---|---|---|
| Electrolyte: 20 mM $NH_4OAc$, pH 9.4 | Voltage: 2.7 kV | Sheath flow: 13.5 lpm |
| Sample: NaCl | Current: 300-400 nA | Pressure: 1 psid |
| Concentration: NaCl : 0.5 mM | $CO_2$: 0.1 lpm | median of 6 measurements |
| Capillary: 25 µm id | Air: 1 lpm | mode: CM, 2 s plug |

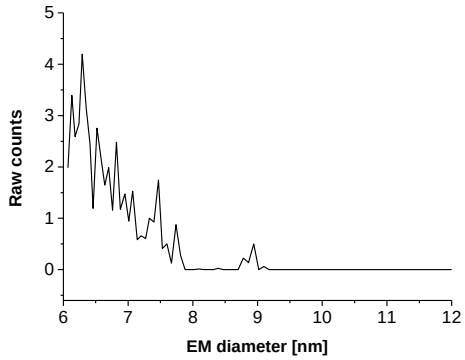


**Figure 5.23: GEMMA spectra obtained for blanks corresponding to Figure 5.20 (sample with sodium chloride 0.5 mM) in NM**

| | | |
|---|---|---|
| Electrolyte: 20 mM $NH_4OAc$, pH 9.4 | Voltage: 2.7 kV | Sheath flow: 13.5 lpm |
| Sample: NaCl | Current: 300-400 nA | Pressure: 1 psid |
| Concentration: NaCl : 0.5 mM | $CO_2$: 0.1 lpm | median of 6 measurements |
| Capillary: 25 µm id | Air: 1 lpm | mode: NM |

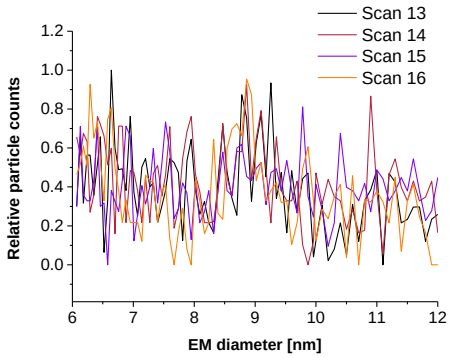


**Figure 5.24: GEMMA spectra obtained for blanks corresponding to Figure 5.21 (sample with sodium chloride 2 mM) in CM**

| | | |
|---|---|---|
| Electrolyte: 20 mM $NH_4OAc$, pH 9.4 | Voltage: 2.7 kV | Sheath flow: 13.5 lpm |
| Sample: NaCl | Current: 300-400 nA | Pressure: 1 psid |
| Concentration: NaCl : 2 mM | $CO_2$: 0.1 lpm | median of 6 measurements |
| Capillary: 25 µm id | Air: 1 lpm | mode: CM, 2 s plug |

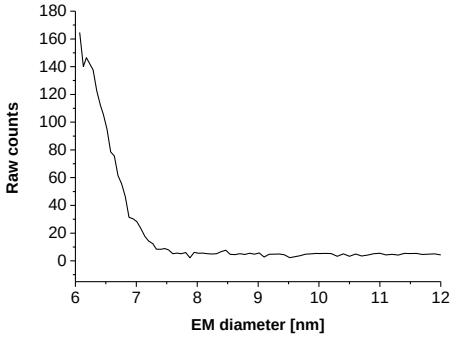


**Figure 5.25: GEMMA spectra obtained for blanks corresponding to Figure 5.21 (sample with sodium chloride 2 mM) in NM**

| | | |
|---|---|---|
| Electrolyte: 20 mM $NH_4OAc$, pH 9.4 | Voltage: 2.7 kV | Sheath flow: 13.5 lpm |
| Sample: NaCl | Current: 300-400 nA | Pressure: 1 psid |
| Concentration: NaCl : 2 mM | $CO_2$: 0.1 lpm | median of 6 measurements |
| Capillary: 25 µm id | Air: 1 lpm | mode: NM |

From Figures 5.20 – 5.21 the online desalting of the samples can be observed. In NM the EM diameter of BSA and IgG significantly increases (in 2 mM NaCl BSA ~ 7.5 nm, IgG ~ 9.5 nm) due to salt molecules attaching on the surface of protein molecules during drying of droplets from ES process. With increasing salt concentration a concomitant increase in EM diameters can be detected (see Figure 5.20 – 5.21).

In CM the desalted BSA (EM diameter ~ 7 nm) and IgG (EM diameter ~ 9 nm) can be detected, the analytes were also separated from each other, BSA and IgG are detected in different scans of CM. Additionally, no interaction with insoluble salt molecules is observed. In the blanks (see Figures 5.22 – 5.25) no peaks between 6 nm and 12 nm are detected confirming the online desalting and separation of BSA and IgG.

## 5.2 Amino acid sequences of analyzed proteins and protein complexes

Amino acid sequence of m-Cherry vault unit (average molecular weight 123.6 kDa) consisting of m-Cherry molecule (in red) and linker (in yellow) followed by MVP unit:

MVSKGEEDNMAIIKEFMRFKVHMEGSVNGHEFEIEGEGEGRPYEGTQTAKLKVTKG
GPLPFAWDILSPQFMYGSKAYVKHPADIPDYLKLSFPEGFKWERVMNFEDGGVVTVT
QDSSLQDGEFIYKVKLRGTNFPSDGPVMQKKTMGWEASSERMYPEDGALKGEIKQR
LKLKDGGHYDAEVKTTYKAKKPVQLPGAYNVNIKLDITSHNEDYTIVEQYERAEGR
HSTGGMDELYKLMAGCGCPCGCGAMATEEAIIRIPPYHYIHVLDQNSNVSRVEVGPK
TYIRQDNERVLFAPVRMVTVPPRHYCIVANPVSRDTQSSVLFDITGQVRLRHADQEIR
LAQDPFPLYPGEVLEKDITPLQVVLPNTALHLKALLDFEDKNGDKVMAGDEWLFEGP
GTYIPQKEVEVVEIIQATVIKQNQALRLRARKECFDREGKGRVTGEEWLVRSVGAYL
PAVFEEVLDLVDAVILTEKTALHLRALQNFRDLRGVLHRTGEEWLVTVQDTEAHVP
DVYEEVLGVVPITTLGPRHYCVILDPMGPDGKNQLGQKRVVKGEKSFFLQPGERLER
GIQDVYVLSEQQGLLLKALQPLEEGESEEKVSHQAGDCWLIRGPLEYVPSAKVEVVE
ERQAIPLDQNEGIYVQDVKTGKVRAVIGSTYMLTQDEVLWEKELPSGVEELLNLGHD
PLADRGQKGTAKPLQPSAPRNKTRVVSYRVPHNAAVQVYDYRAKRARVVFGPELVT
LDPEEQFTVLSLSAGRPKRPHARRALCLLLGPDFFTDVITIETADHARLQLQLAYNWH
FELKNRNDPAEAAKLFSVPDFVGDACKAIASRVRGAVASVTFDDFHKNSARIIRMAV
FGFEMSEDTGPDGTLLPKARDQAVFPQNGLVVSSVDVQSVEPVDQRTRDALQRSVQ
LAIEITTNSQEAAAKHEAQRLEQEARGRLERQKILDQSEAEKARKELLELEAMSMAV
ESTGNAKAEAESRAEAARIEGEGSVLQAKLKAQALAIETEAELERVKKVREMELIYA
RAQLELEVSKAQQLANVEAKKFKEMTEALGPGTIRDLAVAGPEMQVKLLQSLGLKS
TLITDGSSPINLFSTAFGLLGLGSDGQPPAQK

Amino acid sequence of vsvg vault unit (average molecular weight 96.8 kDa) consisting of vsvg tag (in blue) followed by MVP unit:

MAGCGCPCGCGAMATEEAIIRIPPYHYIHVLDQNSNVSRVEVGPKTYIRQDNERVLFA
PVRMVTVPPRHYCIVANPVSRDTQSSVLFDITGQVRLRHADQEIRLAQDPFPLYPGEV
LEKDITPLQVVLPNTALHLKALLDFEDKNGDKVMAGDEWLFEGPGTYIPQKEVEVVE
IIQATVIKQNQALRLRARKECFDREGKGRVTGEEWLVRSVGAYLPAVFEEVLDLVDA
VILTEKTALHLRALQNFRDLRGVLHRTGEEWLVTVQDTEAHVPDVYEEVLGVVPITT
LGPRHYCVILDPMGPDGKNQLGQKRVVKGEKSFFLQPGERLERGIQDVYVLSEQQGL

LLKALQPLEEGESEEKVSHQAGDCWLIRGPLEYVPSAKVEVVEERQAIPLDQNEGIYV
QDVKTGKVRAVIGSTYMLTQDEVLWEKELPSGVEELLNLGHDPLADRGQKGTAKPL
QPSAPRNKTRVVSYRVPHNAAVQVYDYRAKRARVVFGPELVTLDPEEQFTVLSLSA
GRPKRPHARRALCLLLGPDFFTDVITIETADHARLQLQLAYNWHFELKNRNDPAEAA
KLFSVPDFVGDACKAIASRVRGAVASVTFDDFHKNSARIIRMAVFGFEMSEDTGPDG
TLLPKARDQAVFPQNGLVVSSVDVQSVEPVDQRTRDALQRSVQLAIEITTNSQEAAA
KHEAQRLEQEARGRLERQKILDQSEAEKARKELLELEAMSMAVESTGNAKAEAESR
AEAARIEGEGSVLQAKLKAQALAIETEAELERVKKVREMELIYARAQLELEVSKAQQ
LANVEAKKFKEMTEALGPGTIRDLAVAGPEMQVKLLQSLGLKSTLITDGSSPINLFST
AFGLLGLGSDGQPPAQK

Amino acid sequence of the human hemoglobin subunit alpha (average molecular weight 15.1 kDa):

VLSPADKTNVKAAWGKVGAHAGEYGAEALERMFLSFPTTKTYFPHFDLSHGSAQVK
GHGKKVADALTNAVAHVDDMPNALSALSDLHAHKLRVDPVNFKLLSHCLLVTLAA
HLPAEFTPAVHASLDKFLASVSTVLTSKYR

Amino acid sequence of the human hemoglobin subunit beta (average molecular weight 16.0 kDa):

MVHLTPEEKSAVTALWGKVNVDEVGGEALGRLLVVYPWTQRFFESFGDLSTPDAV
MGNPKVKAHGKKVLGAFSDGLAHLDNLKGTFATLSELHCDKLHVDPENFRLLGNVL
VCVLAHHFGKEFTPPVQAAYQKVVAGVANALAHKYH

Amino acid sequence of the N2N3 receptor (average molecular weight 38.8 kDa):

ADESLQDAIKNPAIIDKEHTADNWRPIDFQMKNDKGERQFYHYASTVEPATVIFTKTG
PIIELGLKTASTWKKFEVYEGDKKLPVELVSYDSDKDYAYIRFPVSNGTREVKIVSSIE
YGENIHEDYDYTLMVFAQPITNNPDDYVDEETYNLQKLLAPYHKAKTLERQVYELE
KLQEKLPEKYKAEYKKKLDQTRVELADQVKSAVTEFENVTPTNDQLTDLQEAHFVV
FESEENSESVMDGFVEHPFYTATLNGQKYVVMKTKDDSYWKDLIVEGKRVTTVSKD
PKNNSRTLIFPYIPDKAVYN AIVKVVVANIGYEGQYHVRIINQDINTKDD

Amino acid sequence of Mmm1-D5-Fusion Complex (average molecular weight 31.2 kDa):

MGKQHYELNEEAENEHLQELALILEKTYYNVDVHPAESLDWFNVLVAQIIQQFRSEA
WHRDNILHSLNDFIGRKSPDLPEYLDTIKITELDTGDDFPIFSNCRIQYSPNSGNKKLEA
KIDIDLNDHLTLGVETKLLLNYPKPGIAALPINLVVSIVRFQACLTVSLTNAEEFASTSN
GSSSENGMEGNSGYFLMFSFSPEYRMEFEIKSLIGSRSKLENIPKIGSVIEYQIKKWFVE
RCVEPRFQFVRLPSMWPRSKNTREEKPTELLVPR

Amino acid sequence of TriC subunit alpha (average molecular weight 60.3 kDa):

MEGPLSVFGDRSTGETIRSQNVMAAASIANIVKSSLGPVGLDKMLVDDIGDVTITNDG
ATILKLLEVEHPAAKVLCELADLQDKEVGDGTTSVVIIAAELLKNADELVKQKIHPTS
VISGYRLACKEAVRYINENLIVNTDELGRDCLINAAKTSMSSKIIGINGDFFANMVVD
AVLAIKYTDIRGQPRYPVNSVNILKAHGRSQMESMLISGYALNCVVGSQGMPKRIVN
AKIACLDFSLQKTKMKLGVQVVITDPEKLDQIRQRESDITKERIQKILATGANVILTTG
GIDDMCLKYFVEAGAMAVRRVLKRDLKRIAKASGATILSTLANLEGEETFEAAMLG
QAEEVVQERICDDELILIKNTKARTSASIILRGANDFMCDEMERSLHDALCVVKRVLE
SKSVVPGGGAVEAALSIYLENYATSMGSREQLAIAEFARSLLVIPNTLAVNAAQDSTD
LVAKLRAFHNEAQVNPERKNLKWIGLDLSNGKPRDNKQAGVFEPTIVKVKSLKFATE
AAITILRIDDLIKLHPESKDDKHGSYEDAVHSGALND

Amino acid sequence of TriC subunit beta (average molecular weight 57.5 kDa):

MASLSLAPVNIFKAGADEERAETARLTSFIGAIAIGDLVKSTLGPKGMDKILLSSGRDA
SLMVTNDGATILKNIGVDNPAAKVLVDMSRVQDDEVGDGTTSVTVLAAELLREAES
LIAKKIHPQTIIAGWREATKAAREALLSSAVDHGSDEVKFRQDLMNIAGTTLSSKLLT
HHKDHFTKLAVEAVLRLKGSGNLEAIHIIKKLGGSLADSYLDEGFLLDKKIGVNQPKR
IENAKILIANTGMDTDKIKIFGSRVRVDSTAKVAEIEHAEKEKMKEKVERILKHGINCF
INRQLIYNYPEQLFGAAGVMAIEHADFAGVERLALVTGGEIASTFDHPELVKLGSCKL
IEEVMIGEDKLIHFSGVALGEACTIVLRGATQQILDEAERSLHDALCVLAQTVKDSRT
VYGGGCSEMLMAHAVTQLANRTPGKEAVAMESYAKALRMLPTIIADNAGYDSADL
VAQLRAAHSEGNTTAGLDMREGTIGDMAILGITESFQVKRQVLLSAAEAAEVILRVD
NIIKAAPRKRVPDHHPC

Amino acid sequence of TriC subunit gamma (average molecular weight 60.5 kDa):

MMGHRPVLVLSQNTKRESGRKVQSGNINAAKTIADIIRTCLGPKSMMKMLLDPMGGI
VMTNDGNAILREIQVQHPAAKSMIEISRTQDEEVGDGTTSVIILAGEMLSVAEHFLEQ
QMHPTVVISAYRKALDDMISTLKKISIPVDISDSDMMLNIINSSITTKAISRWSSLACNI

ALDAVKMVQFEENGRKEIDIKKYARVEKIPGGIIEDSCVLRGVMINKDVTHPRMRRYI
KNPRIVLLDSSLEYKKGESQTDIEITREEDFTRILQMEEEYIQQLCEDIIQLKPDVVITEK
GISDLAQHYLMRANITAIRRVRKTDNNRIARACGARIVSRPEELREDDVGTGAGLLEI
KKIGDEYFTFITDCKDPKACTILLRGASKEILSEVERNLQDAMQVCRNVLLDPQLVPG
GGASEMAVAHALTEKSKAMTGVEQWPYRAVAQALEVIPRTLIQNCGASTIRLLTSLR
AKHTQENCETWGVNGETGTLVDMKELGIWEPLAVKLQTYKTAVETAVLLLRIDDIV
SGHKKKGDDQSRQGGAPDAGQE

Disulfide bond 366 ↔ 372

Amino acid sequence of TriC subunit delta (average molecular weight 57.9 kDa):

MPENVAPRSGATAGAAGGRGKGAYQDRDKPAQIRFSNISAAKAVADAIRTSLGPKG
MDKMIQDGKGDVTITNDGATILKQMQVLHPAARMLVELSKAQDIEAGDGTTSVVIIA
GSLLDSCTKLLQKGIHPTIISESFQKALEKGIEILTDMSRPVELSDRETLLNSATTSLNSK
VVSQYSSLLSPMSVNAVMKVIDPATATSVDLRDIKIVKKLGGTIDDCELVEGLVLTQK
VSNSGITRVEKAKIGLIQFCLSAPKTDMDNQIVVSDYAQMDRVLREERAYILNLVKQI
KKTGCNVLLIQKSILRDALSDLALHFLNKMKIMVIKDIEREDIEFICKTIGTKPVAHIDQ
FTADMLGSAELAEEVNLNGSGKLLKITGCASPGKTVTIVVRGSNKLVIEEAERSIHDA
LCVIRCLVKKRALIAGGGAPEIELALRLTEYSRTLSGMESYCVRAFADAMEVIPSTLA
ENAGLNPISTVTELRNRHAQGEKTAGINVRKGGISNILEELVVQPLLVSVSALTLATET
VRSILKIDDVVNTR

Amino acid sequence of TriC subunit epsilon (average molecular weight 59.7 kDa):

MASMGTLAFDEYGRPFLIIKDQDRKSRLMGLEALKSHIMAAKAVANTMRTSLGPNG
LDKMMVDKDGDVTVTNDGATILSMMDVDHQIAKLMVELSKSQDDEIGDGTTGVVV
LAGALLEEAEQLLDRGIHPIRIADGYEQAARVAIEHLDKISDSVLVDIKDTEPLIQTAK
TTLGSKVVNSCHRQMAEIAVNAVLTVADMERRDVDFELIKVEGKVGGRLEDTKLIK
GVIVDKDFSHPQMPKKVEDAKIAILTCPFEPPKPKTKHKLDVTSVEDYKALQKYEKE
KFEEMIQQIKETGANLAICQWGFDDEANHLLLQNNLPAVRWVGGPEIELIAIATGGRI
VPRFSELTAEKLGFAGLVQEISFGTTKDKMLVIEQCKNSRAVTIFIRGGNKMIIEEAKR
SLHDALCVIRNLIRDNRVVYGGGAAEISCALAVSQEADKCPTLEQYAMRAFADALEV
IPMALSENSGMNPIQTMTEVRARQVKEMNPALGIDCLHKGTNDMKQQHVIETLIGKK
QQISLATQMVRMILKIDDIRKPGESEE

Amino acid sequence of TriC subunit zeta (average molecular weight 44.7 kDa):

MAAVKTLNPKAEVARAQAALAVNISAARGLQDVLRTNLGPKGTMKMLVSGAGDIK
LTKDGNVLLHEMQIQHPTASLIAKVATAQDDITGDGTTSNVLIIGELLKQADLYISEGL
HPRIITEGFEAAKEKALQFLEEVKVSREMDRETLIDVARTSLRTKVHAELADVLTEAV
VDSILAIKKQDEPIDLFMIEIMEMKHKSETDTSLIRGLVLDHGARHPDMKKRVEDAYI
LTCNVSLEYEKTEVNSGFFYKSAEEREKLVKAERKFIEDRVKKIIELKRKVCGDSDKG
FVVINQKGIDPFSLDALSKEGIVALRRAKRRNMERLTLACGGVALNSFDDLSPDCLGH
AGLVYEYTLGEEKFTFIEKCNNPRSVTLLIKGPNKHTLTQIKDAVRDGLRAVKNAIDD
GCVVPGAGAVEVAMAEALIKHKPSVKGRAQLGVQAFADALLIIPKVLAQNSGFDLQ
ETLVKIQAEHSESGQLVGVDLNTGEPMVAAEVGVWDNYCVKKQLLHSCTVIATNIL
LVDEIMRAGMSSLKG

Amino acid sequence of TriC subunit eta (average molecular weight 59.4 kDa):

MMPTPVILLKEGTDSSQGIPQLVSNISACQVIAEAVRTTLGPRGMDKLIVDGRGKATIS
NDGATILKLLDVVHPAAKTLVDIAKSQDAEVGDGTTSVTLLAAEFLKQVKPYVEEGL
HPQIIIRAFRTATQLAVNKIKEIAVTVKKADKVEQRKLLEKCAMTALSSKLISQQKAFF
AKMVVDAVMMLDDLLQLKMIGIKKVQGGALEDSQLVAGVAFKKTFSYAGFEMQPK
KYHNPKIALLNVELELKAEKDNAEIRVHTVEDYQAIVDAEWNILYDKLEKIHHSGAK
VVLSKLPIGDVATQYFADRDMFCAGRVPEEDLKRTMMACGGSIQTSVNALSADVLG
RCQVFEETQIGGERYNFFTGCPKAKTCTFILRGGAEQFMEETERSLHDAIMIVRRAIKN
DSVVAGGGAIEMELSKYLRDYSRTIPGKQQLLIGAYAKALEIIPRQLCDNAGFDATNI
LNKLRARHAQGGTWYGVDINNEDIADNFEAFVWEPAMVRINALTAASEAACLIVSV
DETIKNPRSTVDAPTAAGRGRGRGRPH

Amino acid sequence of TriC subunit theta (average molecular weight 59.6 kDa):

MALHVPKAPGFAQMLKEGAKHFSGLEEAVYRNIQACKELAQTTRTAYGPNGMNKM
VINHLEKLFVTNDAATILRELEVQHPAAKMIVMASHMQEQEVGDGTNFVLVFAGAL
LELAEELLRIGLSVSEVIEGYEIACRKAHEILPNLVCCSAKNLRDIDEVSSLLRTSIMSK
QYGNEVFLAKLIAQACVSIFPDSGHFNVDNIRVCKILGSGISSSSVLHGMVFKKETEGD
VTSVKDAKIAVYSCPFDGMITETKGTVLIKTAEELMNFSKGEENLMDAQVKAIADTG
ANVVVTGGKVADMALHYANKYNIMLVRLNSKWDLRRLCKTVGATALPRLTPPVLE
EMGHCDSVYLSEVGDTQVVVFKHEKEDGAISTIVLRGSTDNLMDDIERAVDDGVNT
FKVLTRDKRLVPGGGATEIELAKQITSYGETCPGLEQYAIKKFAEAFEAIPRALAENSG
VKANEVISKLYAVHQEGNKNVGLDIEAEVPAVKDMLEAGILDTYLGKYWAIKLATN
AAVTVLRVDQIIMAKPAGGPKPPSGKKDWDDDQND

Average molecular weight of TriC complex 919.2 kDa

# 6 References


[1] M. Vert, Y. Doi, K. H. Hellwich, M. Hess, P. Hodge, P. Kubisa, M. Rinaudo and F. Schue, *Pure Appl Chem* **2012**, *84*, 377-408.

[2] T. Muthukumar, S. Prabhavathi, M. Chamundeeswari and T. P. Sastry, *Mater Sci Eng C Mater Biol Appl* **2014**, *36*, 14-19.

[3] N. Li, P. Zhao and D. Astruc, *Angew Chem Int Ed Engl* **2014**, *53*, 1756-1789.

[4] W. Shen, X. Zhang, Q. Huang, Q. Xu and W. Song, *Nanoscale* **2014**, *6*, 1622-1628.

[5] W. H. De Jong and P. J. Borm, *Int J Nanomed* **2008**, *3*, 133-149.

[6] K. S. Lin, K. Dehvari, Y. J. Liu, H. Kuo and P. J. Hsu, *J Nanosci Nanotechnol* **2013**, *13*, 2675-2681.

[7] P. Krystek, J. Tentschert, Y. Nia, B. Trouiller, L. Noel, M. E. Goetz, A. Papin, A. Luch, T. Guerin and W. H. de Jong, *Anal Bioanal Chem* **2014,** *406*, 3853-3861.

[8] S. L. Kaufman, J. W. Skogen, F. D. Dorman, F. Zarrin and K. C. Lewis, *Anal Chem* **1996**, *68*, 1895-1904.

[9] a) C. S. Kaddis, S. H. Lomeli, S. Yin, B. Berhane, M. I. Apostol, V. A. Kickhoefer, L. H. Rome and J. A. Loo, *J Am Soc Mass Spectrom* **2007**, *18*, 1206-1216; b) J. Kemptner, M. Marchetti-Deschmann, R. Muller, A. Ivens, P. Turecek, H. P. Schwarz and G. Allmaier, *Rapid Commun Mass Spectrom* **2010**, *24*, 761-767; c) J. Kemptner, M. Marchetti-Deschmann, J. Siekmann, P. L. Turecek, H. P. Schwarz and G. Allmaier, *J Pharm Biomed Anal* **2010**, *52*, 432-437; d) L. Malm, U. Hellman and G. Larsson, *Glycobiol* **2012**, *22*, 7-11; e) V. U. Weiss, X. Subirats, A. Pickl-Herk, G. Bilek, W. Winkler, M. Kumar, G. Allmaier, D. Blaas and E. Kenndler, *Electrophoresis* **2012**, *33*, 1833-1841; f) P. Kallinger, V. U. Weiss, A. Lehner, G. Allmaier and W. W. Szymanski, *Particuology* **2013**, *11*, 14-19.

[10] G. Bacher, W. W. Szymanski, S. L. Kaufman, P. Zollner, D. Blaas and G. Allmaier, *J Mass Spectrom* **2001**, *36*, 1038-1052.

[11] P. Intra and N. Tippayawong, *Songklanakarin J. Sci. Technol.* **2008**, *30*, 243-256.

[12] D. R. Chen, D. Y. H. Pui, D. Hummes, H. Fissan, F. R. Quant and G. J. Sem, *J Aerosol Sci* **1998**, *29*, 497-509.

[13] J. A. Koropchak, S. Sadain, X. Yang, L. E. Magnusson, M. Heybroek, M. Anisimov and S. L. Kaufman, *Anal Chem* **1999**, *71*, 386A-394A.

[14] a) J. A. Loo, B. Berhane, C. S. Kaddis, K. M. Wooding, Y. Xie, S. L. Kaufman and I. V. Chernushevich, *J Am Soc Mass Spectrom* **2005**, *16*, 998-1008; b) G. Allmaier, C. Laschober and W. W. Szymanski, *J Am Soc Mass Spectrom* **2008**, *19*, 1062-1068; c) C. Laschober, J. Wruss, D. Blaas, W. W. Szymanski and G. Allmaier, *Anal Chem* **2008**, *80*, 2261-2264; d) K. D. Cole, L. F. Pease, 3rd, D. H. Tsai, T. Singh, S. Lute, K. A. Brorson and L. Wang, *J Chromatogr A* **2009**, *1216*, 5715-5722; e) D. H. Tsai, L. F. Pease, R. A. Zangmeister, M. J. Tarlov and M. R. Zachariah, *Langmuir* **2009**, *25*, 140-146; f) L. F. Pease, 3rd, D. H. Tsai, J. A. Fagan, B. J. Bauer, R. A. Zangmeister, M. J. Tarlov and M. R. Zachariah, *Small* **2009**, *5*, 2894-2901; g) L. F. Pease, 3rd, D. I. Lipin, D. H. Tsai, M. R. Zachariah, L. H. Lua, M. J. Tarlov and A. P. Middelberg, *Biotechnol Bioeng* **2009**, *102*, 845-855; h) L. F. Pease, 3rd, D. H. Tsai, J. L. Hertz, R. A. Zangmeister, M. R. Zachariah and M. J. Tarlov, *Langmuir* **2010**, *26*, 11384-11390; i) V. U. Weiss, A. Lehner, L. Kerul, R. Grombe, M. Kratzmeier, M. Marchetti-Deschmann and G. Allmaier, *Electrophoresis* **2013**; j) H. Hinterwirth, S. K. Wiedmer, M. Moilanen, A. Lehner, G. Allmaier, T. Waitz, W. Lindner and M. Lammerhofer, *J Sep Sci* **2013**, *36*, 2952-2961.

[15] A. Jouyban and E. Kenndler, *Electrophoresis* **2006**, *27*, 992-1005.

[16] K. C. Lewis, J. W. Jorgenson and S. L. Kaufman, *J Capillary Electrophor* **1996**, *3*, 229-235.

[17] T. Ma and Y. Fung, *ECS Meeting Abstracts* **2012,** MA 2012-02, 2773

[18] a) N. L. Kedersha, M. C. Miquel, D. Bittner and L. H. Rome, *J Cell Biol* **1990**, *110*, 895-901; b) L. Rome, N. Kedersha and D. Chugani, *Trends Cell Biol* **1991**, *1*, 47-50.

[19] L. B. Kong, A. C. Siva, L. H. Rome and P. L. Stewart, *Structure* **1999**, *7*, 371-379.

[20] N. L. Kedersha, J. E. Heuser, D. C. Chugani and L. H. Rome, *J Cell Biol* **1991**, *112*, 225-235.

[21] U. K. Kar, M. K. Srivastava, A. Andersson, F. Baratelli, M. Huang, V. A. Kickhoefer, S. M. Dubinett, L. H. Rome and S. Sharma, *PLoS One* **2011**, *6*, e18758.

[22] M. Han, V. A. Kickhoefer, G. R. Nemerow and L. H. Rome, *ACS Nano* **2011**, *5*, 6128-6137.

[23] D. H. Anderson, V. A. Kickhoefer, S. A. Sievers, L. H. Rome and D. Eisenberg, *PLoS Biol* **2007**, *5*, e318.

[24] H. Tanaka, K. Kato, E. Yamashita, T. Sumizawa, Y. Zhou, M. Yao, K. Iwasaki, M. Yoshimura and T. Tsukihara, *Science* **2009**, *323*, 384-388.

[25] K. A. Suprenant, *Biochemistry* **2002**, *41*, 14447-14454.

[26] J. Yang, A. Srinivasan, Y. Sun, J. Mrazek, Z. Shu, V. A. Kickhoefer and L. H. Rome, *Integr Biol (Camb)* **2013**, *5*, 151-158.

[27] J. C. White and G. H. Beaver, *J Clin Pathol* **1954**, *7*, 175-200.

[28] B. D. Sidell and K. M. O'Brien, *J Exp Biol* **2006**, *209*, 1791-1802.

[29] T. Spirig, G. R. Malmirchegini, J. Zhang, S. A. Robson, M. Sjodt, M. Liu, K. Krishna Kumar, C. F. Dickson, D. A. Gell, B. Lei, J. A. Loo and R. T. Clubb, *J Biol Chem* **2013**, *288*, 1065-1078.

[30] R. J. Hill, W. Konigsberg, G. Guidotti and L. C. Craig, *J Biol Chem* **1962**, *237*, 1549-1554.

[31] A. Leitner, L. A. Joachimiak, A. Bracher, L. Monkemeyer, T. Walzthoeni, B. Chen, S. Pechmann, S. Holmes, Y. Cong, B. Ma, S. Ludtke, W. Chiu, F. U. Hartl, R. Aebersold and J. Frydman, *Structure* **2012**, *20*, 814-825.

[32] V. A. Kickhoefer, A. C. Siva, N. L. Kedersha, E. M. Inman, C. Ruland, M. Streuli and L. H. Rome, *J Cell Biol* **1999**, *146*, 917-928.

[33] Y. Mikyas, M. Makabi, S. Raval-Fernandes, L. Harrington, V. A. Kickhoefer, L. H. Rome and P. L. Stewart, *J Mol Biol* **2004**, *344*, 91-105.

[34] a) M. J. Poderycki, V. A. Kickhoefer, C. S. Kaddis, S. Raval-Fernandes, E. Johansson, J. I. Zink, J. A. Loo and L. H. Rome, *Biochemistry* **2006**, *45*, 12184-12193; b) L. E. Goldsmith, M. Yu, L. H. Rome and H. G. Monbouquette, *Biochemistry* **2007**, *46*, 2865-2875.

[35] a) R. Esfandiary, V. A. Kickhoefer, L. H. Rome, S. B. Joshi and C. R. Middaugh, *J Pharm Sci* **2009**, *98*, 1376-1386; b) J. Yang, V. A. Kickhoefer, B. C. Ng, A. Gopal, L. A. Bentolila, S. John, S. H. Tolbert and L. H. Rome, *ACS Nano* **2010**, *4*, 7229-7240.

[36] L. F. Pease, 3rd, J. T. Elliott, D. H. Tsai, M. R. Zachariah and M. J. Tarlov, *Biotechnol Bioeng* **2008**, *101*, 1214-1222.